THE ROLES OF FIBROBLAST GROWTH FACTORS IN INNER EAR DEVELOPMENT

by

Ekaterina Hatch

A dissertation submitted to the faculty of
The University of Utah
in partial fulfillment of the requirements for the degree of

Doctor of Philosophy

Department of Human Genetics

The University of Utah

August 2007

THE UNIVERSITY OF UTAH GRADUATE SCHOOL

SUPERVISORY COMMITTEE APPROVAL

of a dissertation submitted by

Ekaterina Hatch

This dissertation has been read by each member of the following supervisory committee and by majority vote has been found to be satisfactory.

5/21/07 — Chair: [redacted] Mansour, Ph.D.

21 May 07 — David Grunwald, Ph.D.

[redacted] — Anthea Letsou, Ph.D.

[redacted] — Edward Levine, Ph.D.

5/21/07 — Tatjana Pitotrowski, Ph.D.

THE UNIVERSITY OF UTAH GRADUATE SCHOOL

FINAL READING APPROVAL

To the Graduate Council of the University of Utah:

I have read the dissertation of Ekaterina Hatch in its final form and have found that (1) its format, citations, and bibliographic style are consistent and acceptable; (2) its illustrative materials including figures, tables, and charts are in place; and (3) the final manuscript is satisfactory to the supervisory committee and is ready for submission to The Graduate School.

Suzanne L. Mansour, Ph.D.
Chair: Supervisory Committee

Approved for the Major Department

Mark F. Leppert, Ph.D.
Co-Chair, Dept. of Human Genetics

Mario R.
Co-Chair, Dept. of Human Genetics

Approved for the Graduate Council

David S. Chapman
Dean of The Graduate School

ABSTRACT

Understanding the molecular and genetic mechanisms responsible for the development of the vertebrate inner ear, which mediates hearing and equilibrium, is an ongoing quest in developmental biology. Most of the cells found in the sensory tissue of the mature inner ear are derived from an ectodermal placode that is located adjacent to the developing hindbrain. This tissue undergoes complex morphogenesis to form auditory and vestibular compartments which have distinct morphologic characteristics along each of the developmental axes. Otic development involves signaling interactions within and between otic and non-otic tissues. However, the molecular basis of otic morphogenesis and axis formation remains relatively unexplored.

This study uses the mouse model to assess the role of the Fibroblast Growth Factor (FGF) signaling system in otic development. The work described herein analyses expression patterns of the members of *Fgf* gene family and examines specific roles of *Fgf3* and *Fgf16* in inner ear morphogenesis.

We show that *Fgf16* is one of the earliest regionally restricted transcripts expressed in otic tissue and is polarized along the antero-posterior otic axis. Simultaneous knock out of *Fgf16* function and expression of *Cre* recombinase in its place allowed us to determine the consequences of inactivating *Fgf16* and to examine the fate of mouse posterior otic cells. We show that *Fgf16* does not have a unique role in inner ear development and describe the fates of *Fgf16* expressing otic cells in anterior and

posterior semicircular canals, the three ampullary cristae, and the cochlear stria vascularis.

In addition, this thesis shows that *Fgf3* is required for dorsal pattering and morphogenesis of the inner ear epithelium. The range of malformations observed in *Fgf3* mutants has close parallels with those seen in hearing impaired patients. Through a series of conditional mutagenesis experiments, we also suggest that there is an early placode stage requirement for hindbrain-expressed *Fgf3* to induce proper development of the endolymphatic duct.

Taken together, this study provides new information on the normal development of the inner ear and the factors that regulate the process of otic morphogenesis, providing insights into genetic mechanisms responsible for the myriad of human inner ear malformations.

TABLE OF CONTENTS

ACKNOWLEDGEMENTS

I am grateful for the guidance, advice, and friendship of many people over the course of my graduate studies. The person who has influenced me the most during the course of my graduate career is my mentor, Dr. Susanne L. Mansour. Her guidance was very helpful during the time I was still developing my interest in science. Suzi took on the role as my undergraduate advisor and allowed me to work on my own project, introducing me to the excitement of biological experimentation. During this time I gained practical research experience in an academic setting and began to explore questions associated with fundamental developmental biology, influencing some of my early decisions to pursue a doctorate degree in science. Over the past several years Suzi has been a true mentor, who always expected excellence, gave praise when it was earned, and was patient and understanding during difficult times. She has always pushed me forward and offered encouragement when I struggled with hard decisions in and out of the lab. Suzi impressed me both as a researcher, who taught me how to think scientifically, and as a human being, who is unselfish in sharing both her time and thoughts.

I would like to emphasize my appreciation to the past and present members of the Mansour lab. They all deserve thanks for their scientific input and for their friendship. I gained a lot from the experience they all willingly shared. Without them I would not have brought the project to such a successful conclusion. Much of the work described here has been the result of collaborative efforts with Xiaofen Wang, Albert Noyes and Lisa

Urness. They assisted me with much of my work and taught me how to effectively generate experimental data. I would like to specifically thank Doctor Tracy Wright for her struggles with the Fibroblast Growth Factor expression analysis screen that was the seed for many subsequent projects. I also admire her guidance, critical comments and open suggestions towards biological problems.

I appreciate all the help and collaborative effort of Dr. Mario Capecchi's lab members. Many of them offered valuable conversation and critique in many aspects of mouse embryonic development. In particular I would like to thank Anne Boulet, Ben Arenkiel, Amir Pozner and Nadja Makki for taking their time to share technical experience and genetic tools. I also thank members of Dr. Gary Schoenwolf's lab for their contributions to the work presented in Chapter 2.

I must extend thanks and appreciation to the members of my supervisory committee: David Grunwald, Anthea Letsou, Edward Levine and Tatjana Piotrowski for their guidance throughout my graduate career. Taking time away from their own work, my committee consistently evaluated my progress and offered helpful suggestions. I have been fortunate to develop a genuine personal relationship with many of them, which provided me with a combination of challenge and support and helped to shape the course of my research. They are all role models I will always try to emulate.

I would like to emphasize my appreciation to the people who have taken their time to offer critical comments to help me build both my experimentation and communication skills, which are essential in writing and speaking about science. I appreciate the energetic thinking and constructive criticism of all those who participated in Friday group meetings. In particular I would like to thank Carl Thummel, who always

takes the extra initiative to challenge and support the students. Financial support for much of this work was provided by the National Institutes of Health Genetics Training Grant. Interactions with many of the student trainees gave me the opportunity to develop a different perspective towards the biological problems and made me a better researcher and person.

My spirits have been buoyed at times by many friends over the past several years offering advice, support and encouragement. Special thanks go to my husband's family for their support of me throughout my education. I would also like to extend my thanks and appreciation to my mother, Natalia Kopaneva, who has helped me tremendously after the birth of my son, allowing me to continue my graduate career. Above all I am grateful for the loving support of my husband and son, Shandon and Dimitry, who are my greatest sources of joy. To them I owe a world of thanks for the love, patience and understanding over the years.

Each of you has, at one time or another, motivated and inspired me; your love, friendship and encouragement are a large part of this achievement. Thank you all for sharing it with me.

CHAPTER 1

INTRODUCTION

Development of the inner ear

The inner ear is a morphologically complex sensory organ responsible for hearing and balance. In higher vertebrates, the mechanoreceptor cells responsible for auditory sensation are housed in the ventrally located cochlear duct. The remaining mechanoreceptors are housed within the dorsally located vestibular system, which functions in gravity and motion perception required for balance (Figure 1.1). Dysfunction of the inner ear is a frequent congenital disorder, affecting at least 1 in 500 births (Morton and Nance, 2006) and up to 39% of sensorineural deafness is associated with inner ear malformations (Mafong et al., 2002; Wu et al., 2005). The mouse inner ear is functionally and structurally very similar to that of humans and provides an excellent model system with which to investigate the genetic mechanisms responsible for the myriad of human inner ear malformations (Fritzsch et al., 2006; Kiernan et al., 2002; Mansour and Schoenwolf, 2005).

In the mouse, inner ear formation initiates at embryonic day (E) 8.0 (in an embryo with 7-11 pairs of somites) as a placodal thickening of the head ectoderm adjacent to rhombomeres (r) 5 and 6 of the hindbrain (Figure1.2A). The placode subsequently invaginates to form the otic cup. By E9.5, the cup closes and separates from the surface ectoderm, forming the oval-shaped otic vesicle or otocyst. During the period of late otic

Figure 1.1 Structures of the inner ear

Lateral view of a paint-filled left inner ear from an E15.5 wild type mouse. Structures labeled are as follows: aa, anterior ampulla; asc, anterior semicircular canal; cc, common crus; cd, cochlear duct; ed, endolymphatic duct; es, endolymphatic sac; la, lateral ampulla; lsc, lateral semicircular canal; pa, posterior ampulla; psc, posterior semicircular canal; s, saccule; u, utricle.

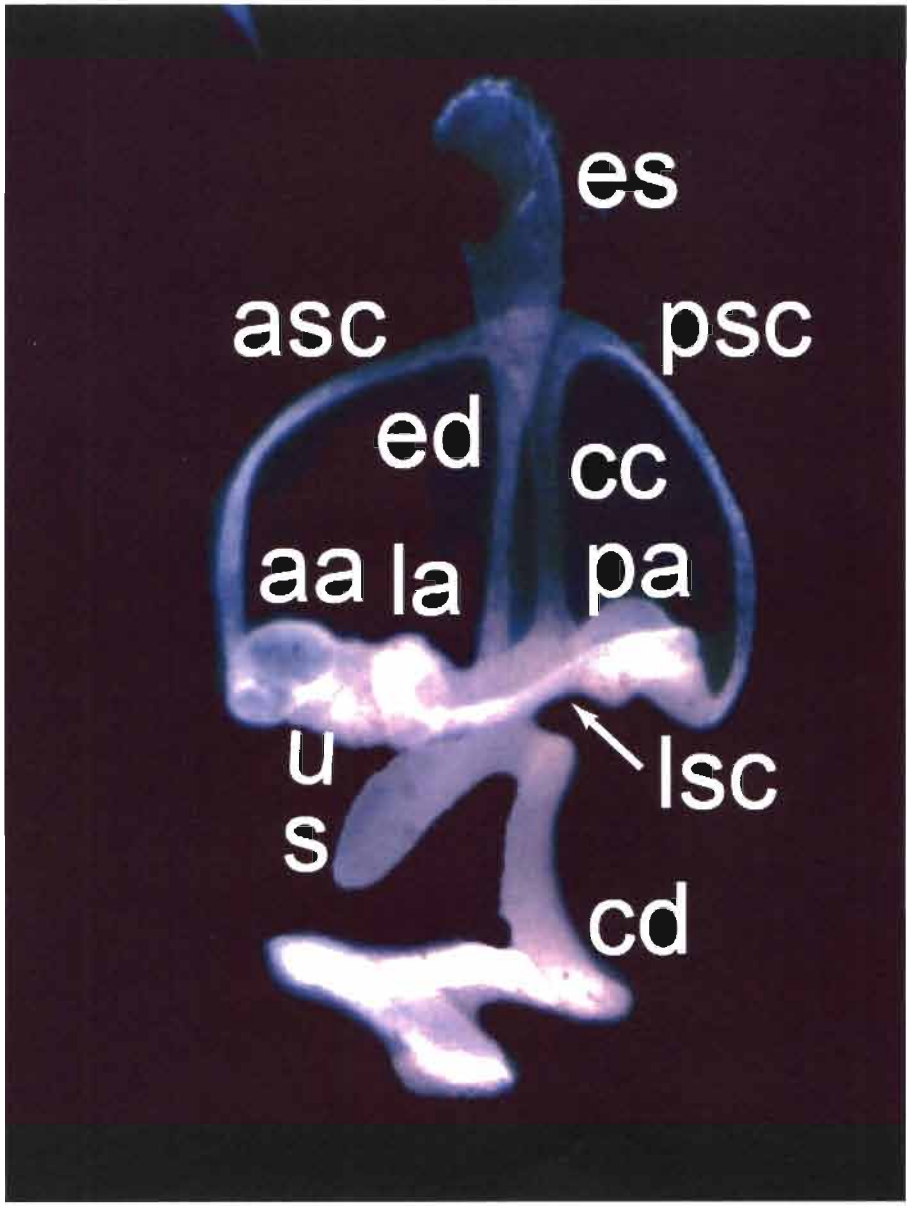
es
asc
psc
ed
cc
aa
la
pa
u
s
lsc
cd

cup and early otocyst formation, cells in the anteroventral portion of the vesicle delaminate from the epithelium and migrate medially to form the eighth cranial ganglion (GVIII). During the next 6 days of development, this relatively simple epithelium acquires its mature and complex morphology and begins to differentiate its multitude of distinct sensory and non-sensory cell types. Morphogenesis of the vesicle initiates at E10.5 with a dorsomedially directed outgrowth of the endolymphatic duct/sac (EDS) anlage and a ventrally directed outgrowth of the cochlear duct (Figure 1.2A, B). At about E11.5, the otic epithelium evaginates dorsolaterally to form the vertical canal plate, the precursor of the anterior and posterior semicircular canals, which are separated by the common crus, and shortly thereafter evaginates laterally to form the lateral canal plate, the precursor of the lateral semicircular canal (Figure 1.2B). The canals are formed by fusion at E12.5 of cells within two central regions of the vertical plate and a single central region of the lateral canal plate, followed at E13.5 by resorption of the fused cells into the epithelium. During this period, there are additional evaginations of the central region to form the more dorsally situated utricle and the more ventrally situated saccule. By E15.5, the inner ear epithelium has acquired its mature morphology, but is still undergoing cellular differentiation within the six sensory patches (Figure 1.2B).

Signaling in inner ear development

The initial induction and subsequent morphogenesis and differentiation of the otic epithelium involves signaling interactions within and between otic and non-otic tissues (Fekete, 1999; Kiernan et al., 2002). Members of the Fibroblast growth factor (FGF) family, namely, FGF3, FGF8, FGF10 and FGF19, are expressed by tissues relevant for

Figure 1.2 Development of the mouse inner ear

(A) Schematic depiction of half-transverse sections taken through the generic inner ear forming region spanning pre-placodal through vesicle stages. (B) Figure modified from Morsli et al. (1998), illustrating lateral view of paint-filled membranous labyrinths ranging from E10.5 to E17.0. Orientation shown in (B) also applies to (A) and indicates dorsal (D) toward the top and ventral (V) toward the bottom.

Abbreviations: coch, cochlea; ed, endolymphatic duct; og, otic ganglion; s, somites.

A

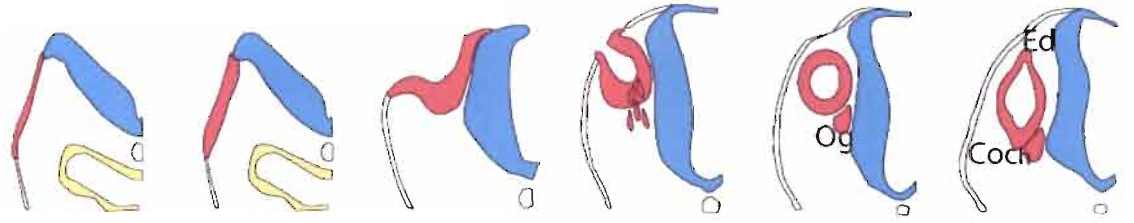

Preplacodal ectoderm 0-4s

Ectodermal thickening of the **placode** 4-11s

Otic **cup** invagination 13-20s

Formation of the 8th cranial ganglion 20-23s

Complete **vesicle** is formed 21-29s

Morphogenetic changes 35s

-Placodal ectoderm -Neuroectoderm -Endoderm

B

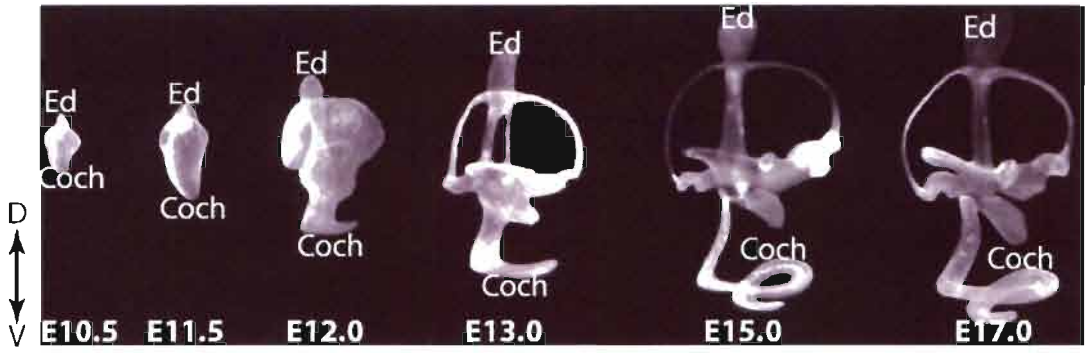

otic development in different species (Ladher et al., 2000; Leger and Brand, 2002; Mahmood et al., 1996; Mansour et al., 1993; Maroon et al., 2002; McKay et al., 1996; Pauley et al., 2003; Phillips et al., 2001; Pirvola et al., 2000; Vendrell et al., 2000; Wilkinson et al., 1988). In particular, FGF signals from the endoderm induce a mesenchymal FGF that is required together with hindbrain FGFs for expression of otic placode genes and for otic placode induction and vesicle formation. Based on genetic data, these signals are likely to be provided in the mouse by FGF8, FGF10 and FGF3, expressed by the endoderm, mesenchyme and hindbrain, respectively (Alvarez et al., 2003; Ladher et al., 2005; Wright and Mansour, 2003)(Figure 1.3A). WNT signals, presumably from the hindbrain, are required to limit the region of the ectoderm that forms the otic placode (Ohyama et al., 2006). In response to the inductive signals, the developing otic placode expresses several transcription factors in a uniform fashion including *Pax2*, *Dlx5*, and *Gbx2* (Ladher et al., 2005; Wright and Mansour, 2003)(Figure 1.3A, B).

By the otocyst stage, the expression domains of most otic markers become confined to restricted domains of the vesicle specified to give rise to different ear structures (Fekete and Wu, 2002)(Figure 1.3B). This division of the otocyst into gene expression domains required for normal morphogenesis also depends on signals from the hindbrain. Removal or rotation of the neural tube in the vicinity of the developing otic tissue disrupts otic vesicle molecular patterning and development (Bok et al., 2005; Hutson et al., 1999). Mutations in hindbrain-expressed genes, such as *Mafb* (*Kreisler*) and *Hoxa1*, which cause defects in the development of r5 and r6, also show aberrant

Figure 1.3 Signaling in inner ear development

(A) Oblique view of the developing hindbrain and otic vesicle during the initiation of otic morphogenesis. The model integrates various data published previously. Otic placode (yellow) induction is initiated by FGF3, FGF8 and FGF10 signals provided redundantly from the hindbrain (blue), endoderm (white) and mesenchyme (beige). Hindbrain WNT signals act to limit the region of the ectoderm that forms the otic placode. In response to these inductive signals, the developing otic placode expresses several transcription factors in a uniform fashion, including *Pax2*, *Dlx5*, and *Gbx2*. (B) Marker gene expression in the inner ear placode (*Pax2*), cup (*Fgf10*) and vesicle (*Pax2*, *Dlx5*). Embryos were probed with *Pax2* (A, C), *Fgf10* (B), or *Dlx5* (D) and sectioned transversely as indicated by the black lines. At E8.5, *Pax2* transcripts are detected throughout the otic placode. At E9.0, *Fgf10* expression is detected throughout the otic cup. At E9.5, *Pax2* expression marks the ventromedial compartment of the vesicle and *Dlx5* marks the dorsolateral region. Abbreviations: oc, otic cup; op, otic placode; ov, otic vesicle.

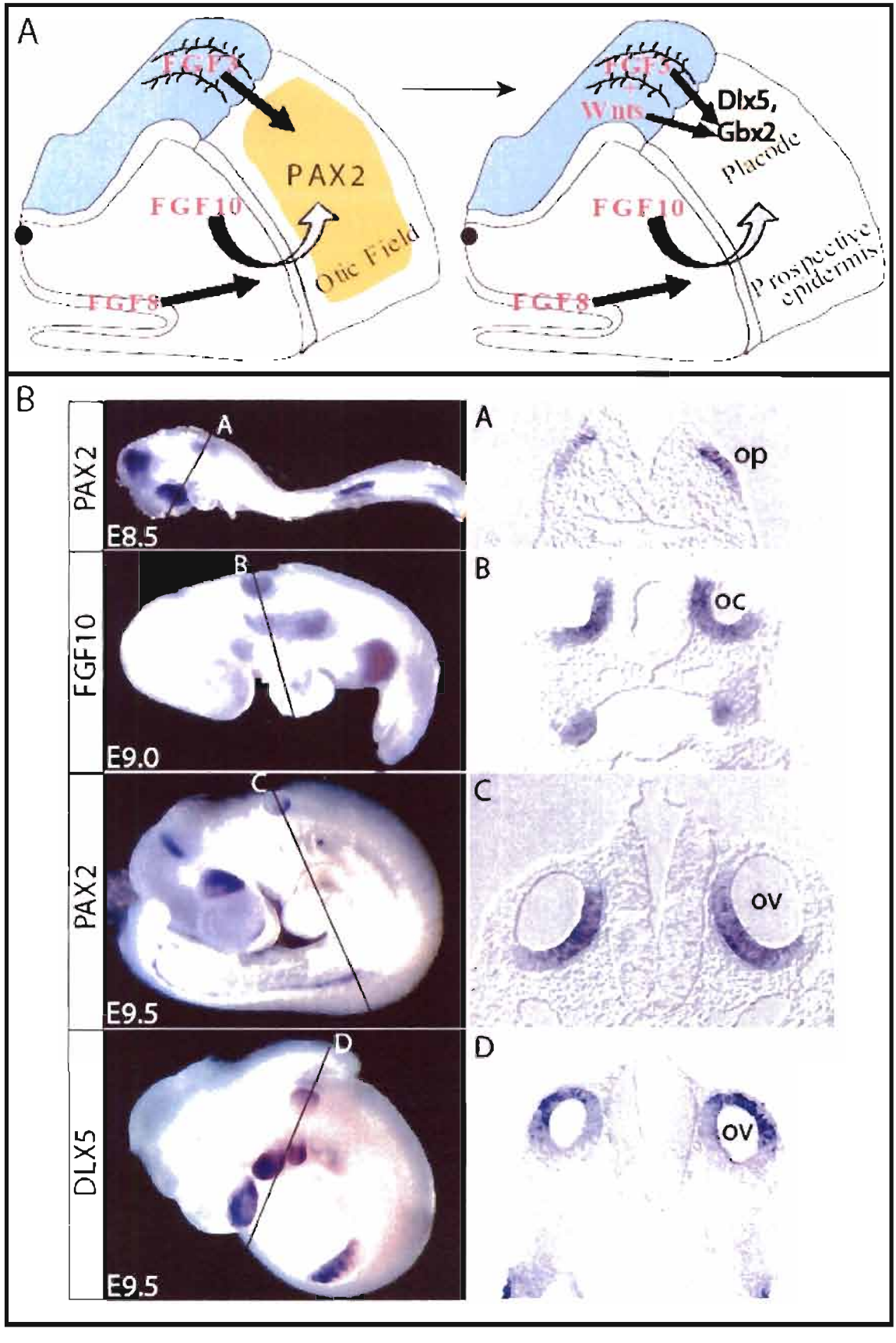
A
FGF3
PAX2
FGF10
Otic Field
FGF8
FGF3
Wnts
Dlx5,
Gbx2
placode
FGF10
Prospective
epidermis
FGF8
B
PAX2
A
E8.5
FGF10
B
E9.0
PAX2
C
E9.5
DLX5
D
E9.5
A
op
B
oc
C
ov
D
ov

patterning of the otic vesicle that presages inner ear malformations (Choo et al., 2006; Pasqualetti et al., 2001). WNT signaling from the hindbrain is sufficient to maintain the expression of some dorsal otic genes and *Wnt1* and *Wnt3a*, which are expressed in the dorsal hindbrain, are required redundantly for formation of the vestibular structures (Riccomagno et al., 2005).

FGF signaling also plays a major role in inner ear morphogenesis. Global inhibition of FGF signaling by application of SU5402 to chick E2.5-E3 otic vesicles just prior to canal pouch evagination inhibits semicircular canal formation (Chang et al., 2004). Mice lacking the "b" splice isoform of FGF receptor (R) 2 form otic vesicles that subsequently develop dysmorphologies that include failure of semicircular canal formation (Pirvola et al., 2000). Most *Fgf10* mutants completely lack semicircular canals (Ohuchi et al., 2005; Pauley et al., 2003). *Fgf3* null mutants develop highly variable and incompletely penetrant inner ear dysmorphologies that and show a reduction in the size of the otic ganglion (Mansour et al., 1993). There is also genetic evidence for transmission of FGF signals needed for several phases of otic development through FGFR1, FGFR3 (isoforms not established), and FGFR2b (Deng et al., 1994; Eswarakumar et al., 2002; Mueller et al., 2002; Partanen et al., 1998; Pirvola et al., 2000; Yamaguchi et al., 1994; Yu et al., 2000).

Axial specification and patterning of the inner ear

The inner ear is an asymmetric structure with each of its developmental axes having distinct morphologic characteristics. When and how each of the three axes arise from a simple ectodermal placode is not fully understood. The timing of anteroposterior (AP) vs. dorsoventral (DV) axis formation was addressed in rotation experiments in the

chick (Brigande et al., 2000b; Rinkwitz et al., 2001; Rivolta, 1997; Torres and Giraldez, 1998; Wu et al., 1998). It was concluded that the AP otic axis is established before the DV axis, and in chick this development occurs at the otic cup stage. The axial fixation issue has not been addressed in the mouse. The molecular basis of otic axis formation also remains relatively unexplored. It has been suggested that the complex task of forming all the compartments of the inner ear is simplified by segregation into different compartments, which are marked by asymmetrically expressed genes. Most recent models of inner ear development indicate that boundaries of gene expression are important for patterning of the inner ear (Brigande et al., 2000b; Fekete and Wu, 2002; Rinkwitz et al., 2001). Even though the major role in inner ear morphogenesis has been attributed to signaling coming from the tissues surrounding the otic region, such as the hindbrain and the periotic mesenchyme, a large number of the key transcription factors are expressed by the epithelium itself, often in spatially and temporally complex patterns (Brigande et al., 2000b; Rivolta, 1997; Torres and Giraldez, 1998).

Several studies in the chick have focused on understanding fate maps of the inner ear. The most common approach has been to mark cell populations with vital dyes that enable identification of clonal populations derived from different areas of the early otic cup and vesicle (Brigande et al., 2000a). These experiments have been extremely valuable in expanding our understanding of patterning and fate specification on different inner ear structures. However, similar information is not available for the mouse model system due to technical difficulties associated with traditional lineage tracing experiments. The only available insights into the mouse specification map came from culturing pieces of mouse otocysts *in vitro* for 10 days (Li et al., 1978). According to that

data, dorsal anterior quarters of day 11 and 12 otocysts give rise to the anterior semicircular canal, part of the lateral canal, and the associated cristae, whereas dorsal posterior quarters give rise to the remaining canals (posterior and the rest of the lateral) and posterior cristae. In addition, all three canals can arise from the lateral half of the otocyst. Ventral halves of otocyst almost exclusively give rise to the cochlea. These data indicate that dorsal and ventral inner ear structures arise from dorsal and ventral otocyst regions respectively. However, to expand our knowledge regarding the lineage and specification of different inner ear structures in a mouse, a genetic approach that permits regions of the otocyst to be permanently marked throughout development would be informative.

Fibroblast growth factor signaling

As previously mentioned, FGF signaling is implicated in a variety of stages of otic development and is a focus of this study. FGFs form a large family of 17-30 kD secreted molecules with many important biological activities. They are monomeric polypeptides, encoded by 22 genes in mammals, with a conserved 120 amino acid core that binds tightly to heparin sulphate proteoglycans (HSPGs) present in the extracellular matrix (McKeehan et al., 1998).

The signaling activity of FGFs is mediated through high-affinity receptors, which are encoded by four genes, *Fgfr1-4*. The typical FGFR tyrosine kinase receptor contains two or three immunoglobulin-like (Ig) domains that serve as the FGF binding site, a single-pass transmembrane domain, a heparin-binding sequence, and an intracellular split tyrosine kinase domain. Alternative mRNA splicing of the Ig-III domain of *Fgfr1*, *-2* and *-3* results in either the IIIb or IIIc isoform of these receptors. *Fgfr4* produces only the

IIIc-type isoform. This alternative splicing dramatically affects ligand-receptor binding specificity and each isoform has a distinct expression pattern (Chellaiah et al., 1994; Johnson et al., 1991; Ornitz et al., 1996; Yeh et al., 2003). The IIIb isoforms are expressed preferentially in epithelial lineages, whereas the IIIc isoforms are restricted to mesenchymal lineages (Alarid et al., 1994; Gilbert et al., 1993; Orr-Urtreger et al., 1993). Previous studies have demonstrated that each FGF has a different ability to bind to and activate the various receptor isoforms (Zhang et al., 2006).

FGF signaling initiates following binding of a ligand to heparin sulfate proteoglycan and dimerization of the receptor (Figure 1.4). Interactions between FGFs and heparin sulfate proteoglycan stabilize these ligands and are required for FGFs to effectively activate their receptors (Ornitz, 2000). Briefly, the FGF and heparin sulphate complex binds to the receptor of the tyrosine kinase class (FGFRs) and causes dimer formation. This leads to autophosphorylation of the receptor and the activation of various signal transduction cascades (Figure 1.4). FGF signaling has been implicated in a wide range of developmental functions, such as regionalization of the brain, limb outgrowth and anteroposterior patterning, as well as in tumor growth , angiogenesis, and wound healing (McKeehan et al., 1998; Ornitz and Itoh, 2001; Ornitz and Marie, 2002; Powers et al., 2000).

Vertebrate FGFs are classified into seven subgroups or subfamilies based on their sequence similarities and functional properties (Itoh and Ornitz, 2004). Functional redundancy is likely to occur because members of one subfamily share similar receptor-binding affinities. The phenotypes of mice that individually lack 16 of the family members have been reported, which began to reveal the ways in which the functions of

Figure 1.4 Fibroblast growth factor signaling and activation

Figure modified from McIntosh et al. (2000) illustrating FGF receptor structure and activation. FGF receptor extracellular domain with immunoglobulin-like domains I, II, and III is at the top left. The transmembrane domain is represented as a black box within the membrane. Fibroblast growth factor (FGF) and Heparin sulfate proteoglycan (HSPG) molecules are involved in activation. The FGF receptors are dimerized upon activation and phosphorylated at the tyrosine kinase domain, initiating signaling pathways as shown to the lower right. Molecular surface view of the dimeric FGF/FGF receptor complex with HSPG docked into the heparin-binding site is modified from Plotnikov et al. (1999) and shown to the upper right. The Ig-like domains II and III of the FGF receptor molecules are shown in green and blue, respectively. The two FGF molecules are shown in yellow.

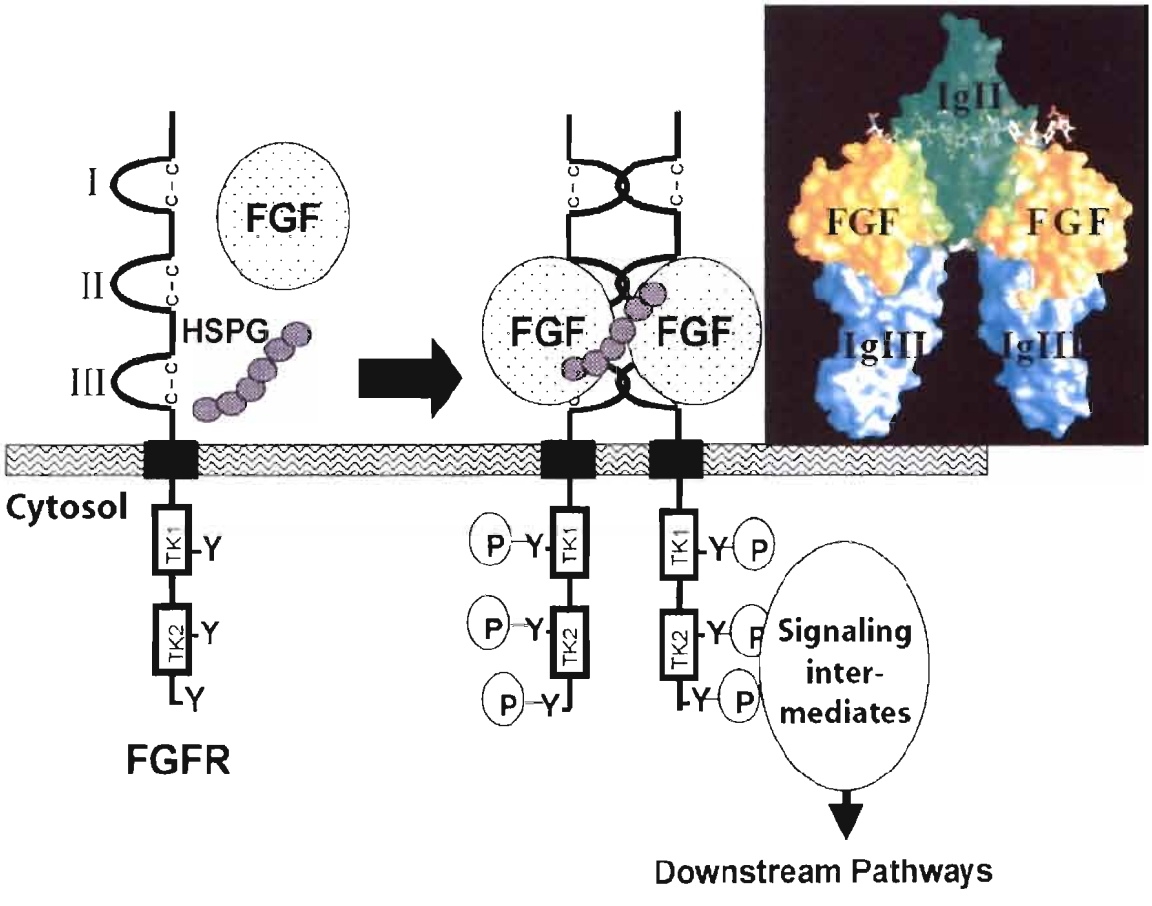
I
II
III
FGF
HSPG
FGF
FGF
IgII
FGF
FGF
IgIII
IgIII
Cytosol
TK1
TK2
Y
P
Signaling inter-mediates
FGFR
Downstream Pathways

FGFs are utilized during normal development of a wide variety of tissues and organs (for review see Itoh and Ornitz, 2004). Many *Fgf* mutant animals have phenotypes, including otic phenotypes, which are more restricted than might be predicted from the expression patterns of the gene. This could be explained, at least in part, by functional redundancy.

The FGF model

The goal of this study is to gain a better understanding of the roles of *Fgf* genes in vertebrate inner ear development. More specifically, this work describes expression patterns of the members of *Fgf* gene family and their receptors and analyzes specific roles of *Fgf3* and *Fgf16* in inner ear morphogenesis.

Expression analysis screen of 18 mouse *Fgf* and 3 *Fgf* receptor (*Fgfr*) genes during early otic development identified two novel sites of *Fgf* expression in the otic epithelium region. More specifically, *Fgf4* transcripts were expressed in the pre-placodal and placodal ectoderm, suggesting potential roles in placode induction and/or maintenance. *Fgf16* was expressed in the posterior otic cup and vesicle, suggesting roles in otic cell fate decisions and/or axis formation. In addition, all three tested members of the *Fgfr* family, *Fgfr2c*, *Fgfr3c*, and *Fgfr4* were expressed in tissues relevant to inner ear development (Wright et al., 2003). Two *Fgf* genes, *Fgf3* and *Fgf16*, were selected for in-depth study of inner ear patterning into compartments by using conventional methods of complete and tissue-specific gene inactivation by targeting, cell lineage and expression analyses.

This thesis shows that *Fgf3* is required for dorsal pattering and morphogenesis of the inner ear epithelium and provides new morphologic data on inner ear dysmorphogenesis in *Fgf3* mutants. The range of malformations observed in *Fgf3*

mutants has close parallels with those seen in hearing impaired patients. The *Fgf3* morphologic data, together with an analysis of changes in the molecular patterning of *Fgf3* mutant otic vesicles and comparisons with other mutations that affect otic morphogenesis, allow placement of *Fgf3* between hindbrain-expressed *Hoxa1* and *Mafb* (*Kreisler*) and otic vesicle-expressed *Gbx2* in the genetic cascade initiated by WNT signaling that leads to dorsal otic patterning and endolymphatic duct and sac formation. In addition, we found that *Fgf3* prevents expansion of *Wnt3a* into more ventral regions of the hindbrain, highlighting a new example of crosstalk between the two signaling systems. Furthermore, we suggest that *Fgf3* also functions, albeit largely redundantly, in the subsequent sensory patch control of non-sensory development.

Through a series of conditional mutagenesis experiments, generating chimeric embryos comprised of both wild type and *Fgf3* mutant cells, we demonstrate that conditional loss of *Fgf3* in the otic placode, the neurogenic region of the otocyst, and the hindbrain at the vesicle stages, does not influence normal inner ear development. We suggest that there is an early placode stage requirement for hindbrain-expressed *Fgf3* to induce proper development of the endolymphatic duct.

We show that *Fgf16* is one of the earliest regionally restricted transcripts expressed in otic tissue with high expression in the posterior otic cup. Germline deletion of *Fgf16* does not have an effect on inner ear morphogenesis or function. Genetic lineage analysis reveals that a significant population of *Fgf16*-expressing, otic cup derived cells is fated to migrate to anterior and posterior semicircular canals, the three ampullary cristae, and the cochlear stria vascularis.

References

Alarid, E. T., Rubin, J. S., Young, P., Chedid, M., Ron, D., Aaronson, S. A. and Cunha, G. R. (1994). Keratinocyte growth factor functions in epithelial induction during seminal vesicle development. *Proc Natl Acad Sci U S A* **91**, 1074-8.

Alvarez, Y., Alonso, M. T., Vendrell, V., Zelarayan, L. C., Chamero, P., Theil, T., Bosl, M. R., Kato, S., Maconochie, M., Riethmacher, D. et al. (2003). Requirements for FGF3 and FGF10 during inner ear formation. *Development* **130**, 6329-38.

Bok, J., Bronner-Fraser, M. and Wu, D. K. (2005). Role of the hindbrain in dorsoventral but not anteroposterior axial specification of the inner ear. *Development* **132**, 2115-24.

Brigande, J. V., Iten, L. E. and Fekete, D. M. (2000a). A fate map of chick otic cup closure reveals lineage boundaries in the dorsal otocyst. *Dev Biol* **227**, 256-70.

Brigande, J. V., Kiernan, A. E., Gao, X., Iten, L. E. and Fekete, D. M. (2000b). Molecular genetics of pattern formation in the inner ear: do compartment boundaries play a role? *Proc Natl Acad Sci U S A* **97**, 11700-6.

Chang, W., Brigande, J. V., Fekete, D. M. and Wu, D. K. (2004). The development of semicircular canals in the inner ear: role of FGFs in sensory cristae. *Development* **131**, 4201-11.

Chellaiah, A. T., McEwen, D. G., Werner, S., Xu, J. and Ornitz, D. M. (1994). Fibroblast growth factor receptor (FGFR) 3. Alternative splicing in immunoglobulin-like domain III creates a receptor highly specific for acidic FGF/FGF-1. *J Biol Chem* **269**, 11620-7.

Choo, D., Ward, J., Reece, A., Dou, H., Lin, Z. and Greinwald, J. (2006). Molecular mechanisms underlying inner ear patterning defects in kreisler mutants. *Dev Biol* **289**, 308-17.

Deng, C. X., Wynshaw-Boris, A., Shen, M. M., Daugherty, C., Ornitz, D. M. and Leder, P. (1994). Murine FGFR-1 is required for early postimplantation growth and axial organization. *Genes Dev* **8**, 3045-57.

Eswarakumar, V. P., Monsonego-Ornan, E., Pines, M., Antonopoulou, I., Morriss-Kay, G. M. and Lonai, P. (2002). The IIIc alternative of Fgfr2 is a positive regulator of bone formation. *Development* **129**, 3783-93.

Fekete, D. M. (1999). Development of the vertebrate ear: insights from knochouts and mutants. *Trends Neusoscience* **22**, 263-269.

Fekete, D. M. and Wu, D. K. (2002). Revisiting cell fate specification in the inner ear. *Curr Opin Neurobiol* **12**, 35-42.

Fritzsch, B., Pauley, S. and Beisel, K. W. (2006). Cells, molecules and morphogenesis: the making of the vertebrate ear. *Brain Res* **1091**, 151-71.

Gilbert, E., Del Gatto, F., Champion-Arnaud, P., Gesnel, M. C. and Breathnach, R. (1993). Control of BEK and K-SAM splice sites in alternative splicing of the fibroblast growth factor receptor 2 pre-mRNA. *Mol Cell Biol* **13**, 5461-8.

Hutson, M. R., Lewis, J. E., Nguyen-Luu, D., Lindberg, K. H. and Barald, K. F. (1999). Expression of Pax2 and patterning of the chick inner ear. *J Neurocytol* **28**, 795-807.

Itoh, N. and Ornitz, D. M. (2004). Evolution of the Fgf and Fgfr gene families. *Trends Genet* **20**, 563-9.

Johnson, D. E., Lu, J., Chen, H., Werner, S. and Williams, L. T. (1991). The human fibroblast growth factor receptor genes: a common structural arrangement underlies the mechanisms for generating receptor forms that differ in their third immunoglobulin domain. *Mol Cell Biol* **11**, 4627-34.

Kiernan, A. E., Steel, K. P. and Fekete, D. M. (2002). Development of the Mouse Inner Ear. Orlando, FL: Academic Press.

Ladher, R. K., Anakwe, K. U., Gurney, A. L., Schoenwolf, G. C. and Francis-West, P. H. (2000). Identification of synergistic signals initiating inner ear development. *Science* **290**, 1965-7.

Ladher, R. K., Wright, T. J., Moon, A. M., Mansour, S. L. and Schoenwolf, G. C. (2005). FGF8 initiates inner ear induction in chick and mouse. *Genes Dev* **19**, 603-13.

Leger, S. and Brand, M. (2002). Fgf8 and Fgf3 are required for zebrafish ear placode induction, maintenance and inner ear patterning. *Mech Dev* **119**, 91-108.

Li, C. W., Van De Water, T. R. and Ruben, R. J. (1978). The fate mapping of the eleventh and twelfth day mouse otocyst: an in vitro study of the sites of origin of the embryonic inner ear sensory structures. *J Morphol* **157**, 249-67.

Mafong, D. D., Shin, E. J. and Lalwani, A. K. (2002). Use of laboratory evaluation and radiologic imaging in the diagnostic evaluation of children with sensorineural hearing loss. *Laryngoscope* **112**, 1-7.

Mahmood, R., Mason, I. J. and Morriss-Kay, G. M. (1996). Expression of Fgf-3 in relation to hindbrain segmentation, otic pit position and pharyngeal arch morphology in normal and retinoic acid-exposed mouse embryos. *Anat Embryol (Berl)* **194**, 13-22.

Mansour, S. L., Goddard, J. M. and Capecchi, M. R. (1993). Mice homozygous for a targeted disruption of the proto-oncogene int-2 have developmental defects in the tail and inner ear. *Development* **117**, 13-28.

Mansour, S. L. and Schoenwolf, G. C. (2005). Morphogenesis of the inner ear. In *Development of the Inner Ear*, vol. 26 (ed. M. W. Kelley D. K. Wu A. N. Popper and R. R. Fay), pp. 43-84. New York: Springer-Verlag.

Maroon, H., Walshe, J., Mahmood, R., Kiefer, P., Dickson, C. and Mason, I. (2002). Fgf3 and Fgf8 are required together for formation of the otic placode and vesicle. *Development* **129**, 2099-108.

McIntosh, I., Bellus, G. A. and Jab, E. W. (2000). The pleiotropic effects of fibroblast growth factor receptors in mammalian development. *Cell Struct Funct* **25**, 85-96.

McKay, I. J., Lewis, J. and Lumsden, A. (1996). The role of FGF-3 in early inner ear development: an analysis in normal and kreisler mutant mice. *Dev Biol* **174**, 370-8.

McKeehan, W. L., Wang, F. and Kan, M. (1998). The heparan sulfate-fibroblast growth factor family: diversity of structure and function. *Prog Nucleic Acid Res Mol Biol* **59**, 135-76.

Morsli, H., Choo, D., Ryan, A., Johnson, R. and Wu, D. K. (1998). Development of the mouse inner ear and origin of its sensory organs. *J Neurosci* **18**, 3327-35.

Morton, C. C. and Nance, W. E. (2006). Newborn hearing screening--a silent revolution. *N Engl J Med* **354**, 2151-64.

Mueller, K. L., Jacques, B. E. and Kelley, M. W. (2002). Fibroblast growth factor signaling regulates pillar cell development in the organ of corti. *J Neurosci* **22**, 9368-77.

Ohuchi, H., Yasue, A., Ono, K., Sasaoka, S., Tomonari, S., Takagi, A., Itakura, M., Moriyama, K., Noji, S. and Nohno, T. (2005). Identification of cis-element regulating expression of the mouse Fgf10 gene during inner ear development. *Dev Dyn* **233**, 177-87.

Ohyama, T., Mohamed, O. A., Taketo, M. M., Dufort, D. and Groves, A. K. (2006). Wnt signals mediate a fate decision between otic placode and epidermis. *Development* **133**, 865-75.

Ornitz, D. M. (2000). FGFs, heparan sulfate and FGFRs: complex interactions essential for development. *Bioessays* **22**, 108-12.

Ornitz, D. M. and Itoh, N. (2001). Fibroblast growth factors. *Genome Biol* **2**, REVIEWS3005.

Ornitz, D. M. and Marie, P. J. (2002). FGF signaling pathways in endochondral and intramembranous bone development and human genetic disease. *Genes Dev* **16**, 1446-65.

Ornitz, D. M., Xu, J., Colvin, J. S., McEwen, D. G., MacArthur, C. A., Coulier, F., Gao, G. and Goldfarb, M. (1996). Receptor specificity of the fibroblast growth factor family. *J Biol Chem* **271**, 15292-7.

Orr-Urtreger, A., Bedford, M. T., Burakova, T., Arman, E., Zimmer, Y., Yayon, A., Givol, D. and Lonai, P. (1993). Developmental localization of the splicing alternatives of fibroblast growth factor receptor-2 (FGFR2). *Dev Biol* **158**, 475-86.

Partanen, J., Schwartz, L. and Rossant, J. (1998). Opposite phenotypes of hypomorphic and Y766 phosphorylation site mutations reveal a function for Fgfr1 in anteroposterior patterning of mouse embryos. *Genes Dev* **12**, 2332-44.

Pasqualetti, M., Neun, R., Davenne, M. and Rijli, F. M. (2001). Retinoic acid rescues inner ear defects in Hoxa1 deficient mice. *Nat Genet* **29**, 34-9.

Pauley, S., Wright, T. J., Pirvola, U., Ornitz, D., Beisel, K. and Fritzsch, B. (2003). Expression and function of FGF10 in mammalian inner ear development. *Dev Dyn* **227**, 203-15.

Phillips, B. T., Bolding, K. and Riley, B. B. (2001). Zebrafish fgf3 and fgf8 encode redundant functions required for otic placode induction. *Dev Biol* **235**, 351-65.

Pirvola, U., Spencer-Dene, B., Xing-Qun, L., Kettunen, P., Thesleff, I., Fritzsch, B., Dickson, C. and Ylikoski, J. (2000). FGF/FGFR-2(IIIb) signaling is essential for inner ear morphogenesis. *J Neurosci* **20**, 6125-34.

Plotnikov, A. N., Schlessinger, J., Hubbard, S. R. and Mohammadi, M. (1999). Structural basis for FGF receptor dimerization and activation. *Cell* **98**, 641-50.

Powers, C. J., McLeskey, S. W. and Wellstein, A. (2000). Fibroblast growth factors, their receptors and signaling. *Endocr Relat Cancer* **7**, 165-97.

Riccomagno, M. M., Takada, S. and Epstein, D. J. (2005). Wnt-dependent regulation of inner ear morphogenesis is balanced by the opposing and supporting roles of Shh. *Genes Dev* **19**, 1612-23.

Rinkwitz, S., Bober, E. and Baker, R. (2001). Development of the vertebrate inner ear. *Ann N Y Acad Sci* **942**, 1-14.

Rivolta, M. N. (1997). Transcription factors in the ear: molecular switches for development and differentiation. *Audiol Neurootol* **2**, 36-49.

Torres, M. and Giraldez, F. (1998). The development of the vertebrate inner ear. *Mech Dev* **71**, 5-21.

Vendrell, V., Carnicero, E., Giraldez, F., Alonso, M. T. and Schimmang, T. (2000). Induction of inner ear fate by FGF3. *Development* **127**, 2011-9.

Wilkinson, D. G., Peters, G., Dickson, C. and McMahon, A. P. (1988). Expression of the FGF-related proto-oncogene int-2 during gastrulation and neurulation in the mouse. *Embo J* **7**, 691-5.

Wright, T. J., Hatch, E. P., Karabagli, H., Karabagli, P., Schoenwolf, G. C. and Mansour, S. L. (2003). Expression of mouse fibroblast growth factor and fibroblast growth factor receptor genes during early inner ear development. *Dev Dyn* **228**, 267-72.

Wright, T. J. and Mansour, S. L. (2003). Fgf3 and Fgf10 are required for mouse otic placode induction. *Development* **130**, 3379-90.

Wu, C. C., Chen, Y. S., Chen, P. J. and Hsu, C. J. (2005). Common clinical features of children with enlarged vestibular aqueduct and Mondini dysplasia. *Laryngoscope* **115**, 132-7.

Wu, D. K., Nunes, F. D. and Choo, D. (1998). Axial specification for sensory organs versus non-sensory structures of the chicken inner ear. *Development* **125**, 11-20.

Yamaguchi, T. P., Harpal, K., Henkemeyer, M. and Rossant, J. (1994). fgfr-1 is required for embryonic growth and mesodermal patterning during mouse gastrulation. *Genes Dev* **8**, 3032-44.

Yeh, B. K., Igarashi, M., Eliseenkova, A. V., Plotnikov, A. N., Sher, I., Ron, D., Aaronson, S. A. and Mohammadi, M. (2003). Structural basis by which alternative splicing confers specificity in fibroblast growth factor receptors. *Proc Natl Acad Sci U S A* **100**, 2266-71.

Yu, C., Wang, F., Kan, M., Jin, C., Jones, R. B., Weinstein, M., Deng, C. X. and McKeehan, W. L. (2000). Elevated cholesterol metabolism and bile acid synthesis in mice lacking membrane tyrosine kinase receptor FGFR4. *J Biol Chem* **275**, 15482-9.

Zhang, X., Ibrahimi, O. A., Olsen, S. K., Umemori, H., Mohammadi, M. and Ornitz, D. M. (2006). Receptor specificity of the fibroblast growth factor family. The complete mammalian FGF family. *J Biol Chem* **281**, 15694-700.

CHAPTER 2

EXPRESSION PATTERNS OF FIBROBLAST GROWTH FACTORS AND FIBROBLAST GROWTH FACTOR RECEPTORS DURING EARLY INNER EAR DEVELOPMENT

Abstract

The inner ear, which mediates hearing and equilibrium, develops from an ectodermal placode located adjacent to the developing hindbrain. Induction of the placode and its subsequent morphogenesis and differentiation into the inner ear epithelium and its sensory neurons, involves signaling interactions within and between otic and non-otic tissues. Several members of the fibroblast growth factor (FGF) family play important roles at various stages of otic development; however, there are additional family members that have not been evaluated. In this study, we surveyed the expression patterns of 18 mouse *Fgf* and 3 *Fgf* receptor (*Fgfr*) genes during early otic development. Two members of the *Fgf* family, *Fgf4* and *Fgf16*, and all three tested members of the *Fgfr* family, *Fgfr2c*, *Fgfr3c*, and *Fgfr4*, were expressed in tissues relevant to inner ear development. *Fgf4* transcripts were expressed in the preplacodal and placodal ectoderm, suggesting potential roles in placode induction and/or maintenance. *Fgf16* was expressed in the posterior otic cup and vesicle, suggesting roles in otic cell fate decisions and/or axis formation.

Introduction

The inner ear, which mediates the sensations of hearing and equilibrium, develops from an ectodermal placode that is located adjacent to the developing hindbrain. Placodal ectoderm becomes committed to an otic fate after receiving inductive signals from the adjacent neurectoderm and underlying mesenchyme. In mouse embryos, the first morphologic evidence of otic placode induction occurs at the 7- to 8-somite stages (embryonic day (E) 8.5), when the committed ectoderm lateral to rhombomeres (r) 5 and 6 thickens. Subsequently, during the 13- to 20-somite stages (E9.0), the placode invaginates to form a cup. During this stage, the otic epithelium delaminates neuroblasts that will ultimately aggregate and differentiate to form the neurons of the eighth (cochleovestibular) ganglion. By the time the embryo has 21–29 somites (E9.5), the cup closes to form a roughly spherical vesicle known as the otocyst or otic vesicle. At E10.5, morphogenesis of the vesicle initiates with the dorsomedial protrusion of the precursor of the endolymphatic duct. During subsequent days, the vesicle undergoes a very complex morphogenesis to elaborate the auditory and vestibular compartments and also embarks on the process of differentiating the numerous sensory and nonsensory cell types found in the mature inner ear (Baker and Bronner-Fraser, 2001; Groves and Bronner-Fraser, 2000; Kiernan et al., 2002; Torres and Giraldez, 1998). Several families of intercellular signaling molecules, including the fibroblast growth factor (FGF) family are involved in induction, morphogenesis, and differentiation of the otic epithelium (Wright and Mansour, 2003b).

The *Fgfs* comprise a 22-member gene family encoding secreted, heparan sulfate-binding proteins that signal through a family of tyrosine kinase receptors, the fibroblast

growth factor receptors (FGFRs), which are encoded by four genes. *Fgfr1*, *-2*, and *-3* mRNAs are alternatively spliced within the region encoding the third extracellular immunoglobulin- like domain, resulting in the production of IIIb and IIIc isoforms of these receptors. *Fgfr4* produces only the IIIc-type isoform. The alternative splicing is regulated in a tissue-specific manner and affects ligand binding specificity and affinity. FGF signaling plays numerous roles during development, including regulation of cell proliferation, migration, differentiation, and survival (Ornitz and Itoh, 2001).

Gain of-function and loss-of-function studies implicate four members of the *Fgf* family, *Fgf3*, *Fgf8*, *Fgf10*, and *Fgf19*, in a variety of stages of otic development in different species (Ladher et al., 2000; Leger and Brand, 2002; Mansour et al., 1993; Maroon et al., 2002; Pauley et al., 2003; Phillips et al., 2001; Vendrell et al., 2000; Wright and Mansour, 2003a). There is also genetic evidence for transmission of FGF signals needed for several phases of otic development through FGFR1, FGFR3 (isoforms not established), and FGFR2b (Deng et al., 1994; Eswarakumar et al., 2002; Mueller et al., 2002; Partanen et al., 1998; Pirvola et al., 2000; Yamaguchi et al., 1994; Yu et al., 2000). In addition, expression profiles have been generated for some *Fgfr* family members during otic development (Orr-Urtreger et al., 1993; Orr-Urtreger et al., 1991; Peters et al., 1993; Peters et al., 1992; Pickles, 2001; Pirvola et al., 2000; Wright and Mansour, 2003a; Yamaguchi et al., 1992). Although these data suggest roles for *Fgfr1*, *Fgfr2*, and *Fgfr3* during otic vesicle morphogenesis and differentiation, little is known about the function of the *Fgfr* isoforms during the early phases of otic induction and vesicle formation.

To determine whether there are other members of the mouse *Fgf* and *Fgfr* families that could participate in early otic development, we evaluated the expression patterns of 18 members of the *Fgf* family, as well as three members of the *Fgfr* family, at four time points during early otic development, spanning the preplacode to vesicle stages. Two members of the *Fgf* family, *Fgf4* and *Fgf16*, and three members of the *Fgfr* family, *Fgfr2c*, *Fgfr3c*, and *Fgfr4*, were expressed in tissues relevant to inner ear development. *Fgf4* was expressed in the preplacodal and placodal ectoderm and *Fgf16* was expressed asymmetrically in the otic cup and vesicle. *Fgfr2c* was expressed in the neurectoderm that lies medial to the otic region throughout early otic development. *Fgfr4* was expressed in a similar pattern but transcripts could be detected only during preplacodal and placodal stages. Temporally, the expression of *Fgfr3c* overlapped with *Fgfr2c*, but *Fgfr3c* was localized to the otic cup and vesicle and was not found in the neurectoderm. These patterns of gene expression suggest that there could be additional roles for FGF signaling during the early phases of otic development.

Results

Expression analysis of *Fgf* and *Fgfr* family members during early otic development

To determine whether any *Fgfs* and *Fgfrs* in addition to those previously determined could play early roles in otic development in the mouse, we examined the normal expression patterns of 18 members of the *Fgf* family (*Fgfs 1*, *2*, *4*, *5*, *6*, *7*, *9*, *11*, *12*, *13*, *14*, *16*, *17*, *18*, *20*, *21*, *22*, and *23*) and 3 members of the *Fgfr* family (*Fgfr2c*, *3c*, and *4*) by whole-mount in situ hybridization at four stages of development. These stages encompassed the early events in otic development that culminate in formation of the otic

vesicle and included preplacodal ectoderm (E8.0, 4-6 somites), otic placode (E 8.5, 7-10 somites), otic cup (E9.0, 11-19 somites), and otic vesicle (E9.5, >20 somites). Of the 18 *Fgfs* examined, two family members, *Fgf4* and *Fgf16*, were expressed in patterns relevant to the early development of the ear. We also detected expression of *Fgfr2c*, *Fgfr3c*, and *Fgfr4*.

Fgf4 is expressed in preplacodal and placodal otic ectoderm

As expected, *Fgf4* transcripts were detected in the remnants of the primitive streak at the four-somite stage. In addition, *Fgf4* was also expressed in a patch of surface ectoderm in these embryos (Figure 2.1A, B)(Drucker and Goldfarb, 1993; Niswander and Martin, 1992). To determine whether this region of the ectoderm was likely to encompass the presumptive otic placode, we compared its location with that of *MafB* (*kreisler*) transcripts by simultaneous hybridization of *Fgf4* and *MafB* probes. *MafB* is expressed in r5 and r6 (Cordes and Barsh, 1994) and the otic placode forms lateral to this region (Figure 2.1C)(Groves and Bronner-Fraser, 2000). Observation of whole mount embryos and coronal sections taken through eight-somite embryos hybridized with both *Fgf4* and *MafB* probes showed that both genes had the same anterior and posterior expression boundaries, suggesting that *Fgf4* is expressed in preplacodal otic ectoderm (Figure 2.1D). This observation was confirmed by hybridizing an eight-somite embryo with *Fgf4* (Figure 2.1E), followed by staining with an antibody directed against PAX2, which is expressed in the otic placode. Colocalization of *Fgf4* and PAX2 in the ectoderm confirmed that *Fgf4* is expressed in the otic placode (Figure 2.1F). In embryos with nine somites, *Fgf4* transcripts were still detected in the otic placode and were also detected in

the pharyngeal endoderm (Figure 2.1G, H). *Fgf4* transcripts were not detected in otic tissue at the 11-somite and older stages but could be seen in the pharyngeal endoderm and tail bud as previously described (Niswander and Martin, 1992).

Fgf16 is expressed asymmetrically in the otic cup and vesicle

Otic expression of *Fgf16* was initially detected very weakly throughout the thickened placode at the 10-somite stage, just before invagination of the placode (Figure 2.1I, J). By 13 somites, *Fgf16* transcripts were more strongly expressed and localized to the posterior region of the invaginating otic cup (Figure 2.1K, L). At this stage, *Fgf16* transcripts were also detected in the pharyngeal endoderm, branchial arches, and the olfactory placode (Figure 2.1K). At 19 somites, *Fgf16* transcripts were still detected in the posterior otic cup but they were no longer found in the branchial arches and pharyngeal endoderm (Figure 2.1M, N). By 24 somites, the otic cup had closed to form an otic vesicle and *Fgf16* continued to be expressed in the dorsolateral wall of the posterior half of the vesicle (Figure 2.1O, P).

Expression of *Fgfr2c*, *Fgfr3c*, and *Fgfr4* during early otic development

If *Fgf4* and *Fgf16* participate in otic development, genes encoding the appropriate receptors should be expressed in the same or in adjacent tissues. FGF4 activates mitogenic signalling through all of the IIIc isoforms of the FGF receptors (Ornitz et al., 1996). Directly comparable studies are not available for FGF16, but this ligand activates proliferation of embryonic brown adipocytes, which express *Fgfr1c*, *Fgfr2c*, and *Fgfr4* and it binds in vitro to FGFR4 but not to FGFR1c or FGFR2c, suggesting that FGFR4

Figure 2.1 *Fgf4* is expressed in the preplacodal and placodal otic ectoderm and *Fgf16* is expressed asymmetrically in the otic cup and vesicle

Whole-mount 4-somite (A), 8-somite (C,E), 9-somite (G), 10-somite (I), 13-somite (K), 19-somite (M), and 24-somite (O) embryos were probed with labeled antisense cDNA for *Fgf4* (A,E,G), *Fgf4* and *MafB/kreisler* (C), or *Fgf16* (I,K,M,O). Rostral is to the left (A,C,E,G) or right (I,K,MO). Lines indicate the plane of transverse (B,F,H,J,L,P) or coronal (N) sections shown in adjacent panels. The section in D was cut horizontally through the *Fgf4*-expressing otic region shown in C. The section shown in F is taken from an 8-somite embryo that was hybridized first with the *Fgf4* probe (not shown) and then subsequently subjected to immunohistochemistry with anti-PAX2 (brown). Op, preplacodal or placodal otic ectoderm; oc, otic cup; ov, otic vesicle; nf, neural folds; nt, neural tube; pe, pharyngeal endoderm; ba, branchial arch; olp, olfactory placode.

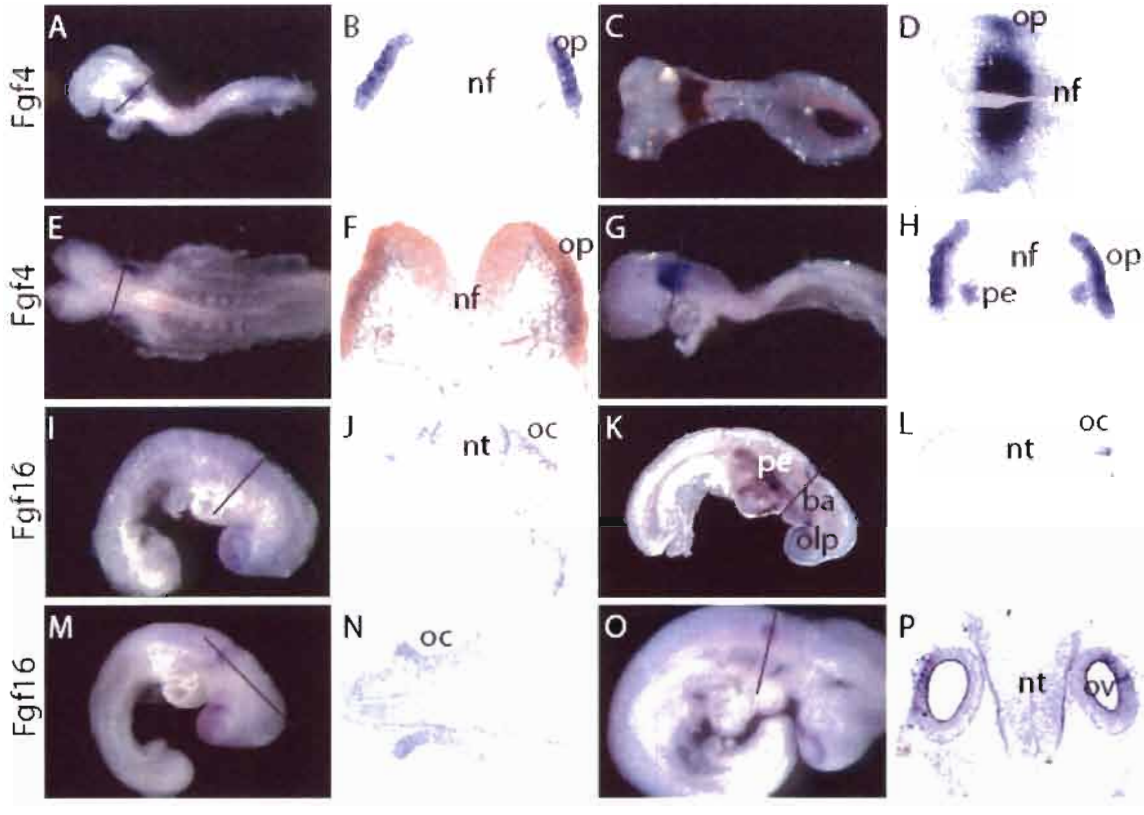
Fgf4
Fgf4
Fgf16
Fgf16
A
B
op
nf
C
D
op
nf
E
F
op
nf
G
H
nf
op
pe
I
J
nt
oc
K
pe
ba
olp
L
oc
nt
M
N
oc
O
P
nt
ov

can act as a receptor for FGF16 (Konishi et al., 2000). Previous studies have shown that at preplacodal and placodal stages, *Fgfr1* transcripts (IIIb and IIIc isoforms not distinguished) are present in the neurectoderm and at E9.5 *Fgfr1* is localized to the hindbrain and to the mesenchyme surrounding the otic vesicle (Pirvola et al., 2002; Wright and Mansour, 2003b; Yamaguchi et al., 1992). We, therefore, examined expression of *Fgfr2c*, *Fgfr3c*, and *Fgfr4* in preplacodal to otic vesicle stages.

Fgfr2c is expressed in the neurectoderm throughout early otic development

Fgfr2c transcripts were not found in the otic tissue itself, but were present in the adjacent neurectoderm medial to the preplacodal otic ectoderm at three somites (Figure 2.2A, B). This expression persisted through otic placode, cup, and vesicle stages (Figure 2.2C-H). By E9.5, *Fgfr2c* transcripts were also detected in the branchial arch mesenchyme, the forelimb bud, and nephrogenic cords as previously observed (Figure 2.2G, H)(Orr-Urtreger et al., 1993).

Fgfr3 is expressed in the otic cup and vesicle

Expression of *Fgfr3c* was not detected in otic tissue until the cup stage. At 19 somites, *Fgfr3c* transcripts were detected throughout the otic cup (Figure 2.2I, J). Expression persisted throughout the otic epithelium as the cup closed to form a vesicle, as seen in a 21-somite embryo (Figure 2.2K, L). *Fgfr3c* expression was also detected in the tail bud, first branchial arch, and optic cup (Figure 2.2I, K).

Fgfr4 is expressed in the neurectoderm during preplacodal and placodal otic development

Just before somite formation, *Fgfr4* was detected in the neurectoderm, extraembryonic endoderm, and caudal lateral plate (Figure 2.2M, N). Expression in the neurectoderm persisted until the otic placode stage at eight somites (Figure 2.2O, P). By 16 somites, when the otic cup had invaginated, expression of *Fgfr4* in the neurectoderm was no longer detected (Figure 2.2Q, R). At this stage, *Fgfr4* transcripts were seen in the rostral somites and hindgut as previously described (Figure 2.2Q; Stark et al., 1991).

Discussion

The identification of five genes, two encoding FGF ligands and three encoding FGF receptors, which were not known previously to be expressed in tissues that are relevant to early otic development, suggests that there may be additional roles for FGF signaling at these stages. *Fgf4* is expressed in the preplacodal and placodal otic ectoderm, coinciding with the PAX2 expression domain. FGF4 signals through the IIIc isoforms of the FGF receptors (Ornitz et al., 1996). We and others have demonstrated *Fgfr1*, *Fgfr2c*, and *Fgfr4* expression in the neurectoderm during preplacodal and placodal stages (Stark et al., 1991; Wright and Mansour, 2003a; Yamaguchi et al., 1992). Therefore, one possible role of FGF4 may be to signal in a paracrine manner to the neurectoderm. A second possibility is that one of the IIIc receptor isoforms is expressed at low levels in the mesenchyme underlying the placode or in the placode itself and that in situ hybridization is not sensitive enough to detect these levels. If this is the case, then FGF4 could signal in a paracrine manner to the mesenchyme or in an autocrine manner to the placode.

If *Fgf4* is signaling to the hindbrain (or even to the mesenchyme) through any of

Figure 2.2 *Fgfr2c* and *Fgfr4* are expressed in the neurectoderm that lies medial to the otic ectoderm, and *Fgfr3c* is expressed in the otic cup and otic vesicle

Whole-mount 3-somite (A), 8-somite (C), E 9 (E), E 9.5 (G), 19-somite (I), 21-somite (K), 0-somite (M), 8-somite (O), and 16-somite (Q) embryos were probed with labeled antisense cDNA for *Fgfr2c* (A,C,E,G), *Fgfr3c* (I,K), or *Fgfr4* (M,O,Q). Rostral is to the left. Lines indicate the plane of transverse sections shown in adjacent panels (B,D,F,H,J,L,N,P,R). nf, neural folds; nt, neural tube; op, preplacodal and placodal otic ectoderm; oc, otic cup; ov, otic vesicle; ba, branchial arch; e, extraembryonic ectoderm; lp, caudal lateral plate.

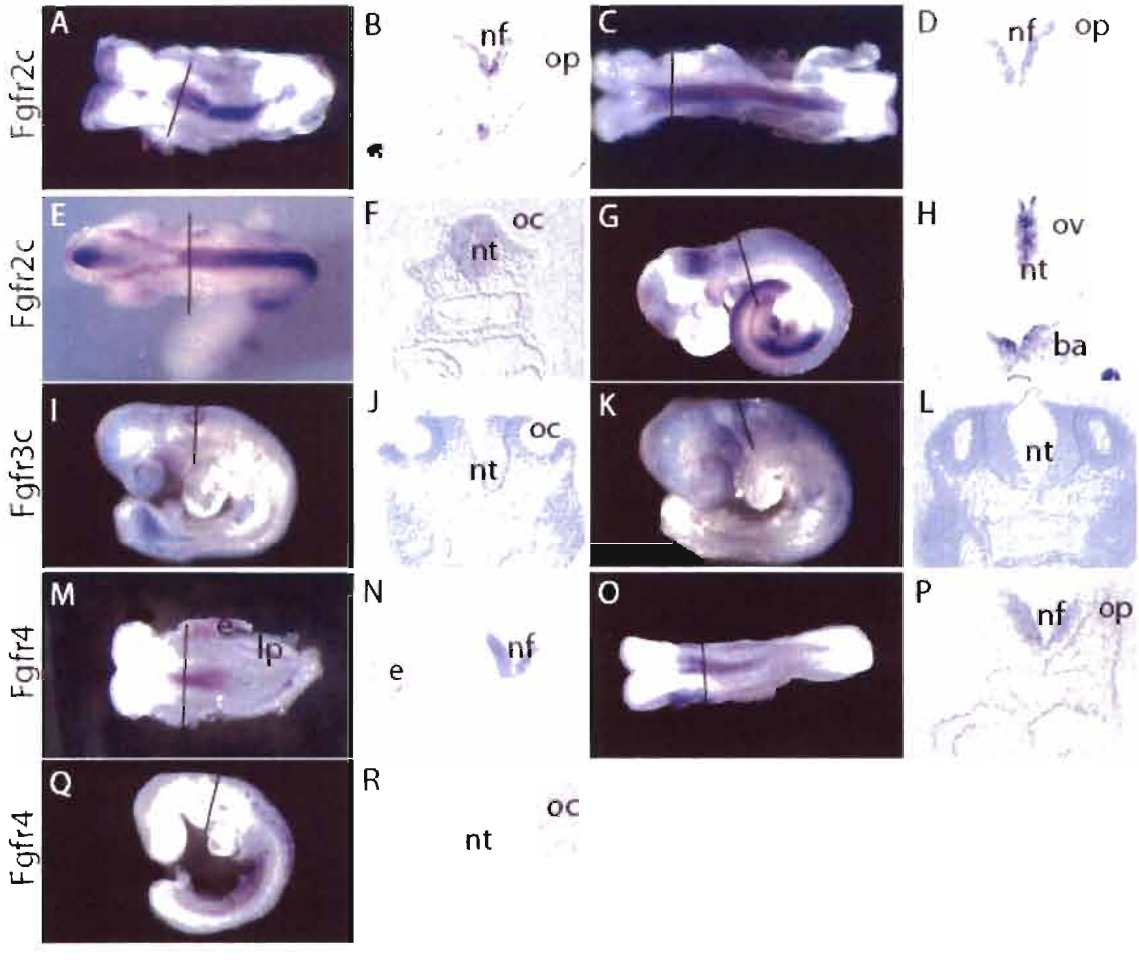
Fgfr2c
Fgfr2c
Fgfr3c
Fgfr4
Fgfr4
A
B
nf
op
C
D
nf
op
E
F
oc
nt
G
H
ov
nt
ba
I
J
oc
nt
K
L
nt
M
e
lp
N
nf
e
O
P
nf
op
Q
R
oc
nt

its receptors, how might this affect otic development? The hindbrain and mesenchyme are sources of otic-inducing signals, including FGF3 and FGF10, respectively (Wright and Mansour, 2003a), so an FGF4 signal from the placode could be used to activate or maintain expression of otic-inducing factors. Similarly, if FGF4 signals in an autocrine manner to the placode, it may regulate or maintain the placodal response to otic induction. As *Fgf4* null mutants are peri-implantation lethal (Feldman et al., 1995), conditional loss-of-function studies will be needed to address these issues.

Fgf16 is initially expressed throughout the invaginating otic placode before becoming localized to the posterior otic cup. Subsequently, *Fgf16* transcripts are detected in the dorsolateral wall of the otic vesicle. Receptor binding studies have shown that FGFR4 but not FGFR1c or FGFR2c can serve as a receptor for FGF16 (Konishi et al., 2000). The potential for binding of FGF16 to FGFR3c was not tested in this study; however, given that FGF9, which is one of the FGFs most closely related to FGF16, activates FGFR3c, it would not be surprising if the same were true for FGF16 (Kim, 2001; Ornitz et al., 1996). Our expression analysis, moreover, shows that *Fgfr3c* is localized appropriately to serve as an FGF16 receptor. *Fgfr3c* is expressed throughout the otic cup and vesicle; therefore, *Fgf16* could signal through *Fgfr3c* in either an autocrine or paracrine manner.

The expression pattern of *Fgf16* suggests possible roles in otic cell fate decisions and/or axis formation. Fate maps generated by injecting chick otic cup with vital dyes suggest that there is an anterior to posterior lineage boundary dividing the endolymphatic duct that is in place by the otic cup stage. Thus, cells in the dorsal posterior portion of the cup give rise to the posterior part of the endolymphatic duct. Cells from more ventral

regions of the posterior cup can adopt a variety of generally posterior fates (Brigande et al., 2000). Similar studies in the frog, however, do not support the existence of the developmental boundaries seen in the chick (Kil and Collazo, 2002). Fate maps of the mouse otocyst lineages have not been produced. As *Fgf16* is one of the earliest regionally restricted transcripts identified in otic tissue to date and is the only transcript known so far to be polarized along the anteroposterior axis of the otic cup, it should be possible to exploit this finding to determine the fate of mouse posterior otic cup cells. Furthermore, targeted mutagenesis of *Fgf16* will show whether it plays a role in specifying particular otic cell fates. Another possible role for *Fgf16* could be to participate in otic axis formation. The anteroposterior otic axis is established before the dorsoventral axis, and in chick, this development occurs at the otic cup stage (Wu et al., 1998). Equivalent information is not available for the mouse. It will be very interesting, therefore, to observe the orientation of otic structures in *Fgf16* null mutants.

Materials and methods

In situ hybridization

Expression patterns of *Fgf* and *Fgfr* genes were determined by using embryos generated by mating wild type CD-1 mice (Charles River Laboratories). Embryos were isolated on the indicated days after detection of a vaginal plug. Digoxigenin-labelled RNA probes were prepared, hybridized to the embryos, and detected as described (Henrique et al., 1995). cDNAs used to prepare probes for *Fgfr2IgIIIc* (accession no. NM010207, bp1599-1737)(Kettunen et al., 1998), *Fgfr3IgIIIc* (accession no. L26492, bp1998-2125)(Kettunen et al., 1998), *Fgf4* (probe contained exon 3 and 3'UTR sequences, accession nos. NM010202, U43515)(Moon et al., 2000), and *Fgf16* (accession

no. NM030614)(Miyake et al., 1998) have been described previously. The *Fgfr4* probe contained 700 bp from the 3'untranslated region (mFgfr4, accession no. XM193720, bp2697-3291). An antisense probe was generated by digestion with *Xho*I, followed by transcription with T7 RNA polymerase.

Immunohistochemistry

After whole-mount in situ hybridization with the *Fgf4* antisense probe, embryos were fixed in 4% paraformaldehyde/ phosphate buffered saline. For whole-mount immunohistochemical detection of PAX2, polyclonal antibodies (Covance), kindly provided by Drs. D. Wellik and M. Capecchi, were used at a 1:62 dilution. The protocol for fixation of the embryos and application and detection of the primary antibodies with horseradish peroxidase–labeled secondary antibodies and diaminobenzidine staining was carried out as described previously for phosphorylated histone H3 antibodies (Gavalas et al., 2001).

Cryosectioning

Embryos stained for analysis of gene expression were cryoprotected in sucrose and sectioned at 14 μm by using a Leica cryostat as described (Stark et al., 2000).

Photography

Whole embryos were photographed by using a Zeiss SV-11 dissecting microscope fitted with a digital camera (Kodak MDS120 or 240). Sections were photographed by using a Zeiss Axioscop fitted with DIC optics and a digital camera (AxioCam).

References

Baker, C. V. and Bronner-Fraser, M. (2001). Vertebrate cranial placodes I. Embryonic induction. *Dev Biol* **232**, 1-61.

Brigande, J. V., Iten, L. E. and Fekete, D. M. (2000). A fate map of chick otic cup closure reveals lineage boundaries in the dorsal otocyst. *Dev Biol* **227**, 256-70.

Cordes, S. P. and Barsh, G. S. (1994). The mouse segmentation gene kr encodes a novel basic domain-leucine zipper transcription factor. *Cell* **79**, 1025-34.

Deng, C. X., Wynshaw-Boris, A., Shen, M. M., Daugherty, C., Ornitz, D. M. and Leder, P. (1994). Murine FGFR-1 is required for early postimplantation growth and axial organization. *Genes Dev* **8**, 3045-57.

Drucker, B. J. and Goldfarb, M. (1993). Murine FGF-4 gene expression is spatially restricted within embryonic skeletal muscle and other tissues. *Mech Dev* **40**, 155-63.

Eswarakumar, V. P., Monsonego-Ornan, E., Pines, M., Antonopoulou, I., Morriss-Kay, G. M. and Lonai, P. (2002). The IIIc alternative of Fgfr2 is a positive regulator of bone formation. *Development* **129**, 3783-93.

Feldman, B., Poueymirou, W., Papaioannou, V. E., DeChiara, T. M. and Goldfarb, M. (1995). Requirement of FGF-4 for postimplantation mouse development. *Science* **267**, 246-9.

Gavalas, A., Trainor, P., Ariza-McNaughton, L. and Krumlauf, R. (2001). Synergy between Hoxa1 and Hoxb1: the relationship between arch patterning and the generation of cranial neural crest. *Development* **128**, 3017-27.

Groves, A. K. and Bronner-Fraser, M. (2000). Competence, specification and commitment in otic placode induction. *Development* **127**, 3489-99.

Henrique, D., Adam, J., Myat, A., Chitnis, A., Lewis, J. and Ish-Horowicz, D. (1995). Expression of a Delta homologue in prospective neurons in the chick. *Nature* **375**, 787-90.

Kettunen, P., Karavanova, I. and Thesleff, I. (1998). Responsiveness of developing dental tissues to fibroblast growth factors: expression of splicing alternatives of FGFR1, -2, -3, and of FGFR4; and stimulation of cell proliferation by FGF-2, -4, -8, and -9. *Dev Genet* **22**, 374-85.

Kiernan, A. E., Steel, K. P. and Fekete, D. M. (2002). Development of the Mouse Inner Ear. Orlando, FL: Academic Press.

Kil, S. H. and Collazo, A. (2002). A review of inner ear fate maps and cell lineage studies. *J Neurobiol* **53**, 129-42.

Kim, H. S. (2001). The human FGF gene family: chromosome location and phylogenetic analysis. *Cytogenet Cell Genet* **93**, 131-2.

Konishi, M., Mikami, T., Yamasaki, M., Miyake, A. and Itoh, N. (2000). Fibroblast growth factor-16 is a growth factor for embryonic brown adipocytes. *J Biol Chem* **275**, 12119-22.

Ladher, R. K., Anakwe, K. U., Gurney, A. L., Schoenwolf, G. C. and Francis-West, P. H. (2000). Identification of synergistic signals initiating inner ear development. *Science* **290**, 1965-7.

Leger, S. and Brand, M. (2002). Fgf8 and Fgf3 are required for zebrafish ear placode induction, maintenance and inner ear patterning. *Mech Dev* **119**, 91-108.

Mansour, S. L., Goddard, J. M. and Capecchi, M. R. (1993). Mice homozygous for a targeted disruption of the proto-oncogene int-2 have developmental defects in the tail and inner ear. *Development* **117**, 13-28.

Maroon, H., Walshe, J., Mahmood, R., Kiefer, P., Dickson, C. and Mason, I. (2002). Fgf3 and Fgf8 are required together for formation of the otic placode and vesicle. *Development* **129**, 2099-108.

Miyake, A., Konishi, M., Martin, F. H., Hernday, N. A., Ozaki, K., Yamamoto, S., Mikami, T., Arakawa, T. and Itoh, N. (1998). Structure and expression of a novel member, FGF-16, on the fibroblast growth factor family. *Biochem Biophys Res Commun* **243**, 148-52.

Moon, A. M., Boulet, A. M. and Capecchi, M. R. (2000). Normal limb development in conditional mutants of Fgf4. *Development* **127**, 989-96.

Mueller, K. L., Jacques, B. E. and Kelley, M. W. (2002). Fibroblast growth factor signaling regulates pillar cell development in the organ of corti. *J Neurosci* **22**, 9368-77.

Niswander, L. and Martin, G. R. (1992). Fgf-4 expression during gastrulation, myogenesis, limb and tooth development in the mouse. *Development* **114**, 755-68.

Ornitz, D. M. and Itoh, N. (2001). Fibroblast growth factors. *Genome Biol* **2**, REVIEWS3005.

Ornitz, D. M., Xu, J., Colvin, J. S., McEwen, D. G., MacArthur, C. A., Coulier, F., Gao, G. and Goldfarb, M. (1996). Receptor specificity of the fibroblast growth factor family. *J Biol Chem* **271**, 15292-7.

Orr-Urtreger, A., Bedford, M. T., Burakova, T., Arman, E., Zimmer, Y., Yayon, A., Givol, D. and Lonai, P. (1993). Developmental localization of the splicing alternatives of fibroblast growth factor receptor-2 (FGFR2). *Dev Biol* **158**, 475-86.

Orr-Urtreger, A., Givol, D., Yayon, A., Yarden, Y. and Lonai, P. (1991). Developmental expression of two murine fibroblast growth factor receptors, flg and bek. *Development* **113**, 1419-34.

Partanen, J., Schwartz, L. and Rossant, J. (1998). Opposite phenotypes of hypomorphic and Y766 phosphorylation site mutations reveal a function for Fgfr1 in anteroposterior patterning of mouse embryos. *Genes Dev* **12**, 2332-44.

Pauley, S., Wright, T. J., Pirvola, U., Ornitz, D., Beisel, K. and Fritzsch, B. (2003). Expression and function of FGF10 in mammalian inner ear development. *Dev Dyn* **227**, 203-15.

Peters, K., Ornitz, D., Werner, S. and Williams, L. (1993). Unique expression pattern of the FGF receptor 3 gene during mouse organogenesis. *Dev Biol* **155**, 423-30.

Peters, K. G., Werner, S., Chen, G. and Williams, L. T. (1992). Two FGF receptor genes are differentially expressed in epithelial and mesenchymal tissues during limb formation and organogenesis in the mouse. *Development* **114**, 233-43.

Phillips, B. T., Bolding, K. and Riley, B. B. (2001). Zebrafish fgf3 and fgf8 encode redundant functions required for otic placode induction. *Dev Biol* **235**, 351-65.

Pickles, J. O. (2001). The expression of fibroblast growth factors and their receptors in the embryonic and neonatal mouse inner ear. *Hear Res* **155**, 54-62.

Pirvola, U., Spencer-Dene, B., Xing-Qun, L., Kettunen, P., Thesleff, I., Fritzsch, B., Dickson, C. and Ylikoski, J. (2000). FGF/FGFR-2(IIIb) signaling is essential for inner ear morphogenesis. *J Neurosci* **20**, 6125-34.

Pirvola, U., Ylikoski, J., Trokovic, R., Hebert, J. M., McConnell, S. K. and Partanen, J. (2002). FGFR1 is required for the development of the auditory sensory epithelium. *Neuron* **35**, 671-80.

Stark, K. L., McMahon, J. A. and McMahon, A. P. (1991). FGFR-4, a new member of the fibroblast growth factor receptor family, expressed in the definitive endoderm and skeletal muscle lineages of the mouse. *Development* **113**, 641-51.

Stark, M. R., Biggs, J. J., Schoenwolf, G. C. and Rao, M. S. (2000). Characterization of avian frizzled genes in cranial placode development. *Mech Dev* **93**, 195-200.

Torres, M. and Giraldez, F. (1998). The development of the vertebrate inner ear. *Mech Dev* **71**, 5-21.

Vendrell, V., Carnicero, E., Giraldez, F., Alonso, M. T. and Schimmang, T. (2000). Induction of inner ear fate by FGF3. *Development* **127**, 2011-9.

Wright, T. J. and Mansour, S. L. (2003a). Fgf3 and Fgf10 are required for mouse otic placode induction. *Development* **130**, 3379-90.

Wright, T. J. and Mansour, S. L. (2003b). FGF signaling in ear development and innervation. *Curr Top Dev Biol* **57**, 225-59.

Wu, D. K., Nunes, F. D. and Choo, D. (1998). Axial specification for sensory organs versus non-sensory structures of the chicken inner ear. *Development* **125**, 11-20.

Yamaguchi, T. P., Conlon, R. A. and Rossant, J. (1992). Expression of the fibroblast growth factor receptor FGFR-1/flg during gastrulation and segmentation in the mouse embryo. *Dev Biol* **152**, 75-88.

Yamaguchi, T. P., Harpal, K., Henkemeyer, M. and Rossant, J. (1994). fgfr-1 is required for embryonic growth and mesodermal patterning during mouse gastrulation. *Genes Dev* **8**, 3032-44.

Yu, C., Wang, F., Kan, M., Jin, C., Jones, R. B., Weinstein, M., Deng, C. X. and McKeehan, W. L. (2000). Elevated cholesterol metabolism and bile acid synthesis in mice lacking membrane tyrosine kinase receptor FGFR4. *J Biol Chem* **275**, 15482-9.

CHAPTER 3

ANALYSIS OF THE ROLE OF FGF16 IN INNER EAR DEVELOPMENT AND ASSAY OF THE FATE OF OTIC FGF16-EXPRESSING CELLS

Introduction

The inner ear is a complex sensory organ specialized for audition and balance. In higher vertebrates, the mechanoreceptor cells responsible for auditory sensation are housed in the ventrally located cochlear duct. The remaining mechanoreceptors, which sense movement of the head, are housed within the dorsally located vestibular system. The three dorsally located semicircular canals each contain within a centrally located ampulla, an associated sensory organ (crista) that functions in angular motion detection. Two additional sensory organs, the maculae of the utricle and saccule, which are situated centrally, between the cochlea and semicircular canals, function in linear motion detection. The inner ear also has a dorsally projecting appendage, the endolymphatic duct and sac (EDS), which does not contain any sensory cells, but plays an important role in maintaining the unique fluid environment that is essential for normal sensory function.

In the mouse, inner ear formation initiates at embryonic day (E)8.0 as a placodal thickening of the head ectoderm adjacent to rhombomeres (r)5 and 6 of the hindbrain. Subsequently, from E8.5-E9.0, the placode invaginates to form the otic cup, which continues to deepen and by E9.5 closes and separates from the surface ectoderm, forming

the roughly spherical otic vesicle or otocyst. Morphogenesis of the vesicle initiates at E10.5 with a dorsomedially directed outgrowth of the endolymphatic duct/sac (EDS) anlage and a ventrally directed outgrowth of the cochlear duct. During the next few days of development, this relatively simple epithelium acquires its mature and complex morphology and begins to differentiate its multitude of distinct sensory and non-sensory cell types. By E15.5, the inner ear epithelium has acquired its mature morphology, but is still undergoing cellular differentiation within the six sensory patches.

The ear is an asymmetric structure with each of its developmental axes having distinct morphologic characteristics. When and how each of the three axes arises from a simple ectodermal placode is not fully understood. The timing of anterior-posterior (AP) vs. dorsal-ventral (DV) axis formation was addressed in salamanders by Harrison (1936). Inner ear grafting and rotation experiments suggested that the AP axis of the ear is established by the placode stage, and that this occurs prior to DV axis specification. In recent otocyst rotation experiments in the chick (Wu et al., 1998), a similar conclusion was reached. It was concluded that the AP otic axis is established before the DV axis, and in chick, this development occurs at the otic cup stage. Axial fixation issue has not been addressed in the mouse.

While relative timing of AP and DV otic axis formation is understood, the nature of otic cell fate specification and compartment formation remains relatively unexplored. Several studies in the chick have focused on understanding fate maps of the inner ear. The most common approach has been to mark the cells with vital dyes that enable the identification of clonal populations that are derived from different areas of the early otic cup and vesicle. Labeling small groups of cells in the early chick epiblast suggests that

up to otic cup stage, there is no subdivision of the prospective otic region into compartments (Streit, 2002). A fate map of cells along the rim of the chick otic cup indicates that the entire dorsal rim of the otic cup becomes the endolymphatic duct (ED), while the posteroventral rim becomes the lateral otocyst wall (Brigande et al., 2000a). Two intersecting boundaries of lineage restriction were identified near the dorsal pole: one bisecting the ED into anterior and posterior halves and the other defining its lateral edge, suggesting that there is a strict anterior to posterior lineage boundary that bisects the endolymphatic duct (Brigande et al., 2000a). Double-labeling of dorsal and ventral regions of the otic vesicle shows that the cells originating from these two regions do not mix, supporting the existence of a sharp boundary between dorsal and ventral regions of the otocyst (Brigande et al., 2000a). These experiments have been extremely valuable in expanding our understanding of patterning and fate specification of different inner ear structures and suggest that the patterning into compartments begins at the otic cup stage.

However, similar information is not available for the mouse model system due to technical difficulties associated with traditional lineage tracing experiments. The only available insights into the mouse specification map come from culturing pieces of mouse otocysts *in vitro* for 10 days (Li et al., 1978). According to that map, dorsal anterior quarters of day 11 and 12 otocysts give rise the anterior semicircular canal, part of the lateral canal and the associated cristae, whereas dorsal posterior quarters gave rise to the remaining canals (posterior and the rest of the lateral) and posterior cristae. In addition, all three canals can arise from the lateral half of the otocyst. The difficulties associated with culturing developing mouse otocysts preclude more detailed dye-labeling or surgical rotation experiments in mouse embryos. Thus, a genetic approach must be used.

The molecular basis of otic axial formation also remains relatively unexplored. It has been suggested that the complex task of forming all the compartments of the inner ear is simplified by segregation of the otic region into gene expression domains. Most recent models of inner ear development indicate that boundaries of gene expression are important for patterning of the inner ear (Brigande et al., 2000b; Fekete and Wu, 2002; Rinkwitz et al., 2001). In fact, by the vesicle stage many genes expressed in the developing inner ear are confined to broad asymmetric domains that are thought to identify different compartments essential to specify various ear structures (Brigande et al., 2000b; Rivolta, 1997; Torres and Giraldez, 1998). To date, there are few gene markers that delineate the AP axis at otic cup stages.

The expression analysis screen described in Chapter 2 has shown that *Fgf16* transcripts are regionally restricted and polarized along the AP axis of the otic cup and vesicle. This expression pattern suggests possible roles in otic cell fate decisions and/or axis formation. As *Fgf16* is one of the earliest regionally restricted transcripts identified in the otic cup, it should be possible to exploit this finding and determine the fate of mouse posterior otic cup cells. To address these possibilities we took a genetic approach and simultaneously knocked out *Fgf16* expression and drove *Cre* recombinase expression in its place. This strategy allowed us to generate the *Fgf16* null phenotype to determine whether it plays a role in specifying particular otic cell fates or participates in otic axis formation. In this chapter we show that *Fgf16* does not have a unique role in inner ear development. In addition, we conducted a genetic lineage analysis to identify the specific ear structures that arise from *Fgf16* expressing cells in an effort to better understand the relationship between the posterior region of the early otic cup and the mature inner ear

structure. We describe the fates of *Fgf16* expressing otic cells during embryogenesis through Cre/LoxP lineage analysis in anterior and posterior semicircular canals, the three ampullary cristae, and the cochlear stria vascularis.

Results

Fgf16 is expressed asymmetrically in the otic cup and vesicle and in the semicircular canal cristae

To obtain a detailed picture of *Fgf16* mRNA expression, we analyzed closely staged embryos by in situ hybridization with an *Fgf16* antisense probe. Otic expression of *Fgf16* was initially detected weakly throughout the posterior otic cup starting at 14 somites (Figure 3.1A, B). By 17 somites, as the cup started to close to form the otic vesicle, *Fgf16* transcripts were more strongly expressed and localized to the posterior region (Figure 3.1C,D). Starting with 21 somites, *Fgf16* transcripts continued to be detected in the posterior half of the vesicle, marking the dorsolateral wall (Figure 3.1E, F, G, H). To determine whether *Fgf16* expression persisted in the otic region later in development, we detected *Fgf16* transcripts at E13.5 in transverse sections taken thought the head. *Fgf16* expression was found in the cristae of all three ampullae (Figure 3.1I, J, L). *Fgf16* transcripts were also expressed in scattered patches of presumptive nonsensory epithelium of the anterior and posterior semicircular canals (for posterior semicircular canal see Figure 3.1L) as well as in lateral cochlear foci (Figure 3.1I, J). In addition, strong *Fgf16* expression persisted in the primitive nasal cavity epithelia (Figure3.1K). These results indicate that *Fgf16* expression in the inner ear persists beyond the stages originally analyzed (Wright et al., 2003).

Figure 3.1 *Fgf16* is expressed asymmetrically in the otic cup and vesicle and in the semicircular canal cristae

Whole-mount 14-somite (A), 17-somite (C), 21-somite (E), and 28-somite (G) embryos were probed with labeled antisense cDNA for *Fgf16*. Rostral is to right (A,C,E,G). Lines indicate the plane of transverse (F) or coronal (B,D,H) sections shown in adjacent panels. Expression pattern of *Fgf16* at E13.5 was detected on paraffin sections probed with labeled antisense cDNA (I-L). *Fgf16* expression can be detected in the posterior cup (B,D) and posterior dorsolateral vesicle (F,H). At E13.5 *Fgf16* transcripts are found in the posterior (I), lateral (J) and anterior (L) semicircular canal cristae, as well as in the cochlear (I) and primitive nasal cavity (K) epithelia. Abbreviations: Coch, cochlea; es, endolymphatic sac; lcc, lateral semicircular canal cristae; oc, otic cup; ov, otic vesicle; pcc, posterior semicircular canal cristae; pnc, primitive nasal cavity; psc, posterior semicircular canal.

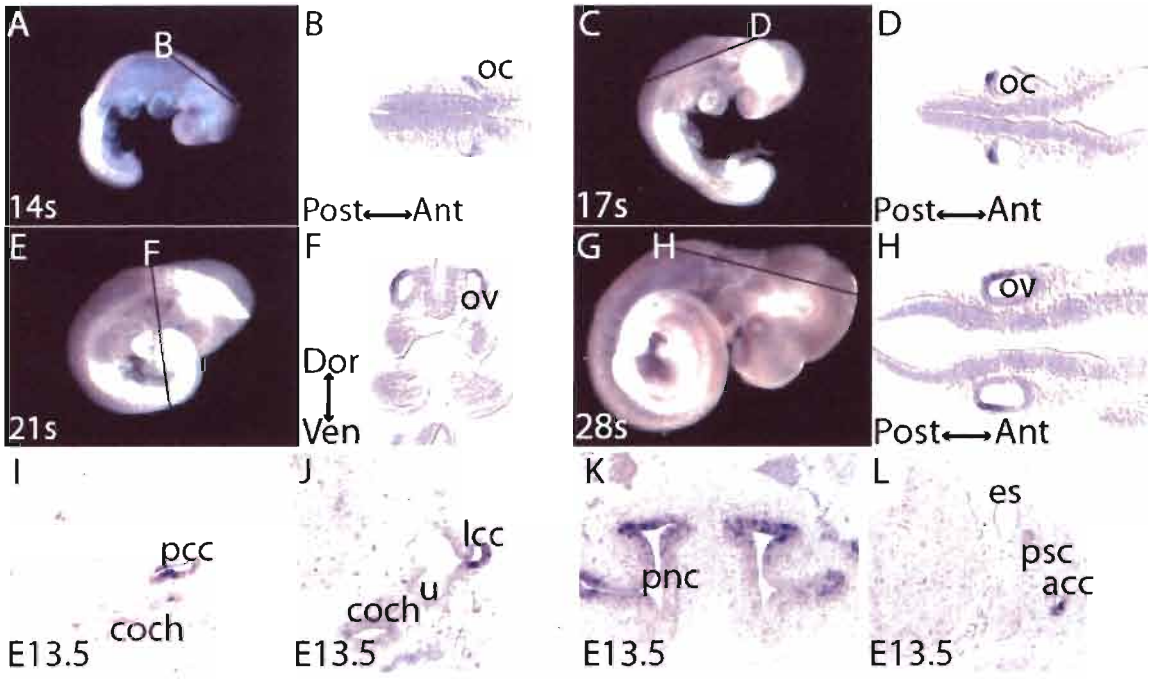
A
B
14s
B
oc
Post⟷Ant
C
D
17s
D
oc
Post⟷Ant
E
F
21s
F
ov
Dor
Ven
G
H
28s
H
ov
Post⟷Ant
I
pcc
coch
E13.5
J
lcc
u
coch
E13.5
K
pnc
E13.5
L
es
psc
acc
E13.5

Gene targeting at the *Fgf16* locus

To follow the fate of *Fgf16*-expresing cells originating in the posterior otic epithelium and to observe the consequences of *Fgf16* inactivation, we targeted the *Fgf16* locus for gene replacement with an engineered vector containing an internal ribosomal entry site (IRES) preceding a gene encoding bacteriophage P1 Cre recombinase (Arenkiel et al., 2003) and an frt-flanked neomyocin (*Neo*) selection cassette (Figure 3.2A). The *IRES-Cre-Neo* cassette was introduced into the first coding exon of *Fgf16* (Figure 3.2A), making a null allele. After FLP-mediated removal of the *Neo* selection gene, in the presence of the ROSA26 reporter allele (Soriano, 1999), the expression of *Cre* recombinase from the *Fgf16* locus drives recombination between two loxP recognition sequences, thereby activating the reporter. This excision is irreversible, thereby permanently marking the clonal derivatives of *Fgf16*-expressing cells, even after they stop expressing *Fgf16*.

The null mutation was introduced into the X-linked *Fgf16* gene through standard gene targeting protocols. Correctly targeted male ES cell clones, hemizygous for the introduced mutation were identified by Southern blot hybridization analysis of Tth111I-digested DNA using a 5' flanking external probe and HindIII-digested DNA using a 3' end internal probes (Figure 3.2A, B). After injection of targeted cells into blastocysts, chimeric mice carrying the *Fgf16-IRES-Cre-Neo* cassette were generated and identified by multiplex polymerase chain reaction (PCR) with primers directed against both wild-type and targeted alleles (data not shown). To determine the efficacy of the disruption strategy, an RT-RCR reaction was performed to detect *Fgf16* mRNA in wild type and mutant animals (Figure 3.2A, C). Using primers that flank the disruption, the expected

Figure 3.2 Gene targeting at the *Fgf16* locus

(A) Structure of the linearized *Fgf16* targeting vector and depiction of the wild type *Fgf16* allele (*Fgf16*+) and the correctly targeted mutant allele in ES cells (*Fgf16* null). Mouse genomic *Fgf16* DNA is depicted with solid lines; dotted lines indicate *Fgf16* genomic DNA that is not present in the targeting vector; untranslated regions are shown as open boxes, protein coding regions as solid boxes. The *IRES-Cre* gene is shown as a dark grey box; the *Neo* cassette flanked by the frt sites as a light grey box; the stop codon in the *Fgf16* frame in axon 3 as an asterisk. The plasmid backbone and the thymidine kinase (TK1) gene are depicted as open boxes. Recognition sites for Tth111I and HindIII, used in Southern analysis are indicated by "T" and "H" respectively. Probes used for Southern analysis are shown as black bars. Numbered arrows indicate the identity, position and directionality of primers used for the RT-PCR assay. (B) Southern blot hybridization assay demonstrating correct targeting of *Fgf16* in ES cells. Tth111I-digested genomic DNA from either the R1 ES cell line (R1) or a targeted cell line (Tar) probed with the external 5' probe, revealed an 8.4kb wild type and a 10.5kb DNA fragments respectively. HindIII-digested genomic DNA probed with the internal 3' probe yielded an 18kb R1 and a 14.8kb targeted cell line DNA fragments. (C) RT-PCR assay used to detect *Fgf16* mRNA in wild type and mutant animals. Total RNA was isolated from female wild type (+/+), female heterozygoute (+/-) and male hemizygoute mutant (-/Y) embryos at E9.0. cDNA fragments were PCR-amplified using primers 418 and 569, producing a 281bp band and primers 570 and 571, producing a 145bp band. 351bp DNA region within the *Hprt* gene was PCR-amplified as a positive control.

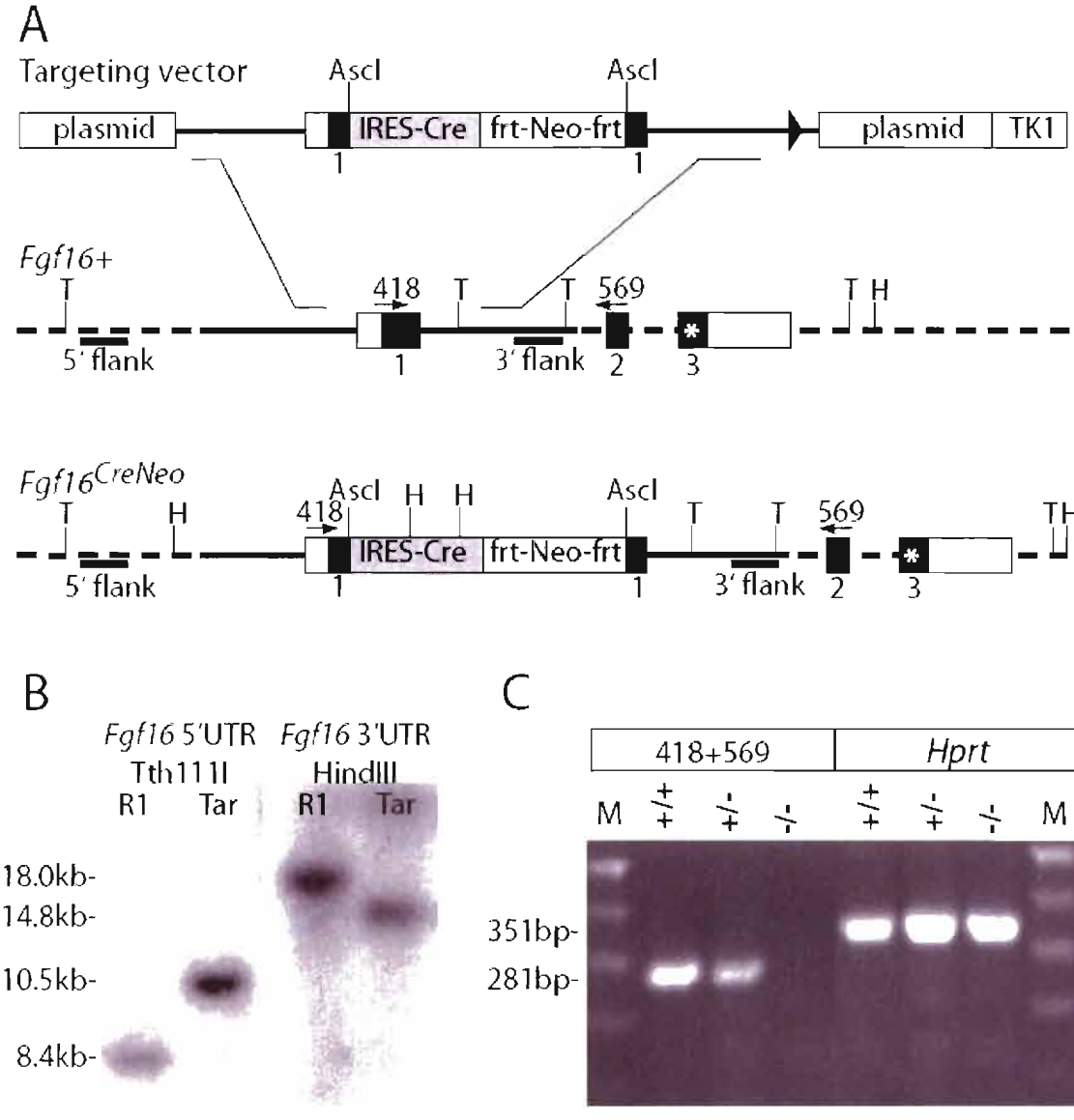
A
Targeting vector
AscI
AscI
plasmid
IRES-Cre
frt-Neo-frt
plasmid
TK1
1
1
Fgf16+
T
418
T
T
569
T H
5' flank
1
3' flank
2
3
Fgf16CreNeo
T
H
418
AscI
H
H
AscI
T
T
569
TH
5' flank
IRES-Cre
frt-Neo-frt
3' flank
2
3
B
Fgf16 5'UTR
Tth111I
R1
Tar
Fgf16 3'UTR
HindIII
R1
Tar
18.0kb-
14.8kb-
10.5kb-
8.4kb-
C
418+569
Hprt
M
+/+
+/-
-/-
+/+
+/-
-/-
M
351bp-
281bp-

band sizes were evident in wild type and heterozygous female samples, but were absent in a male hemizygous mutant, showing that the targeting strategy disrupted production of *Fgf16* mRNA. The $Fgf16^{CreNeo}$ allele was used to analyze any potential inner ear phenotypes associated with the mutation. For *Fgf16* lineage analysis, the *Neo* gene was removed by crossing the $Fgf16^{CreNeo}$ mice to a Flp deleter line (Rodriguez et al., 2000), facilitating recombination and excision of *Neo* sequence between the flanking frt sites. Mice harboring the "Neo-out" allele ($Fgf16^{Cre}$) were tested for appropriate CRE activity by crossing to the ROSA26 reporter strain (Soriano, 1999).

Fgf16 is not required for embryonic development

To determine whether *Fgf16* is required for any aspect of embryonic or postnatal development, the F1 *Fgf16* offspring of germline chimeras were intercrossed and adult progeny were genotyped. The numbers were consistent with a normal Mendelian distribution of wild type and mutant alleles (Table 3.1). No obvious anatomical or behavioral abnormalities were observed in homozygous mutant females or hemizygous mutant males, indicating that *Fgf16* does not have a unique role during mouse development.

The expression pattern of *Fgf16* suggested possible roles in otic cell fate decisions and/or axis formation. To visualize the consequences of loss of *Fgf16* to inner ear morphogenesis, we filled *Fgf16* mutant inner ear epithelia with latex paint at E15.5, a stage when the normal mouse ear has attained its mature morphology (Figure 3.3). At the gross anatomical level, a total of 12 mutant ears had a normal morphology and showed no obvious differences with wild type and heterozygote control littermates (Figure 3.3A, B).

To test for cochlear sensory dysfunction, we measured auditory brainstem

Table 3.1 *Fgf16* backcross and intercross genotypes

Offspring of the indicated crosses were genotyped at weaning. P values were determined using the method of X^2. The $Fgf16^{CreNeo}$ allele is defined as X^{Neo}.

Genotype at weaning	**F1 X C57Bl/6**
$X^{+}X^{+}$	20
$X^{Neo}X^{+}$	23
$X^{+}Y$	14
$X^{Neo}Y$	22
Total	79
P value	0.45
	F1 intercross
$X^{Neo}X^{+}$	5
$X^{Neo}X^{Neo}$	5
$X^{+}Y$	3
$X^{Neo}Y$	6
Total	19
P value	0.75

Figure 3.3 *Fgf16* mutant inner ears are morphologically normal

Representative lateral views of paint-filled inner ears from E15.5 heterozygous control (A) and *Fgf16* homozygous mutant (B). Labeled structures: aa, anterior ampulla; asc, anterior semicircular canal; cc, common crus; cd, cochlear duct; ed, endolymphatic duct; es, endolymphatic sac; la, lateral ampulla; lsc, lateral semicircular canal; pa, posterior ampulla; psc, posterior semicircular canal; s, saccule; u, utricle.

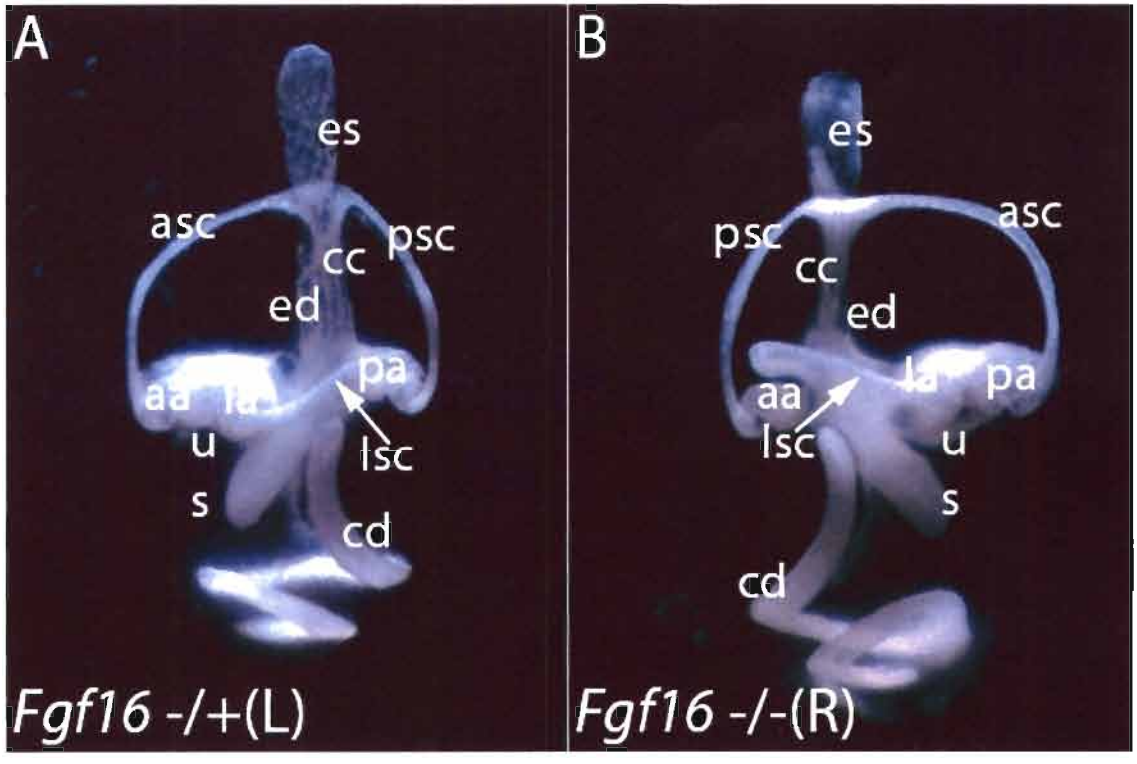
A
es
asc
psc
cc
ed
pa
aa
la
u
lsc
s
cd
Fgf16 -/+(L)
B
es
asc
psc
cc
ed
la
pa
aa
lsc
u
s
cd
Fgf16 -/-(R)

response (ABR) thresholds in each ear individually at approximately 6 weeks of age in animals of all three *Fgf16* genotypes. No significant differences in auditory thresholds were observed between wild type (n=3), heterozygous females (n=3) and hemizygous male mutant (n=7) animals, which showed normal thresholds averaging 19.5 dB, 18.5 dB and 20 dB respectively. Taken together, these results suggest that *Fgf16* mutant inner ears are structurally and functionally normal.

The *Fgf16* lineage is found in both sensory and non-sensory inner ear lineages

By using the ROSA26 reporter, whole-mount *Fgf16* lineage analysis was conducted throughout embryogenesis and at postnatal day one (P1). $Fgf16^{Cre}$ hemizygous males were crossed with ROSA26 homozygous females and stained for ß-galactosidase (ß-gal) expression. Reporter-positive cells were first apparent at E10.5 in both the anterior and posterior dorsolateral regions of the vesicle, although some cells in these regions were reporter-negative (Figure 3.4A, A'). The delay in the initial detection of the ß-gal reporter relative to the initiation of *Fgf16* mRNA detection is likely due to additive effects of the time required for CRE protein synthesis and ß-gal enzyme accumulation. At E11.5, reporter-positive cells mark the region of the developing cristae and are diffusely distributed throughout the vertical canal plate, mainly localizing to the prospective semicircular canal cristae (Figure 3.4B, B'). Few reporter-positive cells are also detected at this time in the cochlear region (Figure 3.4A'). The same pattern of *Fgf16* lineage is seen at E12.5, after the canals are formed by fusion (Figure 3.4C). At E13.5, reporter-positive cells are detected in the developing cristae of the three semicircular canals and are diffusely distributed throughout the anterior and posterior canal non-sensory epithelial

region (Figure 3.4D, D''). In addition to the inner ear, *Cre*-expressing cells are detected in the primitive nasal cavity epithelium (Figure 3.4D'). The cells marked by ß-gal activity at E13.5 corresponded precisely to the domains of *Fgf16* expression, marked by RNA in situ hybridization (Figure 3.1I-L) indicating that the *Fgf16-IRES-Cre* driver recapitulates endogenous *Fgf16* activity and serves as an accurate reporter for in-depth fate mapping analysis. From E15.5 to P1, reporter-positive cells are detected throughout the cristae and mark most of the cells in the non-sensory anterior and posterior semicircular canal epithelia (Figure 3.4E, E', F, F'). Subsets of reporter-positive cells can be found in the lateral edges throughout the length of the cochlear duct (Figure 3.4E'', F''). These cells may develop into the spiral prominence, the function of which is unknown.

Discussion

To determine the role of *Fgf16* in inner ear development and the lineage of *Fgf16*-expressing cells, we generated an $Fgf16^{Cre}$ mouse strain. Analysis of the *Fgf16* null mice indicates that this gene does not have a unique role in inner ear development. Insights coming from the compartment boundary model described for the chick (Fekete and Wu, 2002) can explain the lack of the inner ear phenotype in *Fgf16* mutants. According to that model, the boundaries between regional otic gene expression domains serve as sites that mediate cell fate specification (Fekete and Wu, 2002). Fate-mapping data from the chick supports this argument and shows that the endolymphatic duct arises at the intersection of an anterior-posterior and medial-lateral boundaries (Brigande et al., 2000a). It is possible that one needs to interfere with the expression domains of both sides of the compartment boundary to cause the specific loss of the anterior/posterior structure; therefore, deleting *Fgf16* in the posterior region alone is not sufficient to cause a loss of an inner ear

Figure 3.4 Assay of the lineage of *Fgf16*-expressing cells at E10.5-P1

Embryos harboring both the ROSA26 reporter and *Fgf16-IRES-Cre* driver alleles stained for ß-gal expression at E10.5 (A), E11.5 (B), E12.5 (C), E13.5 (D), E15.5 (E), and P1 (F). Rostral is to right (A-F). Black lines indicate the plane of transverse (A,E,F) or coronal (B,D) sections shown in adjacent panels. Reporter-positive cells can be detected in the dorsolateral otocyst at E10.5 (A'), the primitive nasal cavity (D') the developing cristae (B',D'',E',F') and anterior and superior semicircular canals (B,C,D,F) throughout embryonic development. Abbreviations: Acc, anterior canal cristae; aw, ampullary wall; coch, cochlea; lcc, lateral canal cristae; lsc, lateral semicircular canal; nf, nerve fibers; oc, organ of Corti; ov, otic vesicle; pcc, posterior canal cristae; pnc, primitive nasal cavity; sv, stria vascularis.

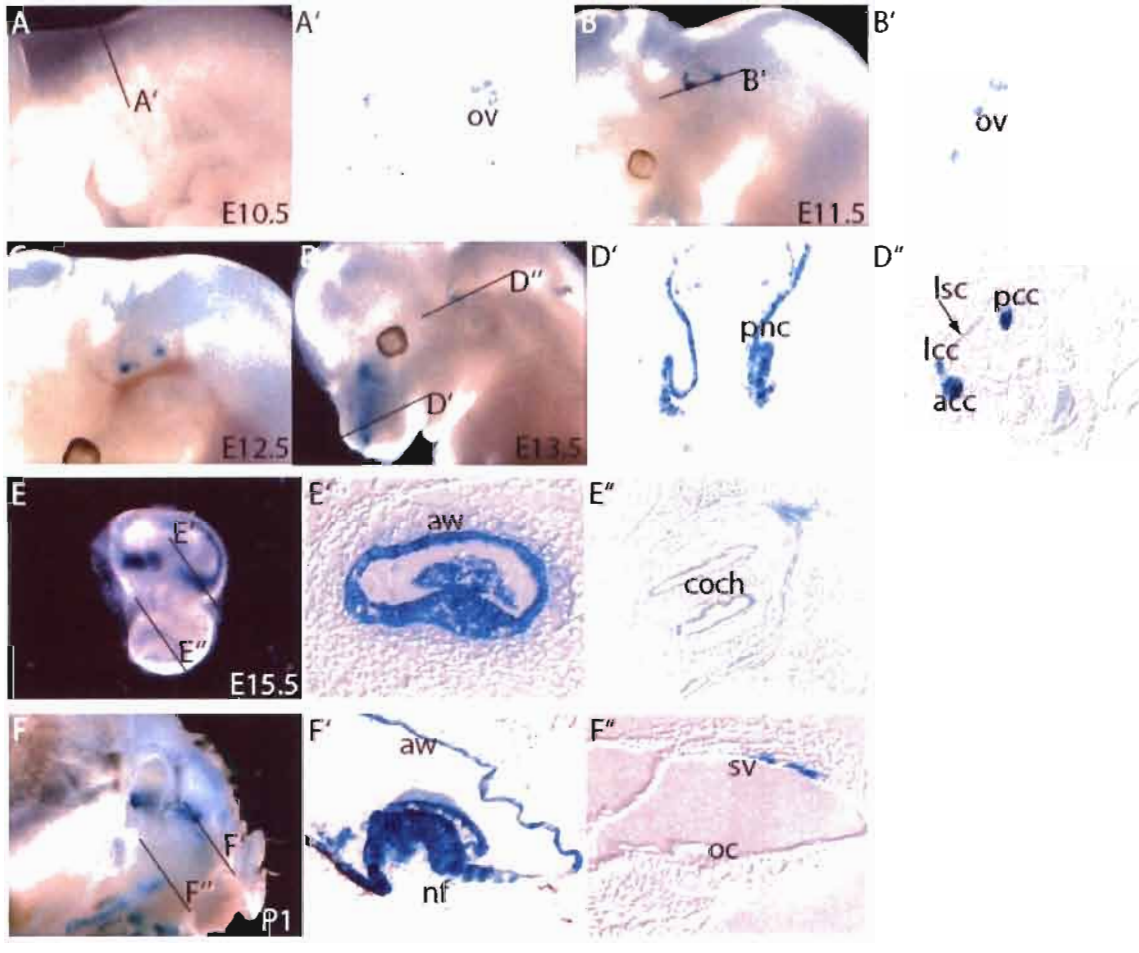
A
A'
E10.5
A'
ov
B
B'
E11.5
B'
ov
D''
D'
E12.5
E13.5
D'
pnc
D''
lsc
pcc
lcc
acc
E
E'
E''
E15.5
E'
aw
E''
coch
F
F'
F''
P1
F'
aw
nf
F''
sv
oc

structure. Thus, functional redundancy with another member of the FGF family, expressed in the same region, needs to be addressed in the future. *Fgf10* is expressed throughout the otic cup when *Fgf16* is only expressed in a posterior domain. By generating double mutants between *Fgf16* and *Fgf10*, we might uncover a role for *Fgf16* if we examine otic vesicles prior to the point at which the *Fgf10*-specific otic phenotype is first evident at E11.5-E12.5 (Pauley et al., 2003).

To better understand the role of *Fgf16* in inner ear development and address the potential redundancy with another gene in otic axial specification, more information is needed about the timing and full range of gene expression in the otic cup and the surrounding tissues. It was suggested that the hindbrain participates in establishing asymmetric AP gene expression in the otocyst (Brigande et al., 2000b). The otic cup develops adjacent to rhombomeres (r)5 and (r)6 of the hindbrain and the boundary between the two rhombomeres alignes precisely with the middle of the otic cup. So it was speculated that anterior and posterior halves of the early otic cup receive different signals from r5 and r6, thus, obtaining differential positional information (Brigande et al., 2000b). At least two signaling systems could potentially be involved in sending differential positional information from r5 and r6 to the developing otic field. One is the Eph/ephrin system, that expresses the ligands at high levels in r6 but only the receptors in r5 (Bergemann et al., 1998; Gale et al., 1996; Mellitzer et al., 2000; Xu et al., 1999). Members of the Hox gene family are also differentially expressed in the rhombomeres of the hindbrain (Duboule, 1994; Wilkinson, 1993) and are likely candidates for inducing differential gene expression in the otic epithelium. In addition, *Fgf3* is differentially expressed in r5 and r6 during the otic cup and vesicle stages, potentially producing low

anterior and high posterior signaling gradient from the hindbrain to the otic epithelium. Potential interactions of *Fgf16* with the hindbrain-expressed genes need to be investigated.

Despite the lack of an otic phenotype, *Fgf16* null mutants are an important genetic tool that could be of potential interest to investigators interested in brown adipose tissue and heart, as they appear to be the two major expression sites of *Fgf16* in late embryos and in the adult (Konishi et al., 2000; Miyake et al., 1998; Sontag and Cattini, 2003). In addition, the *Fgf16-Cre* allele can be utilized to drive CRE-recombinase expression to facilitate conditional loss of genes expressed in the semicircular canal cristae. This strategy could be used to address the question of whether *Fgf3* and/or *Fgf10* signaling from the developing sensory patches induces nonsensory (canal) development and whether these genes are redundant with *Fgf16*.

In this study we have also taken a genetic approach to determine the lineage of *Fgf16* expressing cells. By targeting the *Fgf16* locus for gene replacement with an *IRES-Cre*, we have been able to describe the specific cell fates that arise from the *Fgf16*-expressing region. Reporter-positive cells were first apparent at E10.5 in both the anterior and posterior dorsolateral regions of the vesicle. *Fgf16* lineage analysis at E13.5 faithfully reproduced expression patterns on *Fgf16* transcripts in the base of stria vascularis of the cochlea, nonsensory regions of the anterior and posterior semicircular canals and the three cristae, in the pattern consistently detected throughout embryonic development up until P1. As the detailed expression pattern of *Fgf16* was not analyzed between E10.5 and E13.5, it remains to be determined whether *Fgf16* continues to be expressed in the otic region throughout development, or disappears from the otic vesicle

and switches back on in the cristae. However, these results are consistent with the previously described expression pattern of the chick ortholog of *Fgf16*, which was shown to be restricted to the anterior and posterior domains of the otocyst that partially overlap with those of *Bmp4*, a marker of the developing sensory patches, the cristae of the anterior and posterior semicircular canals (Chapman et al., 2006).

Fgf16 lineage analysis has been extremely valuable in supporting the compartment boundary model proposed for inner ear development. Fate mapping and gene expression data were complied from studies of both mouse and chicken into a predicted fate map for the early otocyst, which indicates where cells from each compartment are likely to reside after morphogenesis (Fekete and Wu, 2002). According to this model, the dorsolateral region of the otocyst gives rise to the anterior and posterior semicircular canals with the associated cristae. The lateral crista is likely to arise at the posterior dorsoventral border. The expression pattern of *Fgf16* and the lineage of *Fgf16*-expressing cells now support this contention and serve as evidence to support the compartment-boundary model of inner ear cell fate specification. To date, very few data are available to define the location of compartments and boundaries within the cochlear region, making the predicted fate map of the cochlear duct especially hypothetical, therefore, the identity of the few reporter-positive cells found in the cochlear stria vascularis remains to be determined.

Materials and methods

Construction of the *Fgf16* allele

A lambda phage carrying the first coding exon of *Fgf16* gene flanked by the 4.5 kb of the noncoding sequences was isolated by recombination cloning (Zhang et al.,

2002) from a 129sv mouse genomic library. A total of 9.3kb of *Fgf16* genomic DNA with a single loxP insertion 4.8kb downstream of the coding region was isolated in the plasmid backbone harboring the thymidine kinase gene for negative selection. The *IRES-Cre-PGKNeo* cassette (Arenkiel et al., 2003) was inserted into an artificial AscI site generated in the first exon of *Fgf16*, followed by the 2bp exchange to produce the following sequence: GATCCTGCGGCGCgcCCAGCTCTACTGC (the mutated sequence is in lowercase). A total 12.3kb of the targeting vector (shown in Figure 3.2A) was linearized with AhdI, electroporated into R1-45 ES cells, and selected in 380μg/ml G418 by weight (Invitrogen) and 2 mM ganciclovir (Sigma). Drug resistant colonies were expanded for DNA isolation. The presence of only one copy of X-linked *Fgf16* gene in male ES cells allowed for PCR analysis to exclude the clones with a random insertion of the targeting vector. The mix containing primers 501 (5'-CCCACTGTTCTTGCCTCTTC-3') and 502 (5'-GGTTTTGGTGCTGGAGATTG-3'), flanking loxP site, yielded a 376bp wild type band and a 450bp loxP-insertion band. ES clones without the random insertion of the targeting vector, as identified by the single 376bp wild type band, were analyzed by Southern blot hybridization on Tth111I-difested DNA using 5' flanking external and HindIII-digested 3' end internal probes. Positive ES clones were further verified by Southern blotting using a variety of enzymes and probes. Of 192 drug resistant cell lines, 5 had a targeted insertion in the first coding exon of at this time in the cochlear region (Figure 3.4A'). The same pattern of *Fgf16* lineage is seen at E12.5, after the canals are formed by fusion (Figure 3.4C). At E13.5, reporter-positive cells are detected in the developing cristae of the three semicircular canals and *Fgf16* gene.

Fgf16 mutant mouse generation and genotyping

All work with mice complied with protocols approved by the University of Utah Institutional Animal Care and Use Committee. Several correctly targeted cell lines were injected into host blastulas and the resulting chimeric males, hemizygous for the targeted mutation, transmitted the targeted allele to offspring. In subsequent crosses, the wild type and mutant alleles were distinguished by PCR analysis using a three primer mix. The mix containing primers 73 (5'-TTCAGTGACAACGTCGAGCAC-3'), 418 (5'-GTCTTTGCCTCCTTGGACTG-3') and 419 (5'-CCGTTGGGGAAGATCTCAAG -3') produced a wild type band of 218bp and a mutant band of 691bp. No difference between intercross offspring produced from different targeted alleles were observed, therefore one line was selected for further analysis and backcrossing. An RT-PCR assay was performed to detect *Fgf16* mRNA in wild type and mutant animals. Total RNA was isolated from the female wild type (+/+), female heterozygoute (+/-) and male mutant (-/Y) embryos at E9.0 The reverse transcriptase (RT) reaction was performed at 42°C with Superscript II reverse transcriptase and oligo(dT) primer. cDNA fragments were PCR-amplified using primers 418 and 569, producing a 281bp band and primers 570 and 571, producing a 145bp band. 351bp DNA region within the *Hprt* gene was PCR-amplified as a positive control, using 33 (5'-CCTGCTGGATTACATTAAAGCACTG-3') and 34 (5'-GTCAAGGGCATATCCAACAACAAAC-3') primers (shown in Figure 3.2C).

Mice homozygous for the targeted "knock-in" allele resembled wild type littermates. For *Fgf16* lineage analysis chimeric males derived from a positive ES clone were mated to *Flp*-expressing mice (Rodriguez et al., 2000) and the progeny were screened for the absence of the *PGK-Neo* selection cassette by PCR analysis. The mix

containing primers 418 (5'-GTCTTTGCCTCCTTGGACTG-3'), 419 (5'-CCGTTGGGGAAGATCTCAAG-3') and 557 (5'-CAATACCGGAGATCATGCAAG-3') produced a wild type band of 218bp and a mutant "Neo-out" band of 360bp. Lineage analysis was conducted by crossing the males hemizygous for the *Fgf16*^{Cre} allele to the previously described ROSA26 reporter strain (Soriano, 1999).

X-gal staining

Embryos harboring both the ROSA26 reporter and *Fgf16-IRES-Cre* driver alleles were isolated from pregnant females in PBS with 1 mM $MgCl_2$. Embryos were then fixed (2% paraformaldehyde, 1.25 mM EGTA, 2 mM $MgCl_2$, 0.1 M PIPES pH6.9), washed in PBS/1 mM $MgCl_2$, and immersed into X-gal staining solution (5 mM $K_3Fe(CN)_6$/5 mM $K_4Fe(CN)_6$-$3H_2O$/ 1 mM $MgCl_2$/ 0.01% Na Deoxycholate/ 0.02% NP40 in PBS pH7.5). Staining was carried out at 37°C in a humidified atmosphere.

Paint filling and RNA in situ hybridization

E15.5 embryos were cleared in methyl salicylate and the ears were filled through the saccule with white latex paint as described (Morsli et al., 1998). The *Fgf16* expression pattern was analyzed at E8.5-10.5 and E13.5 by whole mount RNA in situ hybridization. Embryos were isolated on the indicated days following detection of a vaginal plug and age-matched based on the total number of somite pairs. The normal expression pattern of *Fgf16* was determined using wild type CD-1 (Charles River Laboratories) embryos. The antisense *Fgf16* RNA probe was generated as described previously (Wright et al., 2003), hybridised to the embryos and detected as described (Henrique et al., 1995). Embryos stained for analysis of gene expression were

cryoprotected in sucrose and sectioned at 14 µm using a Leica CM1900 cryostat as described (Stark et al., 2000). For expression analysis of *Fgf16* at E13.5, whole heads were fixed in a modified Carnoy's solution at 4°C. The samples were then dehydrated in 100% ethanol overnight at 4°C, embedded in paraffin and sectioned. Sections (10 µm thick) were collected on SuperFrost slides, air dried for 12 hr and stained for analysis of gene expression as described (Hayashi et al., 2007).

Photography

Whole embryos were photographed using a Zeiss SV-11 dissecting microscope fitted with a digital camera (QImaging). Sections were photographed using a Zeiss Axioscop fitted with DIC optics and a digital camera (AxioCam).

Auditory brainstem response measurements

Mice were anesthetized using 0.02 ml/g Avertin. Auditory brainstem response (ABR) thresholds for click stimuli (47 µsec duration, 29.3/sec) presented to each ear individually were determined using high frequency transducers controlled and analyzed by SmartEP software (Intelligent Hearing Systems)(Zheng et al., 1999).

References

Arenkiel, B. R., Gaufo, G. O. and Capecchi, M. R. (2003). Hoxb1 neural crest preferentially form glia of the PNS. *Dev Dyn* **227**, 379-86.

Bergemann, A. D., Zhang, L., Chiang, M. K., Brambilla, R., Klein, R. and Flanagan, J. G. (1998). Ephrin-B3, a ligand for the receptor EphB3, expressed at the midline of the developing neural tube. *Oncogene* **16**, 471-80.

Brigande, J. V., Iten, L. E. and Fekete, D. M. (2000a). A fate map of chick otic cup closure reveals lineage boundaries in the dorsal otocyst. *Dev Biol* **227**, 256-70.

Brigande, J. V., Kiernan, A. E., Gao, X., Iten, L. E. and Fekete, D. M. (2000b). Molecular genetics of pattern formation in the inner ear: do compartment boundaries play a role? *Proc Natl Acad Sci U S A* **97**, 11700-6.

Chapman, S. C., Cai, Q., Bleyl, S. B. and Schoenwolf, G. C. (2006). Restricted expression of Fgf16 within the developing chick inner ear. *Dev Dyn* **235**, 2276-81.

Duboule, D. (1994). Temporal colinearity and the phylotypic progression: a basis for the stability of a vertebrate Bauplan and the evolution of morphologies through heterochrony. *Dev Suppl*, 135-42.

Fekete, D. M. and Wu, D. K. (2002). Revisiting cell fate specification in the inner ear. *Curr Opin Neurobiol* **12**, 35-42.

Gale, N. W., Flenniken, A., Compton, D. C., Jenkins, N., Copeland, N. G., Gilbert, D. J., Davis, S., Wilkinson, D. G. and Yancopoulos, G. D. (1996). Elk-L3, a novel transmembrane ligand for the Eph family of receptor tyrosine kinases, expressed in embryonic floor plate, roof plate and hindbrain segments. *Oncogene* **13**, 1343-52.

Harrison, R. G. (1936). Relations of Symmetry in the Developing Ear of Amblystoma Punctatum. *Proc Natl Acad Sci U S A* **22**, 238-47.

Hayashi, T., Cunningham, D. and Bermingham-McDonogh, O. (2007). Loss of Fgfr3 leads to excess hair cell development in the mouse organ of Corti. *Dev Dyn* **236**, 525-33.

Henrique, D., Adam, J., Myat, A., Chitnis, A., Lewis, J. and Ish-Horowicz, D. (1995). Expression of a Delta homologue in prospective neurons in the chick. *Nature* **375**, 787-90.

Konishi, M., Mikami, T., Yamasaki, M., Miyake, A. and Itoh, N. (2000). Fibroblast growth factor-16 is a growth factor for embryonic brown adipocytes. *J Biol Chem* **275**, 12119-22.

Li, C. W., Van De Water, T. R. and Ruben, R. J. (1978). The fate mapping of the eleventh and twelfth day mouse otocyst: an in vitro study of the sites of origin of the embryonic inner ear sensory structures. *J Morphol* **157**, 249-67.

Mellitzer, G., Xu, Q. and Wilkinson, D. G. (2000). Control of cell behaviour by signalling through Eph receptors and ephrins. *Curr Opin Neurobiol* **10**, 400-8.

Miyake, A., Konishi, M., Martin, F. H., Hernday, N. A., Ozaki, K., Yamamoto, S., Mikami, T., Arakawa, T. and Itoh, N. (1998). Structure and expression of a novel member, FGF-16, on the fibroblast growth factor family. *Biochem Biophys Res Commun* **243**, 148-52.

Morsli, H., Choo, D., Ryan, A., Johnson, R. and Wu, D. K. (1998). Development of the mouse inner ear and origin of its sensory organs. *J Neurosci* **18**, 3327-35.

Pauley, S., Wright, T. J., Pirvola, U., Ornitz, D., Beisel, K. and Fritzsch, B. (2003). Expression and function of FGF10 in mammalian inner ear development. *Dev Dyn* **227**, 203-15.

Rinkwitz, S., Bober, E. and Baker, R. (2001). Development of the vertebrate inner ear. *Ann N Y Acad Sci* **942**, 1-14.

Rivolta, M. N. (1997). Transcription factors in the ear: molecular switches for development and differentiation. *Audiol Neurootol* **2**, 36-49.

Rodriguez, C. I., Buchholz, F., Galloway, J., Sequerra, R., Kasper, J., Ayala, R., Stewart, A. F. and Dymecki, S. M. (2000). High-efficiency deleter mice show that FLPe is an alternative to Cre-loxP. *Nat Genet* **25**, 139-40.

Sontag, D. P. and Cattini, P. A. (2003). Cloning and bacterial expression of postnatal mouse heart FGF-16. *Mol Cell Biochem* **242**, 65-70.

Soriano, P. (1999). Generalized lacZ expression with the ROSA26 Cre reporter strain. *Nat Genet* **21**, 70-1.

Stark, M. R., Biggs, J. J., Schoenwolf, G. C. and Rao, M. S. (2000). Characterization of avian frizzled genes in cranial placode development. *Mech Dev* **93**, 195-200.

Streit, A. (2002). Extensive cell movements accompany formation of the otic placode. *Dev Biol* **249**, 237-54.

Torres, M. and Giraldez, F. (1998). The development of the vertebrate inner ear. *Mech Dev* **71**, 5-21.

Wilkinson, D. G. (1993). Molecular mechanisms of segmental patterning in the vertebrate hindbrain. *Perspect Dev Neurobiol* **1**, 117-25.

Wright, T. J., Hatch, E. P., Karabagli, H., Karabagli, P., Schoenwolf, G. C. and Mansour, S. L. (2003). Expression of mouse fibroblast growth factor and fibroblast growth factor receptor genes during early inner ear development. *Dev Dyn* **228**, 267-72.

Wu, D. K., Nunes, F. D. and Choo, D. (1998). Axial specification for sensory organs versus non-sensory structures of the chicken inner ear. *Development* **125**, 11-20.

Xu, Q., Mellitzer, G., Robinson, V. and Wilkinson, D. G. (1999). In vivo cell sorting in complementary segmental domains mediated by Eph receptors and ephrins. *Nature* **399**, 267-71.

Zhang, P., Li, M. Z. and Elledge, S. J. (2002). Towards genetic genome projects: genomic library screening and gene-targeting vector construction in a single step. *Nat Genet* **30**, 31-9.

Zheng, Q. Y., Johnson, K. R. and Erway, L. C. (1999). Assessment of hearing in 80 inbred strains of mice by ABR threshold analyses. *Hear Res* **130**, 94-107.

CHAPTER 4

FGF3 IS REQUIRED FOR DORSAL PATTERNING AND MORPHOGENESIS OF THE INNER EAR EPITHELIUM

Abstract

The inner ear, which contains sensory organs specialized for hearing and balance, develops from an ectodermal placode that invaginates lateral to hindbrain rhombomeres 5 and 6 to form the otic vesicle. Under the influence of signals from intra- and extra-otic sources, the vesicle is molecularly patterned and undergoes morphogenesis and cell type differentiation to acquire its distinct functional compartments. This study shows that *Fgf3*, which is expressed in the hindbrain from the time of otic induction through endolymphatic duct outgrowth and in the prospective neurosensory domain of the otic epithelium as morphogenesis initiates, is required for both auditory and vestibular function. We provide new morphologic data on inner ear dysmorphogenesis in *Fgf3* mutants, which show a range of malformations similar to those seen in *Mafb* (*Kreisler*), *Hoxa1* and *Gbx2* mutants; the most common phenotype being failure of endolymphatic duct and common crus formation, accompanied by epithelial dilatation and reduced cochlear coiling. The range of malformations has close parallels with those seen in hearing impaired patients. The *Fgf3* morphologic data, together with an analysis of changes in the molecular patterning of *Fgf3* mutant otic vesicles, and comparisons with other mutations that affect otic morphogenesis, allow placement of *Fgf3* between

hindbrain-expressed *Hoxa1* and *Mafb* (*Kreisler*) and otic vesicle-expressed *Gbx2* in the genetic cascade initiated by WNT signaling that leads to dorsal otic patterning and endolymphatic duct and sac formation. In addition, we found that *Fgf3* prevents expansion of *Wnt3a* into more ventral regions of the hindbrain, serving to focus the inductive WNT signals on the dorsal otic vesicle and highlighting a new example of crosstalk between the two signaling systems.

Introduction

The inner ear is a morphologically complex sensory organ responsible for hearing and balance. In higher vertebrates, the mechanoreceptor cells responsible for auditory sensation are housed in the ventrally located cochlear duct. The remaining mechanoreceptors, which sense movement of the head, are housed within the dorsally located vestibular system. The three dorsally located semicircular canals each contain within a centrally located ampulla, an associated sensory organ (crista) that functions in angular motion detection. Two additional sensory organs, the maculae of the utricle and saccule, which are situated centrally, between the cochlea and semicircular canals, function in linear motion detection. The inner ear also has a dorsally projecting appendage, the endolymphatic duct and sac (EDS), which does not contain any sensory cells, but plays an important role in maintaining the unique fluid environment that is essential for normal sensory function.

In the mouse, inner ear formation initiates at embryonic day (E)8.0 as a placodal thickening of the head ectoderm adjacent to rhombomeres (r)5 and 6 of the hindbrain. Subsequently, from E8.5-E9.0, the placode invaginates to form the otic cup, from which neuroblasts of the eighth ganglion (GVIII) delaminate anteroventrally and migrate

medially. By E9.5, the cup closes and separates from the surface ectoderm, forming the roughly spherical otic vesicle or otocyst. Morphogenesis of the vesicle initiates at E10.5 with a dorsomedially directed outgrowth of the endolymphatic duct/sac (EDS) anlage and a ventrally directed outgrowth of the cochlear duct. During the next few days of development significant changes occur in the appearance of the dorsally situated semicircular canals joined at the common crus. By E15.5, the inner ear epithelium has acquired its mature morphology, but is still undergoing cellular differentiation within the six sensory patches.

The initial induction and subsequent morphogenesis and differentiation of the otic epithelium involves signaling interactions within and between otic and non-otic tissues (Fekete, 1999; Kiernan et al., 2002). In particular, FGF and WNT signals from the endoderm, mesenchyme and hindbrain are required together for otic placode induction and vesicle formation. In response to the inductive signals, the developing otic placode expresses in a uniform fashion several transcription factors including *Pax2*, *Dlx5*, and *Gbx2* (Ladher et al., 2005; Wright and Mansour, 2003). By the otocyst stage, the expression domains of most otic markers become confined to restricted domains of the vesicle specified to give rise to different ear structures (Fekete and Wu, 2002). This division of the otocyst into gene expression domains required for normal morphogenesis also depends on signals from the hindbrain. Removal or rotation of the neural tube in the vicinity of the developing otic tissue disrupts otic vesicle molecular patterning and development (Bok et al., 2005; Hutson et al., 1999). Mutations in hindbrain-expressed genes, such as *Mafb* (*Kreisler*) and *Hoxa1*, which cause defects in the development of r5 and r6, also show abnormal patterning of the otic vesicle leading to inner ear

malformations (Choo et al., 2006; Pasqualetti et al., 2001). *Wnt1* and *Wnt3a*, which are expressed in the dorsal hindbrain, are required redundantly for formation of the vestibular structures (Riccomagno et al., 2005).

FGF signaling is also implicated in otic vesicle morphogenesis. FGF3 and FGF10 are expressed by prospective otic sensory tissues (Mahmood et al., 1996; McKay et al., 1996; Pauley et al., 2003; Pirvola et al., 2000; Wilkinson et al., 1988) and their major receptor, FGFR2b, is found in prospective nonsensory tissue (Pirvola et al., 2000). Global inhibition of FGF signaling by application of SU5402 to chick E2.5-E3 otic vesicles just prior to canal pouch evagination causes dose-dependent inhibition of semicircular canal formation leading to the concept that developing sensory structures control development of nonsensory structures (Chang et al., 2004). Mutant mouse phenotypes support this concept. Mice lacking the "b" splice isoform of FGFR2 form otic vesicles that subsequently develop dysmorphologies initiating at the stage of EDS outgrowth and include failure of semicircular canal formation (Pirvola et al., 2000). Most *Fgf10* mutants completely lack semicircular canals (Ohuchi et al., 2005; Pauley et al., 2003). *Fgf3* null mutants undergo normal otic vesicle formation, but then go on to develop highly variable and incompletely penetrant inner ear dysmorphologies that, like those of *Fgfr2b* mutants, appear to initiate at the stage of endolymphatic duct outgrowth. These mutants also show a reduction in the size of the otic ganglion (Mansour et al., 1993). Whether loss of hindbrain or otic prosensory sites of *Fgf3* expression or both contribute to this phenotype remains unclear.

To gain insight into the mechanisms by which *Fgf3* functions in otic morphogenesis, we determined the three dimensional structure of *Fgf3* mutant ears and

the changes in their molecular patterning. In addition to the previously described *Fgf3*^{neo} allele (Mansour et al., 1993) we also analyzed a new *Fgf3* exon 2 deletion allele in anticipation of its eventual use in conditional inactivation studies. We show that the two mutant alleles are equivalent and homozygous mutants have variably penetrant and expressive inner ear morphologies that are characterized most typically by loss of the endolymphatic duct and common crus, dilatation of the remaining epithelium and poor coiling of the cochlea; phenotypes that are very similar to those of *Hoxa1*, *Mafb* (*Kr*), and *Gbx2* mutants (Choo et al., 2006; Lin et al., 2005; Pasqualetti et al., 2001). In addition, a very small number of mutants had normal endolymphatic duct and cochlear development, but lacked the posterior semicircular canal. The initial molecular patterning of *Fgf3* mutant otocysts was normal, but by E10-E10.5 these ears lacked or had reduced domains of dorsally expressed otic genes, suggesting a loss of the cells fated to form the EDS. Ventrally expressed genes important for cochlear development were not affected, but markers of the developing vestibular sensory domains, particularly those expressed in the posterior region of the vesicle were downregulated or absent and the eighth ganglion was reduced and displaced dorsomedially. Interestingly, hindbrain expression of *Wnt3a* was ventrally expanded in *Fgf3* mutants. Taken together, our results suggest that *Fgf3* is required for dorsal otic patterning and that its primary role is to sustain and focus the dorsal otic gene expression induced by WNT signals. Furthermore, we suggest that *Fgf3* also functions, albeit largely redundantly, in the subsequent sensory patch control of non-sensory development.

Results

We showed previously that mice homozygous for the *Fgf3*^{neo} allele have defects of inner ear morphogenesis that are incompletely penetrant and variably expressive (Mansour et al., 1993). The earliest morphologic defect appeared to be a failure of endolymphatic duct outgrowth between E9.5 and E10.5. Here we present a more detailed analysis of the inner ear dysmorphology in *Fgf3* mutants and an analysis of otic marker genes using the previously described *Fgf3*^{neo} allele and a newly targeted *Fgf3*$^{\Delta 2}$ allele (Figure 4.1A).

Fgf3^{neo} and *Fgf3*$^{\Delta 2}$ adult homozygotes have similar survival and gross skeletal and otic phenotypes

To determine whether the new *Fgf3*$^{\Delta 2}$ allele was similar to the *Fgf3*^{neo} allele, we first compared the phenotypes of adult homozygotes. Offspring of *Fgf3*$^{+/neo}$ and *Fgf3*$^{+/\Delta 2}$ intercrosses were observed and genotyped at weaning (~4 weeks postnatal). In both cases, although all three genotypes were recovered, the genotypic distribution deviated significantly from the normal Mendelian expectation (Figure 4.1B). Only 10% of the *Fgf3*$^{+/neo}$ intercross offspring and 9% of the *Fgf3*$^{+/\Delta 2}$ intercross offspring were homozygous mutant, showing that there is significant and similar lethality associated with both alleles. In addition, all homozygous mutants exhibited characteristic short, curly tails described previously (Figure 4.1B)(Mansour et al., 1993). Thus, the two *Fgf3* alleles behave similarly at the overt phenotypic level.

Some of the previously described *Fgf3*$^{neo/neo}$ animals had a weak or absent Preyer's reflex and exhibited circling behavior, which suggested auditory and vestibular dysfunction (Mansour et al., 1993). Therefore, we measured auditory brainstem response

(ABR) thresholds in each ear individually at approximately 6 weeks of age in animals of all three *Fgf3*$^{\Delta 2}$ genotypes. No significant differences in auditory thresholds were observed between wild type (n=7) and heterozygous (n=11) animals and all of these controls had normal behavior. In contrast, only one *Fgf3*$^{\Delta 2/\Delta 2}$ animal had normal thresholds in both ears and eight of nine *Fgf3*$^{\Delta 2/\Delta 2}$ animals had ABR thresholds that were significantly elevated (>2 standard deviations above the same side controls) in one (n=3) or both (n=5) ears (Figure 4.1C). Interestingly, all five bilaterally affected homozygous mutants showed circling behavior, whereas, the three unilaterally affected animals had only a slight head tilt. Histologic sections of inner ears isolated from a normal hearing control heterozygote showed typical gross morphology and normal cochlear structure (Figure 4.1D, D'). In contrast, inner ear sections of a deaf homozygote showed only rudimentary partitioning into distended cochlear and vestibular chambers. Nevertheless, the otic epithelium could be identified and showed evidence for sensory differentiation, albeit quite abnormal (Figure 4.1E, E'). Thus, as was concluded using morphologic studies of the *Fgf3*^{neo} homozygotes (Mansour et al, 1993), the *Fgf3*$^{\Delta 2}$ homozygotes have auditory and vestibular phenotypes that are incompletely penetrant and variably expressive.

Most *Fgf3* mutants show abnormal otic morphologies

Prior studies of *Fgf3*^{neo} homozygote relied on histologic sections to provide snapshots of the developing and adult inner ear phenotype (Mansour et al., 1993). To more clearly visualize the consequences of loss of *Fgf3* to inner ear morphogenesis, we filled *Fgf3* mutant inner ear epithelia with latex paint at E15.5, a stage when the normal mouse ear has attained its mature morphology (Figure 4.2A, B) (Morsli et al., 1998).

Figure 4.1 Gene targeting of *Fgf3* and phenotypes of *Fgf3* null adult mice

(A) Depiction of the wild type ($Fgf3^{+}$), originally targeted ($Fgf3^{neo}$) and newly targeted ($Fgf3^{\Delta 2}$) *Fgf3* alleles. Mouse genomic *Fgf3* DNA is depicted with solid lines; protein coding regions as open boxes, untranslated regions as solid boxes, the MC1Neo cassette as a dark grey box. An arrow indicates transcription orientation. (B) Genotypes at weaning of separate $Fgf3^{+/neo}$ and $Fgf3^{+/\Delta 2}$ intercrosses. Numbers and percent of total (in parentheses) wild type (+/+), heterozygous (+/neo or +/Δ2) and homozygous (neo/neo or Δ2/Δ2; photographs to the right) offspring are shown. (C) Auditory brainstem response threshold measurements for the three $Fgf3^{\Delta 2}$ genotypes. Average thresholds for left (L, blue) and right (R, red) ears of +/+ (n=7) and +/Δ2 (n=12) animals are shown as boxes with the bar indicating one standard deviation. Homozygous mutant (Δ2/Δ2) ABR measurements are presented as connected circles (left=blue, right=red) for individual animals, with numbers in parentheses indicating the total number of mutant animals with the specified phenotype. Low (D,E) and high (D',E') magnification views of hematoxylin and eosin-stained mid-modiolar sections of $Fgf3^{+/\Delta 2}$ (hearing, D,D') and $Fgf3^{\Delta 2/\Delta 2}$ (deaf, E,E') ears. Scale bar: 50 μm. oC, organ of Corti; sv, stria vascularis; tm, tectorial membrane.

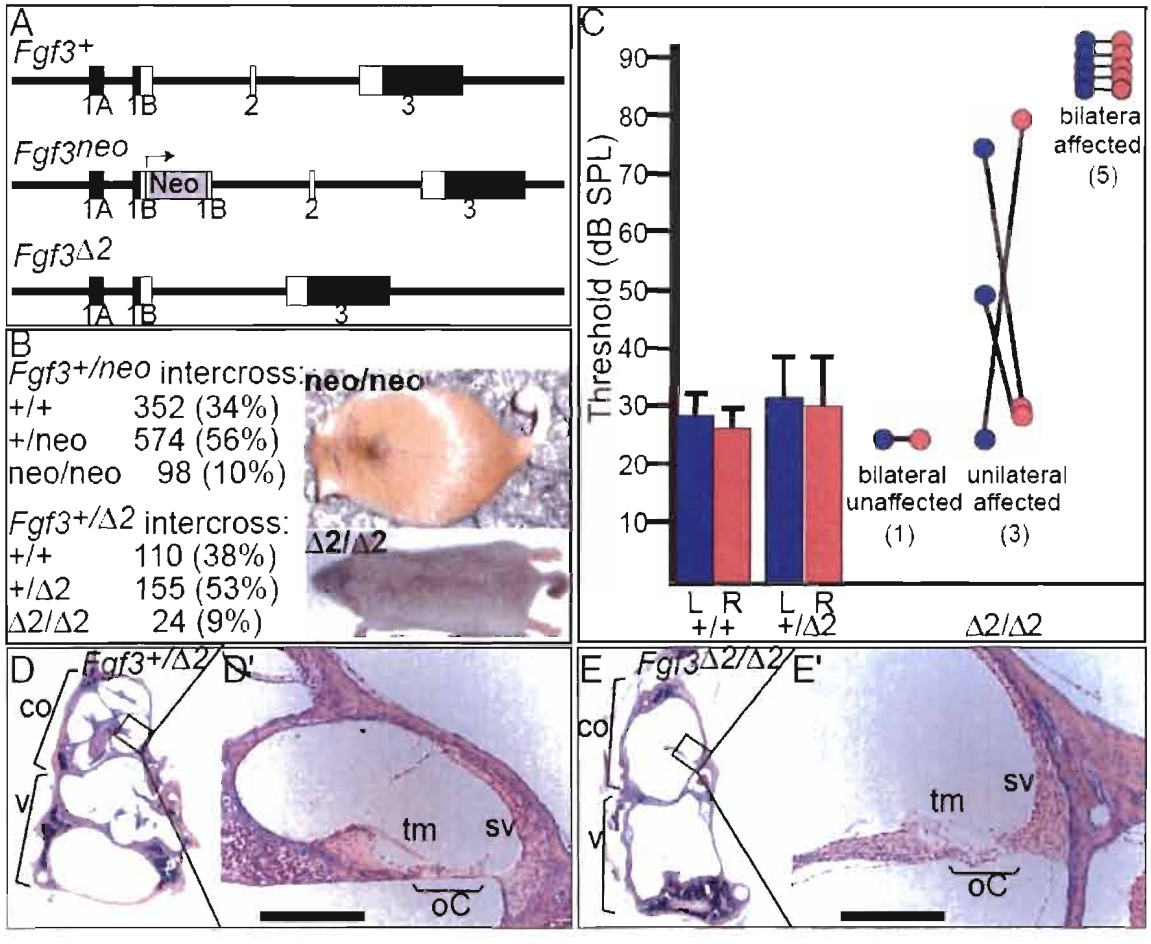
A
Fgf3+
1A 1B 2 3
Fgf3neo
Neo
1A 1B 1B 2 3
Fgf3Δ2
1A 1B 3
B
Fgf3+/neo intercross:
+/+ 352 (34%)
+/neo 574 (56%)
neo/neo 98 (10%)
Fgf3+/Δ2 intercross:
+/+ 110 (38%)
+/Δ2 155 (53%)
Δ2/Δ2 24 (9%)
neo/neo
Δ2/Δ2
C
Threshold (dB SPL)
90
80
70
60
50
40
30
20
10
bilatera
affected
(5)
bilateral
unaffected
(1)
unilateral
affected
(3)
L R L R
+/+ +/Δ2 Δ2/Δ2
D
Fgf3+/Δ2
co
v
D'
tm
sv
oC
E
Fgf3Δ2/Δ2
co
v
E'
tm
sv
oC

Both *Fgf3* alleles were studied, but no obvious differences between them were apparent, so the results for a total of 120 mutant ears were combined. At the gross anatomical level, 50 of 120 E15.5 mutant ears (42%) had a normal morphology, consistent with incomplete penetrance of the adult *Fgf3* auditory and vestibular phenotypes (Figure 4.2C). The remaining 70 (58%) showed graded morphologic defects that were assigned to groups based on the classification of *Gbx2* mutant ears (Lin et al., 2005).

Virtually all affected *Fgf3* mutant ears had a distended membranous labyrinth (n=65/70). In most of these ears, the swollen cochlear duct showed incomplete partition and poor coiling. All of the expected inner ear structures could be identified in Type 1a ears, but the endolymphatic duct appeared truncated dorsally, lacking the endolymphatic sac (Figure 4.2D, n=8/70). Type 1b ears were similar to Type 1a, but lacked entirely the EDS appendage (Figure 4.2E, n=12/70). Type II was the most common phenotype seen in affected *Fgf3* mutant ears and included absence of the EDS as well as the common crus, such that the anterior and posterior canals appeared as a single continuous canal (Figure 4.2F, n=32/70). In addition, the utricle and saccule were fused with the enlarged cochlear duct. Smaller numbers of homozygous mutants were even more severely affected. Type III ears had the EDS and common crus aplasia typical of Type II ears, together with absence or severe truncation of the anterior and posterior semicircular canals (Figure 4.2G, n=5/70). Most of the associated ampullae could be identified, but one ear lacked the posterior ampulla and another lacked the anterior ampulla. These ears all retained the lateral canal and ampulla. The Type III cochlear duct was severely malformed and shortened, with less than one coil. The Type IV phenotype was the most severe, with defects in all inner ear structures. The only discernable formation was a

cochlea-like structure (Figure 4.2H, n=7/70). Taken together, these data show that the abnormal morphologies of most *Fgf3* mutant ears included hypoplasia or aplasia of the EDS, swelling of the remaining labyrinth and in many cases, aplasia of the common crus; similar to the phenotypes seen in *Hoxa1*, *Mafb/Kr* and *Gbx2* mutant ears (Choo et al., 2006; Lin et al., 2005; Pasqualetti et al., 2001).

A small number of affected *Fgf3* mutant ears retained a normal endolymphatic appendage and were not distended. These were grouped into Type O (n=5/70). Three Type O ears lacked the posterior canal and ampulla (Figure 4.2I). One Type O ear lacked the lateral canal and one had an abnormally thickened and posteriorly positioned common crus (data not shown). Thus, Type O ears have dysmorphologies that are also seen in *Fgf10* and *Fgfr2b* null mutants (Ohuchi et al., 2005; Paulcy et al., 2003; Pirvola et al., 2000) and are similar to those of *Fgf10* hypomorphs (X. Wang, T. Wright and S. Mansour, unpublished observations).

Fgf3 is expressed in tissues relevant for otic vesicle morphogenesis

To correlate the spatial and temporal expression pattern of *Fgf3* with major steps in early inner ear morphogenesis, we detected *Fgf3* mRNA transcripts by in situ hybridization of E8.5-E10.5 embryos. Consistent with results described previously, at 3-4 somites *Fgf3* was expressed weakly in a dorsoventrally oriented stripe within the presumptive otic placode and strongly in the adjacent neurectoderm (data not shown, but see McKay et al., 1996; Wright and Mansour, 2003). Ectodermal expression of *Fgf3* disappeared from this region as the placode was induced and began to form a cup (5-12 somite stages, data not shown), whereas neurectodermal expression remained strong

Figure 4.2 The morphologies of *Fgf3* mutant inner ears fall into types of increasing severity

Representative lateral views of paint-filled inner ears from E15.5 control (A, B) and *Fgf3* homozygous mutants (C-I). The percentage of each type among total number of mutants (n=120) is indicated in the upper right-hand corner of each mutant panel. Types were defined as follows (asterisks indicate the expected locations of missing structures). Type Ia: the endolymphatic sac was truncated and the entire membranous labyrinth was distended. Type Ib: Similar to Type Ia, but the entire endolymphatic duct/sac was missing. Type II: In addition to the Type I abnormalities, the common crus was also absent. Type III: In addition to the Type II abnormalities, there was no anterior or posterior semicircular canal. Type IV: These ears consisted of only a distended cochlear duct. Type O: The majority of these ears lacked the posterior semicircular canal ampulla (H). Structures labeled in the wild type left ear (1A) are as follows: aa, anterior ampulla; asc, anterior semicircular canal; cc, common crus; cd, cochlear duct; ed, endolymphatic duct; es, endolymphatic sac; la, lateral ampulla; lsc, lateral semicircular canal; pa, posterior ampulla; psc, posterior semicircular canal; s, saccule; u, utricle.

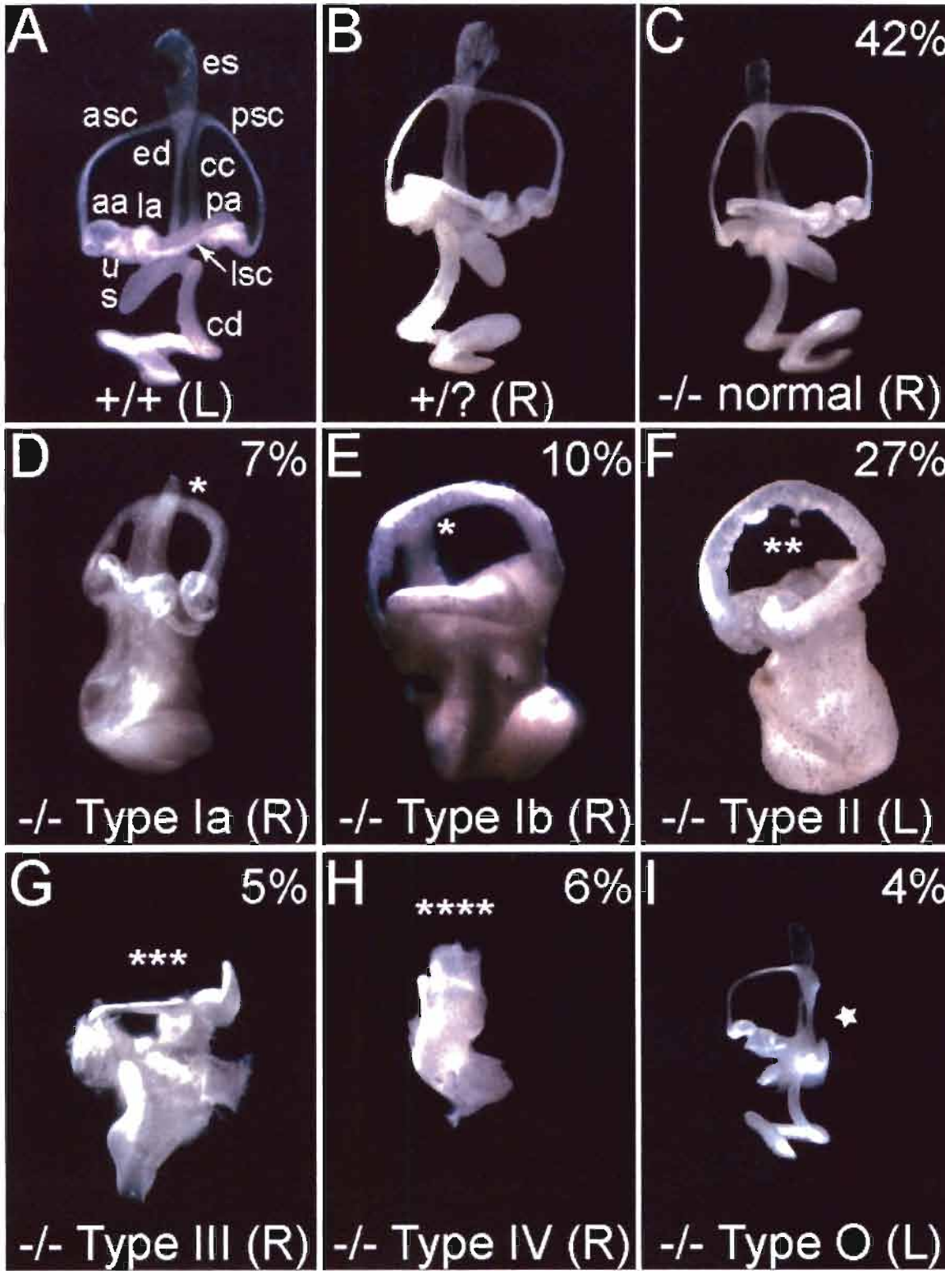
A
es
asc
psc
ed
cc
aa
la
pa
u
s
lsc
cd
+/+ (L)
B
+/? (R)
C
42%
-/- normal (R)
D
7%
*
-/- Type Ia (R)
E
10%
*
-/- Type Ib (R)
F
27%
**
-/- Type II (L)
G
5%
***
-/- Type III (R)
H
6%
****
-/- Type IV (R)
I
4%
-/- Type O (L)

throughout the otic cup stage and was restricted to r5 and r6 (Figure 4.3A-D and Mahmood et al., 1996; McKay et al., 1996; Wright and Mansour, 2003). As the otic cup closed to form the otic vesicle, *Fgf3* expression in the hindbrain became restricted to r6, and the expression was induced in an anteroventrolateral region of the otic vesicle and in early delaminating neuroblasts of the otic ganglion (Figure 4.3E-H). Endolymphatic duct outgrowth was first evident morphologically at the 27-somite stage, just as r6 expression of *Fgf3* diminished (Figure 4.3I-L). At E10.5, *Fgf3* expression was still found in the otic epithelium, localized to the anteroventrolateral patch of cells from which both neuroblasts and sensory cells are derived (Figure 4.3J, K) (Carney and Silver, 1983; Li et al., 1978). The neuroblasts of the otic ganglion, however, no longer expressed *Fgf3*. Thus, *Fgf3* shows a dynamic pattern of expression in the hindbrain, otic ganglion and prospective sensory domains during the transition from the otic cup stage to the initiation of endolymphatic duct outgrowth.

Dorsal otic gene expression is markedly affected in *Fgf3* mutants

The disruption of EDS development in the majority of abnormal *Fgf3* mutant ears suggested that molecular patterning of the dorsal otic epithelium could be perturbed. Thus, we analyzed the expression patterns of various dorsal otic markers by whole mount RNA in situ hybridization at E9.5-10.5, the stage when otic vesicle morphogenesis is initiated by endolymphatic duct outgrowth and when *Fgf3* expression is found in the hindbrain and initiates in the prosensory domain (Figure 4.3). Again, both *Fgf3* mutant alleles were examined, but no allele-specific differences were apparent, so the results were combined (see Figure 4.4). First, we analyzed genes expressed in the developing

Figure 4.3 *Fgf3* is expressed in tissues relevant for inner ear development

Whole-mount embryos probed with labeled *Fgf3* cDNA and sectioned in the transverse plane. (A,E,I,J) lateral views, (B,F) dorsal views. Somite pair numbers indicated at the lower left (A,E,I). Labeled lines in B,F,J indicate the locations of corresponding sections below. At 15s, *Fgf3* is found in r5 (C) and r6 (D). At 21s, *Fgf3* hindbrain expression is restricted to r6 (G,H). *Fgf3* is detected in the anteroventrolateral region of the otic epithelium at 21s as the cup closes to form the vesicle (G) and at 27s, when the endolymphatic duct becomes morphologically evident (K).

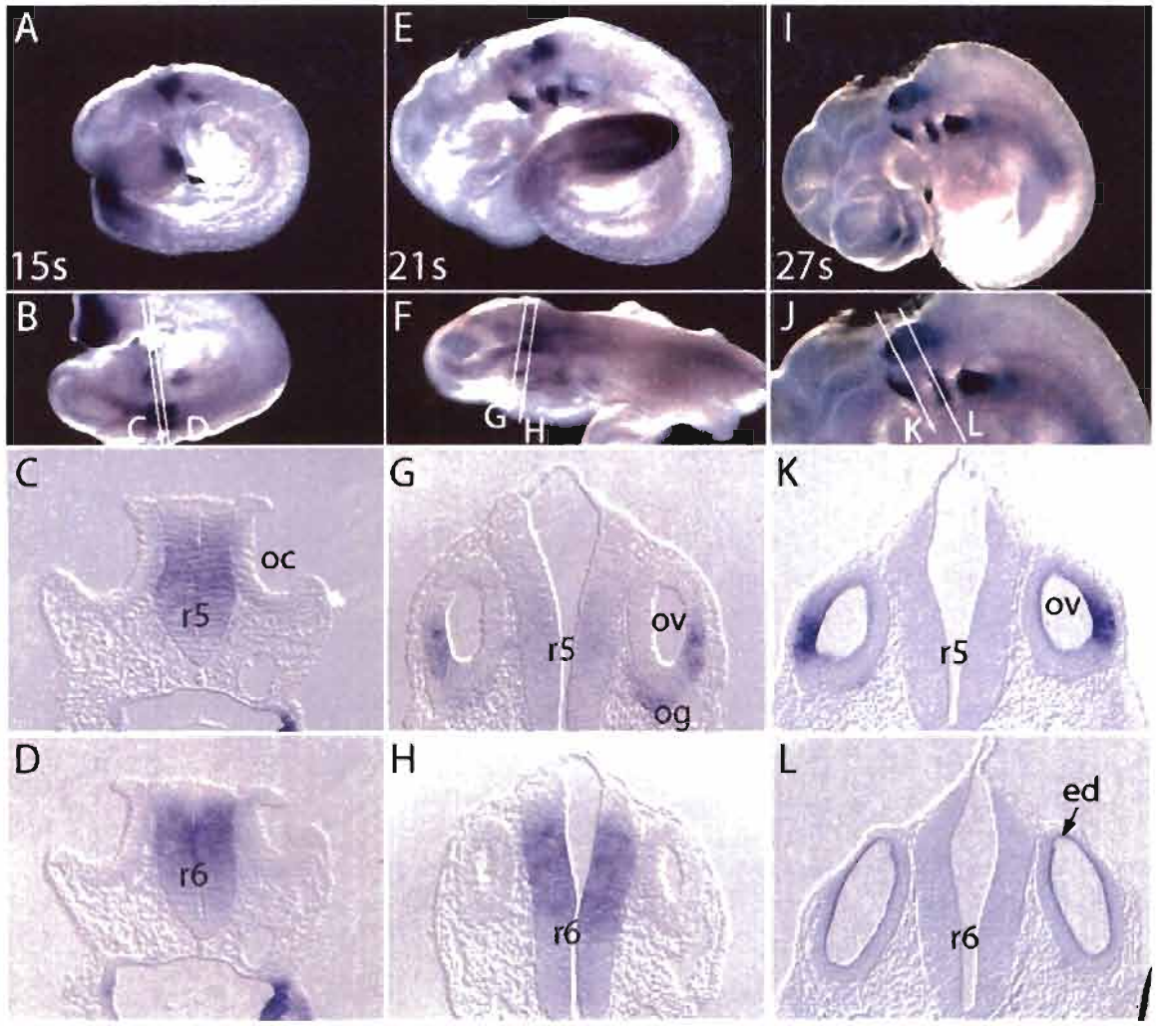
A
15s
E
21s
I
27s
B
C
D
F
G
H
J
K
L
C
oc
r5
G
r5
ov
og
K
r5
ov
D
r6
H
r6
L
ed
r6

Figure 4.4 Expression of dorsal inner ear markers in *Fgf3* control and mutant embryos reveals abnormal patterning starting at E10.5

Embryos were probed with *Gbx2* (A,B,C,D), *Dlx5* (E,F,G,H), *Wnt2b* (I,J), or *Hmx3* (K,L) and sectioned transversely as indicated by the white lines. At E9.5 *Gbx2* transcripts are detected in the dorsomedial otic region in 24s control (A') and 25s mutant (B') embryos. At E10.5, *Gbx2* otic expression is only detected in control (C'), but not mutant (D') embryos. At E9.5 (26s) there is no difference in *Dlx5* dorsolateral otic expression between control (E') and mutant (F') embryos. At E10.5, *Dlx5* transcripts are detected in control embryos in the broad dorsal otic domain (G'), but in mutant embryos there is a reduction in the extent of the *Dlx5* domain both medially and dorsally (H'). At E10.5, *Wnt2b* transcripts are detected in the dorsomedial otic epithelium in control (I') but not mutant (J') embryos. At E10.5, *Hmx3* is expressed in the dorsolateral otic ectoderm (K'). In mutant embryos there is a medial shift of the *Hmx3* expression domain (L'). Stage and genotype of each embryo are indicated in the lower left and right, respectively, of each panel. Abbreviations: ov, otic vesicle; nt, neural tube.


A
Gbx2
24s
+/-
A'
nt
ov
B
Gbx2
25s
-/-
B'
nt
ov
C
Gbx2
E10.5
+/+
C'
nt
ov
D
Gbx2
E10.5
-/-
D'
nt
ov
E
Dlx5
26s
+/-
E'
nt
ov
F
Dlx5
26s
-/-
F'
nt
ov
G
Dlx5
E10.5
+/-
G'
nt
ov
H
Dlx5
E10.5
-/-
H'
nt
ov
I
Wnt2b
35s
+/-
I'
nt
ov
J
Wnt2b
33s
-/-
J'
nt
ov
K
Hmx3
E10.5
+/-
K'
nt
ov
L
Hmx3
E10.5
-/-
L'
nt
ov

endolymphatic duct (*Wnt2b*) and/or whose mutant phenotypes included an EDS phenotype (*Gbx2* and *Dlx5*, Depew et al., 1999; Lin et al., 2005). In addition, we studied *Hmx3(Nkx5.1)*, a marker that broadly identifies the vestibular portion of the otocyst and is required redundantly with *Hmx2(Nkx5-2)* for vestibular development (Wang et al., 2001; Wang et al., 2004; Wang et al., 1998).

Gbx2 expression, which marks a broad dorsomedial region of the vesicle, including the prospective endolymphatic duct as well as more anterior and posterior dorsal otic tissue, was generally not affected in E9.5 *Fgf3* mutants (Figure 4.4A, A', B, B'). Only one such *Fgf3* mutant showed a slight reduction in the extent of the medial *Gbx2* domain (2/8 mutant ears, data not shown). The dorsomedial *Gbx2* expression domain persisted in E10.5 control inner ears (Figure 4.4C, C'). In contrast, otic *Gbx2* expression was strongly affected by E10.5 in the *Fgf3* mutant otocysts, which were noticeably smaller than control otocysts (Figure 4.4D, D'). In 8 of 12 *Fgf3* mutant ears no *Gbx2* staining was found in the otic epithelium (Figure 4.4D, D', right ear) and in the remaining 4 ears, weak staining was detected in the dorsomedial wall of the otocyst; however, the expression domain was severely reduced (Figure 4.4D', left ear). At E10.5, *Gbx2* was also expressed in the mid-hindbrain region (Lin et al., 2005). This *Gbx2* domain was not affected in any *Fgf3* mutant (Figure 4.4C, C', D, D').

Starting at E9.5, *Dlx5* was found in the dorsomedial region of the otocyst and its expression was comparable in *Fgf3* mutants and littermate controls (Figure 4.4E, E', F, F'). At E10.5, control specimens showed initiation of endolymphatic duct outgrowth and expression of *Dlx5* in the dorsal half of the otocyst (Figure 4.4G, G'). However, in *Fgf3* mutants there was a slight reduction in the extent of the *Dlx5* domain – both medially and

laterally, possibly due to the physical loss of the prospective endolymphatic duct domain (n=6/6 ears; Figure 4.4H, H').

Wnt2b expression was first detected in control specimens at E10.5 in the dorsomedial otic epithelium, marking the outgrowing endolymphatic duct (Figure 4.4I, I'). In contrast, *Wnt2b* expression was entirely absent from the dorsal otocyst in 4 out of 10 *Fgf3* mutant ears, and was severely reduced, showing only weak staining on the medial wall of the otocyst in 6 out of 10 mutant ears, suggesting a failure of endolymphatic duct specification (Figure 4.4J, J'). *Hmx3(Nkx5.1)* was expressed in the dorsolateral region of E10.5 control otocysts (Figure 4.4K, K') marking the prospective lateral canal plate region. In *Fgf3* mutants, however, *Hmx3(Nkx5.1)* expression shifted medially (n=8/8 ears; Figure 4.4L, L').

Ventrally expressed otic genes important for cochlear development are not affected by loss of *Fgf3*

As the cochlear ducts in affected E15.5 *Fgf3* mutant inner ears were greatly enlarged and poorly coiled, we analyzed the expression patterns of ventral otic markers. *Pax2* marks the ventromedial region of the otocyst and is important for the development of the cochlear duct (Burton et al., 2004; Torres et al., 1996). The expression pattern of *Pax2* was the same in control and *Fgf3* mutant embryos at E9.5 (Figure 4.5A, A', B, B') and E10.5 (Figure 4.5C, C', D, D'). At E10.5, *Otx2* is normally expressed in a posterior ventrolateral patch (Morsli et al., 1998) (Figure 4.5E, E'). In most of the *Fgf3* mutant ears, the *Otx2* expression pattern was unchanged (n=4/6 ears; Figure 4.5F, F'). However, in one specimen, the *Otx2* signal was reduced in one ear and absent in the other (data not shown).

Figure 5.5 Expression of ventral inner ear markers is similar in E10.5 *Fgf3* control and mutant embryos

Whole-mount embryos were probed with *Pax2* (A,B,C,D) or *Otx2* (E,F) and sectioned transversely as indicated by the white lines. *Pax2* expression in the ventromedial wall of the otocyst is similar in E9.5 and E10.5 control (A',C') and mutant (B',D') embryos. At E10.5, *Otx2* transcripts are detected in the posterior ventromedial otic epithelium in control (E') and mutant embryos (F'). Abbreviations: ov, otic vesicle; nt, neural tube.

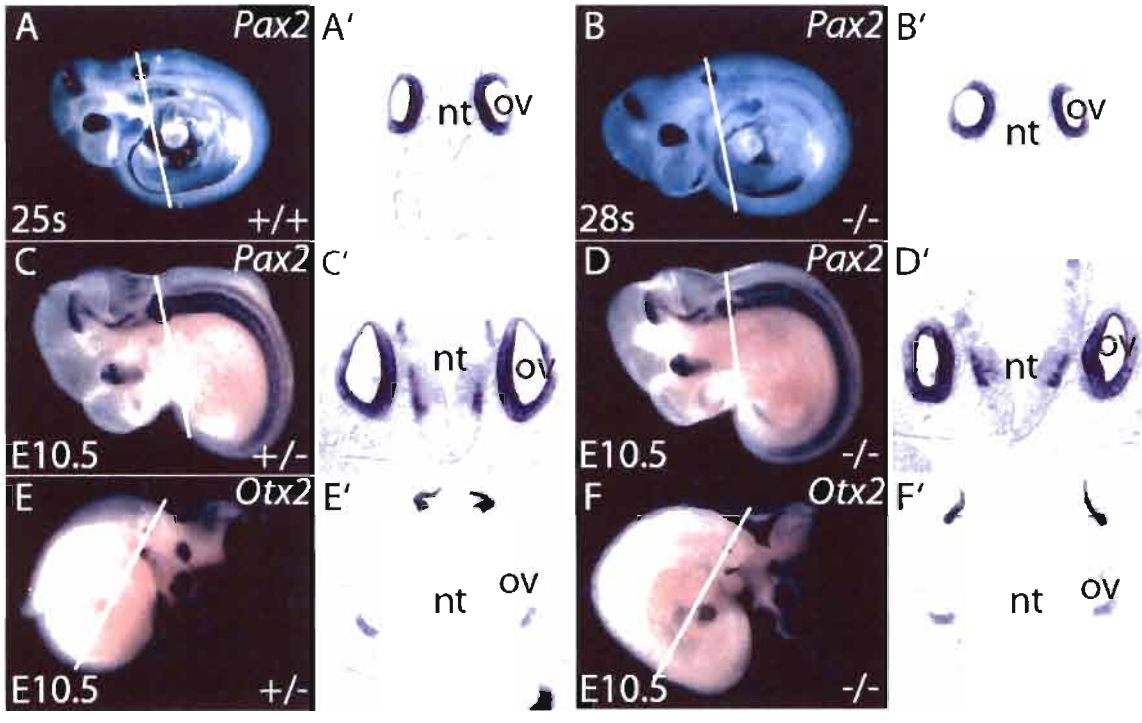
A
Pax2
25s
+/+
A'
nt
ov
B
Pax2
28s
-/-
B'
nt
ov
C
Pax2
E10.5
+/-
C'
nt
ov
D
Pax2
E10.5
-/-
D'
nt
ov
E
Otx2
E10.5
+/-
E'
nt
ov
F
Otx2
E10.5
-/-
F'
nt
ov

Markers of the developing posterior sensory domain are downregulated in *Fgf3* mutants

The expression of *Fgf3* in the anteroventrolateral otocyst domain that gives rise to sensory cells of the inner ear and to neuroblasts of the eighth ganglion, together with the reduced size of the eighth ganglion in E11.5 $Fgf3^{neo}$ mutants, suggested roles for *Fgf3* in sensory organ and ganglion development (Mansour et al., 1993). Therefore, we assessed the expression patterns of the sensory markers, *Lnfg* and *Bmp4* in *Fgf3* mutant otocysts. *Fgf10* expression was used as a marker of both neural and sensory domains (Pauley et al., 2003; Pirvola et al., 2000).

Lnfg is normally detected in the anteroventral region of the otocyst; in the precursors of the cochlear, saccular and utricular sensory organs (Morsli et al., 1998). No significant differences in the distribution of *Lnfg*-expressing cells were detected between control (Figure 4.6A, A', A") and mutant (Figure 4.6B, B', B'') specimens at E10.5. *Bmp4* is a marker of the presumptive cristae (Morsli et al., 1998). At E10.5, *Bmp4* expression was detected in two patches; one anterodorsolateral (Figure 4.6C, C') and the other posteroventral (Figure 4.6C, C"). The anterior *Bmp4* patch is thought to contain precursors of the superior and lateral cristae, whereas the posterior *Bmp4* domain (Figure 4.6C, arrowhead) is thought to house precursors of the posterior crista (Morsli et al., 1998). The anterior *Bmp4* domain was present in all E10.5 *Fgf3* mutant embryos (Figure 4.6D, D'); however, there was a reduction in the extent of the staining and a lateral shift of that domain. The posterior patch of *Bmp4* expression was not detected in 4 out of 6 mutant inner ears (Figure 4.6D, D"). Thus, loss of *Fgf3* can affect posterior crista development.

To assess the development of the eighth ganglion together with the prospective otic sensory domains, we examined *Fgf10* expression in control and mutant embryos at E9.5-10.5. At E9.5, *Fgf10* was expressed throughout the otic vesicle in control and *Fgf3* mutant embryos (data not shown). At E10.5, *Fgf10* was detected in the anterior pole of control vesicles, which includes the prospective sensory domain, and in the delaminating neuroblasts of the forming eighth ganglion (Figure 4.6E, E'). During this time, *Fgf10* was also expressed in a second, smaller posterior patch, which is destined to give rise to the posterior crista (Pauley et al., 2003) (Figure 4.6E, E"). The posterior patch of *Fgf10* expression appeared to be missing in 8 out of 12 *Fgf3* mutant ears (Figure 4.6F, arrowhead), but examination of sections showed that it was shifted anteriorly and slightly medially (Figure 4.6F"). Interestingly, there was also a medial shift of the *Fgf10*-expressing anterior domain in the otic epithelium together with a corresponding positional shift of the eighth ganglion in 6 of 12 mutant ears (Figure 4.6F').

Fgf3 negatively regulates *Wnt3a* in the region of rhombomeres 5 and 6

WNT signaling from the dorsal neural tube is required for dorsal otocyst patterning, with *Wnt1* and *Wnt3a* identified genetically as the specific (redundant) ligands (Riccomagno et al., 2005). The complete loss of all dorsal otic structures in *Wnt1/Wnt3a* mutants was attributed to the additive effects of losing both *Dlx5* and *Gbx2* expression from the dorsal otic epithelium. We therefore examined the expression patterns of *Wnt1* and *Wnt3a* in *Fgf3* mutants. As expected at E9.5, both *Wnt1* and *Wnt3a* marked the dorsal-most region of the developing neurectoderm in control embryos (Figure 4.7A, A', C, C') (Parr et al., 1993). *Wnt1* expression was unchanged in all three *Fgf3* mutants

Figure 4.6 Expression of sensory inner ear markers in E10.5 *Fgf3* control and mutant embryos reveals changes in the posterior sensory and neural patterning

Whole-mount embryos were probed with *Lfng* (A,B), *Bmp4* (C,D) and *Fgf10* (E,F) and sectioned transversely as indicated by white lines. Hybridization of *Lfng* to both E10.5 control (A',A") and mutant (B',B") embryos detects transcripts in the anteroventral region of the otocyst. At E10.5, *Bmp4* transcripts are detected in control embryos in both presumptive anterior/lateral cristae (C') and in the presumptive posterior cristae (C"). In *Fgf3* mutant embryos there is a slight reduction in the anterior *Bmp4* domain (D'), whereas the posterior domain is absent (D"). At E10.5, *Fgf10* is expressed in control embryos in the anterior region of the otocyst, which includes the prospective sensory domain and the delaminating neuroblasts of the forming eighth ganglion (E') and in the presumptive posterior cristae (E"). In *Fgf3* mutants there is a medial shift in the ganglion and anterior epithelial *Fgf10* expression (F') and a slight medial shift of the posterior patch of *Fgf10* expression (F"). Right and left ears in F' and F'' are photographed separately due to different sectioning angles. Arrowheads point to a posterior expression domain of *Bmp4* (C,D) and *Fgf10* (E,F). Brackets in E' and F' indicate the position of the eighth ganglion relative to the otocyst. Abbreviations: ov, otic vesicle; nt, neural tube.

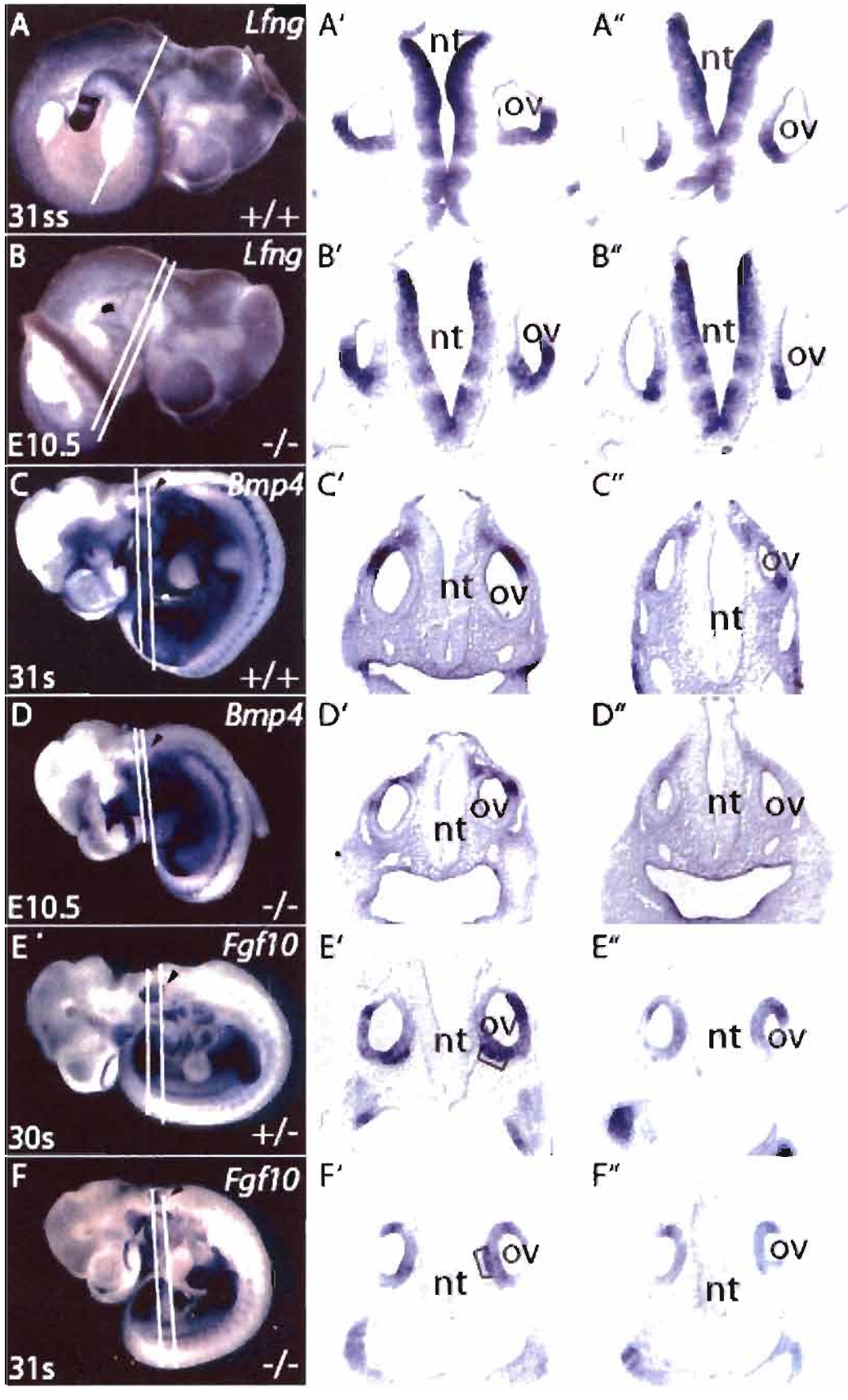
A
Lfng
31ss
+/+
A'
nt
ov
A''
nt
ov
B
Lfng
E10.5
-/-
B'
nt
ov
B''
nt
ov
C
Bmp4
31s
+/+
C'
nt
ov
C''
ov
nt
D
Bmp4
E10.5
-/-
D'
nt
ov
D''
nt
ov
E
Fgf10
30s
+/-
E'
nt
ov
E''
nt
ov
F
Fgf10
31s
-/-
F'
nt
ov
F''
ov
nt

examined (Figure 4.7B, B'). Surprisingly, all six *Fgf3* mutants examined showed a significant ventral expansion of the *Wnt3a* expression domain in the region of r5 and r6 (Figure 4.7D, D"), but not in hindbrain regions anterior (Figure 4.7D') or posterior (Figure 4.7D"') to the otic vesicle. These results show that *Fgf3* negatively regulates *Wnt3a* expression in the dorsal hindbrain.

Discussion

This study provides new morphologic data on the aberrant inner ear morphogenesis in *Fgf3* mutants. These data, together with an analysis of changes in molecular patterning of *Fgf3* mutant otic vesicles and a comparison of similar studies of other mutants that affect inner ear morphogenesis, allow us to propose a placement for *Fgf3* in the genetic cascade leading to EDS formation and draw parallels with human inner ear dysmorphogenesis and deafness.

The role of *Fgf3* in inner ear morphogenesis

Although homozygotes for another *Fgf3* null allele ($Fgf3^{tm1Sng}$, MGI:3027990) from which all coding sequences were removed, failed to show any inner ear phenotypes (Alvarez et al., 2003), we found that both *Fgf3* alleles examined here gave similar otic phenotypes. The phenotypic differences between our alleles and those of Alvarez and colleagues could arise either from differences in the genetic backgrounds of the alleles, or from the particular nature of the mutations, the contributions of which will require additional experiments.

We found that ears from both of our *Fgf3* mutant alleles exhibited a graded series of morphologies ranging from completely normal to complete loss of all vestibular

Figure 4.7 Hindbrain expression of *Wnt3a*, but not *Wnt1*, is expanded ventrally in r5 and r6 of *Fgf3* mutants

Whole-mount embryos were probed with *Wnt1* (A,B) and *Wnt3a* (C,D) and sectioned transversely, as indicated by the white lines. *Wnt1* is found in the dorsal-most region of the neural ectoderm in both control (A') and mutant (B') E 9.5 embryos. The *Wnt3a* probe also detects transcripts in the dorsal-most neural tube in E10.0 control (C', anterior, C", r5 and r6, C'", posterior) and mutant embryos (D', anterior, D", r5 and r6, D'", posterior), but there is a significant ventral expansion of *Wnt3a* expression in r5 and r6 (adjacent to the otic vesicle) of *Fgf3* mutants. Abbreviations: ov, otic vesicle; nt, neural tube.

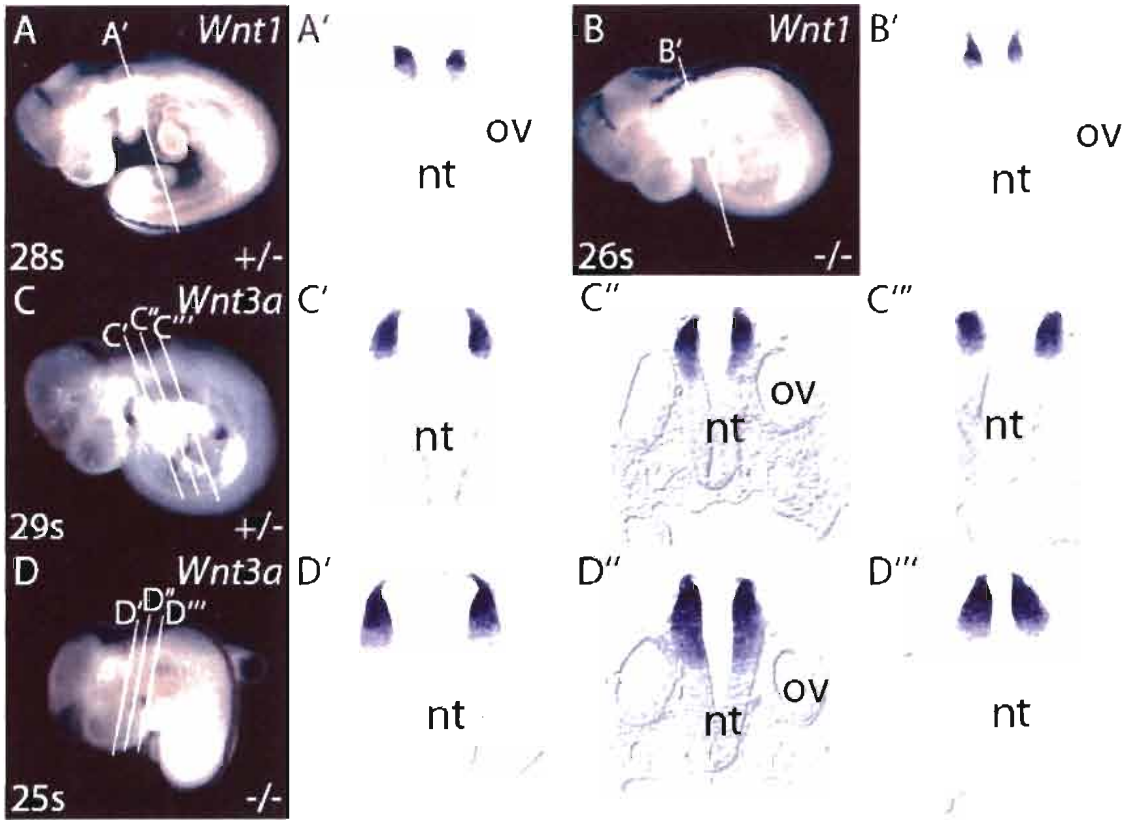
A
A′
Wnt1
A′
ov
nt
28s
+/-
B
B′
Wnt1
B′
ov
nt
26s
-/-
C
C′
C″
C‴
Wnt3a
C′
nt
C″
ov
nt
C‴
nt
29s
+/-
D
D′
D″
D‴
Wnt3a
D′
nt
D″
ov
nt
D‴
nt
25s
-/-

(dorsal) structures. Common to all affected *Fgf3* mutant ears, except for the small Type O group (discussed further below), was hypoplasia or aplasia of the EDS, global swelling of the entire otic epithelium and poor cochlear coiling. This association between abnormal EDS development and otic epithelial swelling is characteristic of both syndromic and non-syndromic human hearing loss (Wu et al., 2005) and is common to mouse mutations that disrupt the hindbrain signaling required for EDS induction (Choo et al., 2006; e.g. *Mafb/Kr*, *Hoxa1*, *Wnt1/Wnt3a* double mutants, Pasqualetti et al., 2001; Riccomagno et al., 2005) or disrupt transcription factors that are expressed early in the dorsal otic vesicle and are required for EDS formation (Lin et al., 2005; Merlo et al., 2002; e.g. *Gbx2*, *Hmx2*, *Hmx3*, *Dlx5*, *Dlx5/6*, Wang et al., 2001). Furthermore, mutations in *Foxi1*, which encodes an EDS-expressed transcription factor, or in its genetic target, *Slc26a4* (encoding the anion transporter, Pendrin), cause abnormal function of the EDS, leading to swelling of the entire endolymphatic space, loss of endocochlear potential and deafness (Everett et al., 2001; Hulander et al., 2003). Indeed, mutations in *SLC26A4* are a common cause of syndromic (Pendred) or non-syndromic deafness (Morton and Nance, 2006). These patients typically show enlarged vestibular aqueduct (the structure that houses the EDS) and may show Mondini defect (dilatation and incomplete partitioning of the cochlear duct), similar to the *Fgf3* Type Ia ears described here (Fitoz et al., 2007; Phelps et al., 1998). Thus it appears that any type of disruption to EDS development, whether leading to EDS hypoplasia or aplasia, as when hindbrain-expressed or early otic-expressed genes are disrupted, or to overall dilatation of a labyrinth that retains an EDS, as in the case of later acting EDS-expressed genes, can cause deafness. The EDS appendage has long been thought to participate in regulation of endolymph homeostasis, which is critical for

hearing function in the mature ear, but the phenotypes exhibited by *Fgf3* and the other mutants with similar dysmorphologies suggest that EDS function may be required from the earliest stages of inner ear morphogenesis. It is interesting to speculate that Meniere's disease, an adult condition that is characterized by both auditory and vestibular symptoms, and is associated with enlarged endolymphatic spaces (hydrops), could be caused either by mutations in EDS-expressed genes that function only after inner ear morphogenesis is complete or by mutations in "developmental" genes that, like *Fgf3*, have a wide spectrum of penetrance and expressivity.

EDS aplasia and general membranous swelling together with common crus aplasia was the most prevalent phenotypic complex observed in affected *Fgf3* mutant inner ears (Type II = 27%) and has also been noted in some *Hoxb1*, *Mafb/Kr* and *Gbx2* mutants (Choo et al., 2006; Lin et al., 2005; Pasqualetti et al., 2001). Such a phenotype has also been reported in the human population (Kim et al., 2004; Manfre et al., 1997), but its cause is unknown. If the EDS aplasia and consequent membranous swelling is explained by failure of FGF3-mediated signaling from the hindbrain to the dorsal otic vesicle, how might the common crus aplasia arise? Since the common crus is formed when two distinct central regions of the vertical canal plate fuse and then resorb to form distinct anterior and posterior canals, one possibility is that *Fgf3*, expressed from the developing cristae, normally functions relatively directly to limit the fusion boundaries or the process of cellular resorption. Alternatively, it could be that the abnormal swelling of the epithelium consequent to failed or incomplete induction of the EDS is itself the cause of excessive cellular fusion and/or resorption in the vertical canal plate. Given the diversity of mutant genes that cause common crus aplasia, most of which are not known

to be expressed in the otic epithelium, the latter possibility seems more likely. Conditional ablation of *Fgf3* in the otic epithelium vs. hindbrain (in progress) could help to address this issue.

Fgf3 signaling is required to maintain dorsal patterning of the otocyst

To understand the effects of the *Fgf3* mutations at the molecular level, we surveyed expression of regionally restricted otic vesicle genes in mutant embryos at a stage just prior to the first morphologic sign of aberrant vesicle development; namely at EDS induction. Generally speaking, dorsally expressed genes were affected (absent or shifted), whereas ventrally expressed marker genes were not strongly affected, suggesting that *Fgf3* is a component of the dorsal determination pathway and EDS specification (Figure 4.8). Just as the dysmorphologies of *Fgf3* mutant ears were similar to those of *Mafb/Kr*, *Hoxa1* and *Gbx2* mutants, so to were the trends for most of the molecular changes. Since *Mafb/Kr* and *Hoxa1* are required for *Fgf3* expression in the hindbrain (Carpenter et al., 1993; Frohman et al., 1993; McKay et al., 1996; Pasqualetti et al., 2001), and both *Mafb/Kr* and *Fgf3* are required for normal dorsal otic expression of *Gbx2*, (Choo et al., 2006 and this study), this places *Fgf3* between *Mafb/Kr* and *Gbx2* in the EDS induction pathway. However, since *Gbx2* expression in *Fgf3* mutants was only strongly affected at E10.5 and not at E9.5, a time when it is affected in *Wnt1/Wnt3a* double mutants, which have no dorsal development at all (Riccomagno et al., 2005), we suggest that WNTs provide the initiating signal for dorsal patterning of the otic vesicle, and that FGF3 directly or indirectly sustains or reinforces expression of dorsal otic genes. This may explain, at least in part, the reduced penetrance and severity of *Fgf3* otic

Figure 4.8 Model for FGF3 function in the initiation of otic morphogenesis

Oblique view of the developing hindbrain and otic vesicle during the initiation of otic morphogenesis. The model integrates present data with those published previously. Otic vesicle molecular patterning and morphogenesis is initiated by WNT signals provided redundantly by *Wnt3a* and *Wnt1* expressed from the roofplate (dark blue). This signal induces otic *Gbx2*, which in turn induces *Wnt2* and *Dlx5* at a minimum, and is required for dorsal outgrowth of the dorsal EDS anlage. *Fgf3*, induced in r5 and r6 by *Hoxa1* and *Mafb* (*Kr*), serves to maintain otic *Gbx2* and its downstream genes, but has no direct effect on ventral otic genes such as *Pax2* and *Otx2*. In addition, *Fgf3* prevents medial expansion of otic *Hmx3* and ventral expansion of hindbrain *Wnt3a*. The role of SHH in ventral otic patterning via induction of *Pax2* and *Otx2* is illustrated, but was not addressed here.

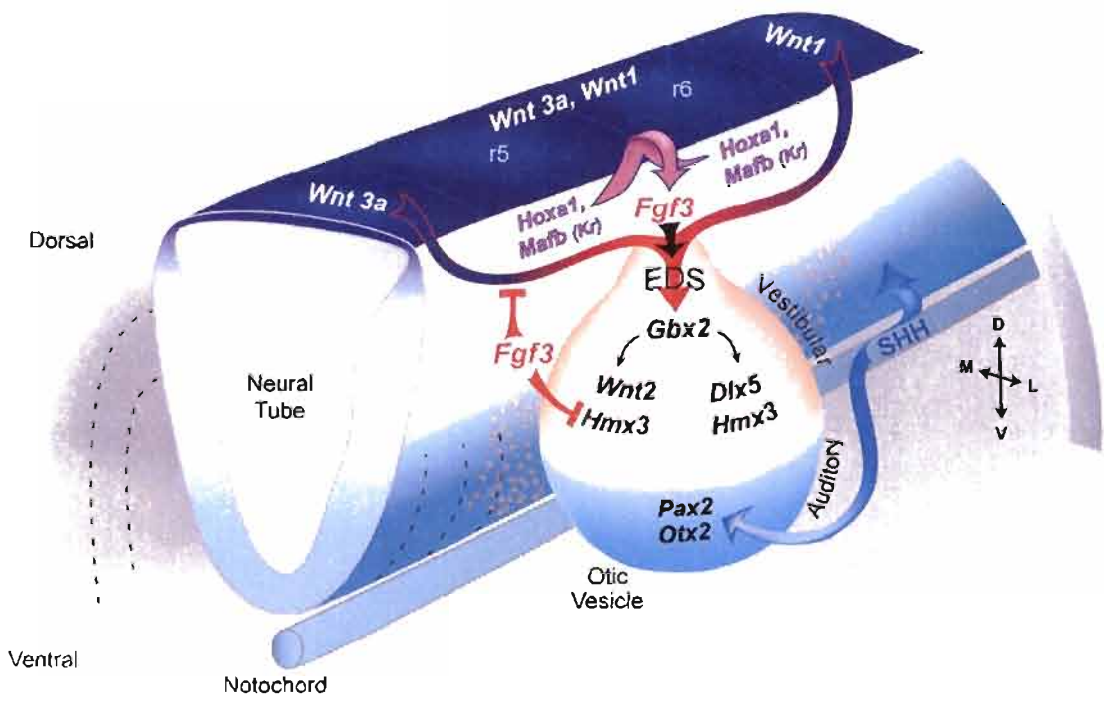
Wnt1
Wnt 3a, Wnt1
r6
r5
Hoxa1,
Mafb (Kr)
Wnt 3a
Hoxa1,
Mafb (Kr)
Fgf3
Dorsal
EDS
Vestibular
SHH
Fgf3
Gbx2
Neural
Tube
Wnt2
Hmx3
Dlx5
Hmx3
D
M
L
V
Auditory
Pax2
Otx2
Otic
Vesicle
Ventral
Notochord

morphologic and molecular phenotypes relative to those of *Gbx2*.

The expression of the other dorsally expressed otic genes downstream of *Gbx2* was also perturbed in *Fgf3* mutants. *Wnt2b*, the gene that most specifically marks the developing EDS, but the otic function of which is unknown, is absent from *Gbx2* mutant ears and was strongly reduced or absent from *Fgf3* mutant ears, consistent with the EDS defects in both mutants. *Dlx5* expression, which normally marks the entire dorsal half of the otocyst and is required for both EDS and semicircular canal development (Merlo et al., 2002), was also affected in both mutants, but in slightly different ways. In *Gbx2* mutants, *Dlx5* expression is lost from the entire dorsomedial domain, whereas in *Fgf3*mutants, the most ventral region of both the medial and lateral *Dlx5* domains were absent. This suggests that *Dlx5* is not likely to be a direct target of *Fgf3* signaling, but is downstream of *Gbx2* and in this instance is revealing the loss of the dorsomedial EDS domain from the vesicle and the consequent dorsal shifts of its most ventromedial and ventrolateral domains. Finally, *Hmx3* is expressed in the dorsolateral otocyst and subsequently in the semicircular canals and is required for canal, but not for EDS development (Wang et al., 2004). *Hmx3* expression is unchanged in *Gbx2* mutants (Lin et al., 2005) and very slightly down regulated in *Wnt1/Wnt3a* double mutants. In contrast, in *Fgf3* mutants there is a medial expansion of the *Hmx3* expression domain, suggesting that *Fgf3* may normally function directly to restrict expansion of *Hmx3* into the medial otocyst or may function indirectly by expanding the *Wnt3a* expression domain ventrally.

Fgf3 does not have a unique role in ventral patterning of the inner ear

Despite the abnormal cochlear development seen in *Fgf3* mutants, expression of *Pax2* and *Otx2*, ventral otic genes downstream of SHH signaling and necessary for cochlear development (Burton et al., 2004; Morsli et al., 1999; Riccomagno et al., 2002), were largely unaffected, except for one case of loss of *Otx2* expression. This was somewhat unexpected, given that both *Mafb/Kr* and *Gbx2* mutants show a medial expansion of otic *Otx2* expression (Choo et al., 2006; Lin et al., 2005). However, since *Fgf3* appears to be required to maintain, rather than to initiate *Gbx2* expression, it is possible that the early phase of *Gbx2* expression is sufficient to establish the *Otx2* domain and that FGF3, on its own, is not a major player in cochlear development. The possibility for redundant roles with *Fgf10*, such as occurs during otic induction, remains and will be tested using conditional mutants.

Fgf3 is required for posterior sensory domain genes and eighth ganglion development

The *Bmp4* and *Fgf10* posterior expression domains thought to mark the developing posterior ampullae were absent or shifted dorsomedially, respectively, in *Fgf3* mutants. Although the vast majority of *Fgf3* mutant ears had a phenotype that seemed most consistent with a loss of FGF3 signaling to properly induce the EDS, a very small number of affected mutants apparently underwent normal EDS induction, but nevertheless developed with abnormal or absent posterior semicircular canals (Type O). This phenotype is consistent with previous suggestions that FGF signals from the developing sensory patches induce nonsensory (canal) development (Chang et al., 2004)

and further suggests that *Fgf3* may participate in posterior sensory domain specification. However, to address this issue directly and to assess the relative contributions of *Fgf3* and *Fgf10* to posterior sensory and non-sensory development, analysis of double conditional mutants in which the hindbrain requirement for *Fgf3* in EDS induction is bypassed will be required.

As in the original study of *Fgf3* mutants, the otic ganglion, as marked in this study by *Fgf10* expression, was notably smaller in affected mutant ears. We also consistently observed a dorsal shift of the ganglion in affected ears, as if either the neurogenic domain itself or the expression domain for an otocyst-derived attractant for delaminating GVIII neuroblasts has shifted. It is interesting to note that a similar dislocation of the otic ganglion and the *Fgf3* expression domain was noted in studies of *Mafb*(*Kr*) mutants (McKay et al., 1996).

Crosstalk between WNTs and FGFs in inner ear development

Our results show that *Fgf3* negatively regulates *Wnt3a* in the region of r5 and r6, preventing a ventral expansion of *Wnt3a* transcripts. This suggests an important role for *Fgf3* not only in reinforcing the inductive effect of WNT signals on the dorsal otocyst, but also in regulating the localization of WNT signals to the dorsal-most region of the neural tube. Since WNT proteins are unlikely to diffuse over long distances, this localization may serve to limit the effects of WNT signals to the dorsal otic vesicle.

FGF/WNT cross-talk is emerging as an important mechanism to regulate various biological processes in different developmental systems (Dailey et al., 2005), including brain, tooth and kidney development (Moon et al., 1997). In some cases, the parallel

activation of FGF and WNT pathways causes developmental changes different from the individual effects of each factor, as exemplified by FGF/WNT interactions to specify neural and epidermal fate in the chick epiblast (Wilson et al., 2001). Evidence to support the role for FGFs in modulating WNT signaling comes from mouse genetic experiments showing that cross-regulation of FGF and WNT signaling is fundamental to normal skull development, when FGFs inhibit WNTs and subsequently osteoblast differentiation (Dailey et al., 2005). There also appear to be additional roles for crosstalk between the WNT and FGF pathways in otic development. During chick otic induction, mesodermal FGF19 induces neurectodermal expression of *Wnt8c* (Ladher et al., 2000). Both types of signals also participate in otic placode induction (Ladher et al., 2000; Ladher et al., 2005; Wright and Mansour, 2003) with WNT signals needed for stabilizing the otic placode cell state by enhancing and sensitizing the response of ectoderm to inductive FGF signaling (Ohyama et al., 2006). Given that WNT and FGF signaling pathway components continue to be expressed in the inner ear epithelia during the later stages of otic morphogenesis and sensory organ patterning and that roles for each pathway are beginning to be defined (Hayashi et al., 2007; Pirvola et al., 2002; Pirvola et al., 2004; Wang et al., 2006), it will not be surprising if further intersections between these pathways in the ear are uncovered.

Materials and methods

Fgf3 alleles and genotyping

All work with mice complied with protocols approved by the University of Utah Institutional Animal Care and Use Committee. The targeted $Fgf3^{neo}$ allele ($Fgf3^{tm1Mrc}$, MGI:1931059, originally designated $int\text{-}2^{neo}$) has been described previously and has an

insertion of a promoter-containing *Neo* gene in the first protein-coding exon (1B) (Mansour et al., 1993). A new *Fgf3* allele ($Fgf3^{\Delta 2}$), which has a deletion of exon 2, was generated by first targeting LoxP sites on either side of exon 2 to generate a conditional allele and then deleting the intervening DNA by exposing the conditional allele to CRE recombinase (X. Wang et al., manuscript in preparation). *Fgf3* transcripts produced from the $Fgf3^{\Delta 2}$ allele contain exon 1 spliced directly to exon 3, which is in a different frame. Thus they encode only the first 73 out of 245 FGF3 amino acids, including only the first 28 out of 137 amino acids of the FGF core homology domain.

Heterozygous intercrosses of each *Fgf3* allele were used to generate homozygous mutant embryos. Genotypes were determined by PCR amplification of yolk sac or tail DNA using 3-primer mixes that distinguish the mutant and wild type alleles. The $Fgf3^{neo}$ PCR genotyping assay was performed as described previously (Wright and Mansour, 2003). The $Fgf3^{\Delta 2}$ genotyping mix, containing primers 455C (5'-CTGCCTATGTGCTATATCCATGG-3'), 456C (5'-GTAGATGACTGAGTGTGTAGG-3') and 485B (5'-GGTTCCTCGATCAAACTCTGG-3'), produced a wild type band of 250 bp and a mutant band of 600 bp. PCR analysis was performed in 20 µl reactions amplified in an MJR thermal cycler for 35 cycles of 30 sec at 94°C, 20 sec at 60°C and 1 min at 72°C.

Paint-filling and RNA in situ hybridization

E15.5 embryos were cleared in methyl salicylate and the ears were filled through the saccule with white latex paint as described by Morsli et al. (1998). Otic vesicle and hindbrain marker genes were analyzed at E9.5-E10.5 (21-39 somite pairs) by whole mount RNA in situ hybridization using a panel of marker genes. Embryos were isolated

on the indicated days following detection of a vaginal plug and age-matched based on the total number of somite pairs. Digoxigenin-labeled probes were prepared, hybridized to the embryos and detected as described (Henrique et al., 1995). Antisense RNA probes were generated from plasmids for: *Pax2* (Dressler et al., 1990), *Dlx5* (Depew et al., 1999), *Gbx2* (Wassarman et al., 1997), *Hmx3(Nkx5.1)* (Merlo et al., 2002), *Lfng* (Morsli et al., 1998), *Fgf10* (Pauley et al., 2003), *Wnt1* (provided by Andy McMahon), *Wnt3a* (provided by Jeff Barrow), *Wnt2b* (provided by Elisabeth Grove), *Bmp4* (provided by Mario Capecchi), *Otx2* (provided by Laure Bally-Cuif). Embryos stained for analysis of gene expression were cryoprotected in sucrose and sectioned at 14 µm using a Leica CM1900 cryostat as described (Stark et al., 2000). Between two to six embryos of each genotype were analyzed for each probe.

Auditory brainstem response threshold measurements

Mice were anesthetized using 0.02 ml/g Avertin. Auditory brainstem response (ABR) thresholds for click stimuli (47 µsec duration, 29.3/sec) presented to each ear individually were determined using high frequency transducers controlled and analyzed by SmartEP software (Intelligent Hearing Systems) according to Zheng et al. (1999).

References

Alvarez, Y., Alonso, M. T., Vendrell, V., Zelarayan, L. C., Chamero, P., Theil, T., Bosl, M. R., Kato, S., Maconochie, M., Riethmacher, D. et al. (2003). Requirements for FGF3 and FGF10 during inner ear formation. *Development* **130**, 6329-38.

Bok, J., Bronner-Fraser, M. and Wu, D. K. (2005). Role of the hindbrain in dorsoventral but not anteroposterior axial specification of the inner ear. *Development* **132**, 2115-24.

Burton, Q., Cole, L. K., Mulheisen, M., Chang, W. and Wu, D. K. (2004). The role of Pax2 in mouse inner ear development. *Dev Biol* **272**, 161-75.

Carney, P. R. and Silver, J. (1983). Studies on cell migration and axon guidance in the developing distal auditory system of the mouse. *J Comp Neurol* **215**, 359-69.

Carpenter, E. M., Goddard, J. M., Chisaka, O., Manley, N. R. and Capecchi, M. R. (1993). Loss of Hox-A1 (Hox-1.6) function results in the reorganization of the murine hindbrain. *Development* **118**, 1063-75.

Chang, W., Brigande, J. V., Fekete, D. M. and Wu, D. K. (2004). The development of semicircular canals in the inner ear: role of FGFs in sensory cristae. *Development* **131**, 4201-11.

Choo, D., Ward, J., Reece, A., Dou, H., Lin, Z. and Greinwald, J. (2006). Molecular mechanisms underlying inner ear patterning defects in kreisler mutants. *Dev Biol* **289**, 308-17.

Dailey, L., Ambrosetti, D., Mansukhani, A. and Basilico, C. (2005). Mechanisms underlying differential responses to FGF signaling. *Cytokine Growth Factor Rev* **16**, 233-47.

Depew, M. J., Liu, J. K., Long, J. E., Presley, R., Meneses, J. J., Pedersen, R. A. and Rubenstein, J. L. (1999). Dlx5 regulates regional development of the branchial arches and sensory capsules. *Development* **126**, 3831-46.

Dressler, G. R., Deutsch, U., Chowdhury, K., Nornes, H. O. and Gruss, P. (1990). Pax2, a new murine paired-box-containing gene and its expression in the developing excretory system. *Development* **109**, 787-95.

Everett, L. A., Belyantseva, I. A., Noben-Trauth, K., Cantos, R., Chen, A., Thakkar, S. I., Hoogstraten-Miller, S. L., Kachar, B., Wu, D. K. and Green, E. D. (2001). Targeted disruption of mouse Pds provides insight about the inner-ear defects encountered in Pendred syndrome. *Hum Mol Genet* **10**, 153-61.

Fekete, D. M. (1999). Development of the vertebrate ear: insights from knochouts and mutants. *Trends Neusoscience* **22**, 263-269.

Fekete, D. M. and Wu, D. K. (2002). Revisiting cell fate specification in the inner ear. *Curr Opin Neurobiol* **12**, 35-42.

Fitoz, S., Sennaroglu, L., Incesulu, A., Cengiz, F. B., Koc, Y. and Tekin, M. (2007). SLC26A4 mutations are associated with a specific inner ear malformation. *Int J Pediatr Otorhinolaryngol* **71**, 479-86.

Frohman, M. A., Martin, G. R., Cordes, S. P., Halamek, L. P. and Barsh, G. S. (1993). Altered rhombomere-specific gene expression and hyoid bone differentiation in the mouse segmentation mutant, kreisler (kr). *Development* **117**, 925-36.

Hayashi, T., Cunningham, D. and Bermingham-McDonogh, O. (2007). Loss of FGFR3 leads to excess hair cell development in the mouse organ of Corti. *Dev Dyn* **in press**.

Henrique, D., Adam, J., Myat, A., Chitnis, A., Lewis, J. and Ish-Horowicz, D. (1995). Expression of a Delta homologue in prospective neurons in the chick. *Nature* **375**, 787-90.

Hulander, M., Kiernan, A. E., Blomqvist, S. R., Carlsson, P., Samuelsson, E. J., Johansson, B. R., Steel, K. P. and Enerback, S. (2003). Lack of pendrin expression leads to deafness and expansion of the endolymphatic compartment in inner ears of Foxi1 null mutant mice. *Development* **130**, 2013-25.

Hutson, M. R., Lewis, J. E., Nguyen-Luu, D., Lindberg, K. H. and Barald, K. F. (1999). Expression of Pax2 and patterning of the chick inner ear. *J Neurocytol* **28**, 795-807.

Kiernan, A. E., Steel, K. P. and Fekete, D. M. (2002). Development of the Mouse Inner Ear. Orlando, FL: Academic Press.

Kim, H. J., Song, J. W., Chon, K. M. and Goh, E. K. (2004). Common crus aplasia: diagnosis by 3D volume rendering imaging using 3DFT-CISS sequence. *Clin Radiol* **59**, 830-4.

Ladher, R. K., Anakwe, K. U., Gurney, A. L., Schoenwolf, G. C. and Francis-West, P. H. (2000). Identification of synergistic signals initiating inner ear development. *Science* **290**, 1965-7.

Ladher, R. K., Wright, T. J., Moon, A. M., Mansour, S. L. and Schoenwolf, G. C. (2005). FGF8 initiates inner ear induction in chick and mouse. *Genes Dev* **19**, 603-13.

Li, C. W., Van De Water, T. R. and Ruben, R. J. (1978). The fate mapping of the eleventh and twelfth day mouse otocyst: an in vitro study of the sites of origin of the embryonic inner ear sensory structures. *J Morphol* **157**, 249-67.

Lin, Z., Cantos, R., Patente, M. and Wu, D. (2005). *Gbx2* is required for the morphogenesis of the mouse inner ear: a downstream target of hindbrain signaling. *Development* **132**, 2309-2318.

Mahmood, R., Mason, I. J. and Morriss-Kay, G. M. (1996). Expression of Fgf-3 in relation to hindbrain segmentation, otic pit position and pharyngeal arch morphology in normal and retinoic acid-exposed mouse embryos. *Anat Embryol (Berl)* **194**, 13-22.

Manfre, L., Genuardi, P., Tortorici, M. and Lagalla, R. (1997). Absence of the common crus in Goldenhar syndrome. *AJNR Am J Neuroradiol* **18**, 773-5.

Mansour, S. L., Goddard, J. M. and Capecchi, M. R. (1993). Mice homozygous for a targeted disruption of the proto-oncogene int-2 have developmental defects in the tail and inner ear. *Development* **117**, 13-28.

McKay, I. J., Lewis, J. and Lumsden, A. (1996). The role of FGF-3 in early inner ear development: an analysis in normal and kreisler mutant mice. *Dev Biol* **174**, 370-8.

Merlo, G. R., Paleari, L., Mantero, S., Zerega, B., Adamska, M., Rinkwitz, S., Bober, E. and Levi, G. (2002). The Dlx5 homeobox gene is essential for vestibular morphogenesis in the mouse embryo through a BMP4-mediated pathway. *Dev Biol* **248**, 157-69.

Moon, R. T., Brown, J. D. and Torres, M. (1997). WNTs modulate cell fate and behavior during vertebrate development. *Trends Genet* **13**, 157-62.

Morsli, H., Choo, D., Ryan, A., Johnson, R. and Wu, D. K. (1998). Development of the mouse inner ear and origin of its sensory organs. *J Neurosci* **18**, 3327-35.

Morsli, H., Tuorto, F., Choo, D., Postiglione, M. P., Simeone, A. and Wu, D. K. (1999). Otx1 and Otx2 activities are required for the normal development of the mouse inner ear. *Development* **126**, 2335-43.

Morton, C. C. and Nance, W. E. (2006). Newborn hearing screening--a silent revolution. *N Engl J Med* **354**, 2151-64.

Ohuchi, H., Yasue, A., Ono, K., Sasaoka, S., Tomonari, S., Takagi, A., Itakura, M., Moriyama, K., Noji, S. and Nohno, T. (2005). Identification of cis-element regulating expression of the mouse Fgf10 gene during inner ear development. *Dev Dyn* **233**, 177-87.

Ohyama, T., Mohamed, O. A., Taketo, M. M., Dufort, D. and Groves, A. K. (2006). Wnt signals mediate a fate decision between otic placode and epidermis. *Development* **133**, 865-75.

Parr, B. A., Shea, M. J., Vassileva, G. and McMahon, A. P. (1993). Mouse Wnt genes exhibit discrete domains of expression in the early embryonic CNS and limb buds. *Development* **119**, 247-61.

Pasqualetti, M., Neun, R., Davenne, M. and Rijli, F. M. (2001). Retinoic acid rescues inner ear defects in Hoxa1 deficient mice. *Nat Genet* **29**, 34-9.

Pauley, S., Wright, T. J., Pirvola, U., Ornitz, D., Beisel, K. and Fritzsch, B. (2003). Expression and function of FGF10 in mammalian inner ear development. *Dev Dyn* **227**, 203-15.

Phelps, P. D., Coffey, R. A., Trembath, R. C., Luxon, L. M., Grossman, A. B., Britton, K. E., Kendall-Taylor, P., Graham, J. M., Cadge, B. C., Stephens, S. G. et

al. (1998). Radiological malformations of the ear in Pendred syndrome. *Clin Radiol* **53**, 268-73.

Pirvola, U., Spencer-Dene, B., Xing-Qun, L., Kettunen, P., Thesleff, I., Fritzsch, B., Dickson, C. and Ylikoski, J. (2000). FGF/FGFR-2(IIIb) signaling is essential for inner ear morphogenesis. *J Neurosci* **20**, 6125-34.

Pirvola, U., Ylikoski, J., Trokovic, R., Hebert, J. M., McConnell, S. K. and Partanen, J. (2002). FGFR1 is required for the development of the auditory sensory epithelium. *Neuron* **35**, 671-80.

Pirvola, U., Zhang, X., Mantela, J., Ornitz, D. M. and Ylikoski, J. (2004). Fgf9 signaling regulates inner ear morphogenesis through epithelial-mesenchymal interactions. *Dev Biol* **273**, 350-60.

Riccomagno, M. M., Martinu, L., Mulheisen, M., Wu, D. K. and Epstein, D. J. (2002). Specification of the mammalian cochlea is dependent on Sonic hedgehog. *Genes Dev* **16**, 2365-78.

Riccomagno, M. M., Takada, S. and Epstein, D. J. (2005). Wnt-dependent regulation of inner ear morphogenesis is balanced by the opposing and supporting roles of Shh. *Genes Dev* **19**, 1612-23.

Stark, M. R., Biggs, J. J., Schoenwolf, G. C. and Rao, M. S. (2000). Characterization of avian frizzled genes in cranial placode development. *Mech Dev* **93**, 195-200.

Torres, M., Gomez-Pardo, E. and Gruss, P. (1996). Pax2 contributes to inner ear patterning and optic nerve trajectory. *Development* **122**, 3381-91.

Wang, W., Chan, E. K., Baron, S., Van de Water, T. and Lufkin, T. (2001). Hmx2 homeobox gene control of murine vestibular morphogenesis. *Development* **128**, 5017-29.

Wang, W., Grimmer, J. F., Van De Water, T. R. and Lufkin, T. (2004). Hmx2 and Hmx3 homeobox genes direct development of the murine inner ear and hypothalamus and can be functionally replaced by Drosophila Hmx. *Dev Cell* **7**, 439-53.

Wang, W., Van De Water, T. and Lufkin, T. (1998). Inner ear and maternal reproductive defects in mice lacking the Hmx3 homeobox gene. *Development* **125**, 621-34.

Wang, Y., Guo, N. and Nathans, J. (2006). The role of Frizzled3 and Frizzled6 in neural tube closure and in the planar polarity of inner-ear sensory hair cells. *J Neurosci* **26**, 2147-56.

Wassarman, K. M., Lewandoski, M., Campbell, K., Joyner, A. L., Rubenstein, J. L., Martinez, S. and Martin, G. R. (1997). Specification of the anterior hindbrain and

establishment of a normal mid/hindbrain organizer is dependent on Gbx2 gene function. *Development* **124**, 2923-34.

Wilkinson, D. G., Peters, G., Dickson, C. and McMahon, A. P. (1988). Expression of the FGF-related proto-oncogene int-2 during gastrulation and neurulation in the mouse. *Embo J* **7**, 691-5.

Wilson, S. I., Rydstrom, A., Trimborn, T., Willert, K., Nusse, R., Jessell, T. M. and Edlund, T. (2001). The status of Wnt signalling regulates neural and epidermal fates in the chick embryo. *Nature* **411**, 325-30.

Wright, T. J. and Mansour, S. L. (2003). Fgf3 and Fgf10 are required for mouse otic placode induction. *Development* **130**, 3379-90.

Wu, C. C., Chen, Y. S., Chen, P. J. and Hsu, C. J. (2005). Common clinical features of children with enlarged vestibular aqueduct and Mondini dysplasia. *Laryngoscope* **115**, 132-7.

Zheng, Q. Y., Johnson, K. R. and Erway, L. C. (1999). Assessment of hearing in 80 inbred strains of mice by ABR threshold analyses. *Hear Res* **130**, 94-107.

CHAPTER 5

CONDITIONAL INACTIVATION OF FGF3

Introduction

It was shown previously that mice homozygous for the *Fgf3*^{neo} null allele have defects of inner ear morphogenesis that are incompletely penetrant and variably expressive (Mansour et al., 1993). We have recently generated new morphologic data on the aberrant inner ear morphogenesis in *Fgf3* mutants and presented a more detailed analysis of the inner ear dysmorphology together with an analysis of otic marker genes using the previously described *Fgf3*^{neo} allele (Mansour et al., 1993) and a newly targeted *Fgf3*$^{\Delta 2}$ allele. We showed that the two mutant alleles are equivalent, and homozygous mutants have variably penetrant and expressive inner ear morphologies that are characterized most typically by loss of the endolymphatic duct and common crus, dilatation of the remaining epithelium, and poor coiling of the cochlea. In addition, a very small number of mutants had normal endolymphatic duct and cochlear development, but lacked the posterior semicircular canal. The initial molecular patterning of *Fgf3* mutant otocysts was normal, but by E10-E10.5 these ears lacked or had reduced domains of dorsally expressed otic genes, suggesting a loss of the cells fated to form the endolymphatic duct and sac (EDS). Ventrally expressed genes important for cochlear development were not affected, but markers of the developing vestibular sensory domains, particularly those expressed in the posterior region of the vesicle were

downregulated or absent and the eighth ganglion was reduced and displaced dorsomedially. Taken together, our results suggest that *Fgf3* is required for the dorsal otic patterning and functions, albeit largely redundantly, in the subsequent sensory patch control of nonsensory development (Chapter 4).

The results of complete inactivation of *Fgf3* in the germline clearly demonstrate that *Fgf3* plays a role in otic development (Mansour et al., 1993), however, it remains unclear which source(s) of *Fgf3* is(are) required. *Fgf3* is expressed in at least three sites that have relevance to inner ear development: the otic placode, rhombomeres 5 and 6 of the hindbrain, and the neurogenic region of the otocyst. It can be hypothesized that *Fgf3* signaling plays distinct roles in different tissues during otic development; the hindbrain being a critical site of *Fgf3* expression, particularly for induction of the endolymphatic duct, and otic-expressed *Fgf3* being required for neuronal differentiation or migration from the otic epithelium. To elucidate the tissue-specific roles for *Fgf3* in inner ear morphogenesis, we have utilized Cre/loxP technology and classical genetic mosaic analysis to inactivate *Fgf3* separately in each of the three inner ear-relevant expression sites.

The use of a conditional strategy allows for analysis of the effects of loss of *Fgf3* signaling in a tissue-specific and temporal fashion. Several appropriate enhancer elements that drive CRE-recombinase expression independently in patterns that overlap with various *Fgf3* expression domains are available. These include *Pax2-Cre* (otic placode), *Foxg1-Cre* (otic vesicle), *Wnt-1-Cre* (dorsal hindbrain), *Hoxb1-Cre* (hindbrain), and *Hoxa3-Cre* (hindbrain). Using these different temporally and spatially restricted *Cre*-drivers, we were able to conditionally inactivate *Fgf3* in different domains of expression.

We show that *Fgf3* signaling from the early placode and the neurogenic region of the otocyst does not play a unique role in otic morphogenesis. Our results also indicate that deleting *Fgf3* throughout the hindbrain or in its dorsal most region at the period immediately prior to the observed *Fgf3* morphologic defects does not phenocopy the null phenotype, suggesting an earlier requirement for the hindbrain-expressed *Fgf3*.

Results

Fgf3 is expressed in tissues relevant for otic vesicle morphogenesis

To correlate the spatial and temporal expression pattern of *Fgf3* with major steps in early inner ear morphogenesis, we detected *Fgf3* mRNA transcripts by in situ hybridization of E8.5-E10.5 embryos. Consistent with results described previously, at 3-4 somites *Fgf3* was expressed weakly in a dorsoventrally oriented stripe within the presumptive otic placode and strongly in the adjacent neurectoderm (data not shown, but see McKay et al., 1996; Wright and Mansour, 2003). Ectodermal expression of *Fgf3* disappeared from this region as the placode was induced and began to form a cup (10-12 somite stages, data not shown), whereas neurectodermal expression remained strong throughout the otic cup stage and was restricted to r5 and r6 (Figure 4.3A-D and Mahmood et al., 1996; McKay et al., 1996; Wright and Mansour, 2003). As the otic cup closed to form the otic vesicle, *Fgf3* expression in the hindbrain became restricted to r6. In addition, *Fgf3* expression was induced in an anteroventrolateral region of the otic vesicle and in early delaminating neuroblasts of the otic ganglion (Figure 4.3E-H). Endolymphatic duct outgrowth was first evident morphologically at the 27-somite stage, just as r6 expression of *Fgf3* diminished (Figure 4.3I-L). At E10.5, *Fgf3* expression was

still found in the otic epithelium, localized to the anteroventrolateral patch of cells from which both neuroblasts and sensory cells are derived (Figure 4.3J,K) (Carney and Silver, 1983; Li et al., 1978). The neuroblasts of the otic ganglion, however, no longer expressed *Fgf3*. Thus, *Fgf3* shows a dynamic pattern of expression in the otic placode, hindbrain, otic ganglion, and prospective sensory domains during the transition from the otic cup stage to the initiation of endolymphatic duct outgrowth.

Conditional inactivation of *Fgf3* in the otic placode, hindbrain, and the neurogenic region of the otocyst

Having generated a detailed analysis of the nature of inner ear malformations in *Fgf3* mutants, we set out to elucidate the tissue-specific roles for *Fgf3* in inner ear morphogenesis. A conditional *Fgf3* allele ($Fgf3^{flox}$) was generated by targeting LoxP sites on either side of exon 2 (X. Wang et al., manuscript in preparation). In the absence of *Cre*, mice homozygous for the *Fgf3* conditional allele are fertile and indistinguishable from control wild-type mice (data not shown). For removal of *Fgf3* in a tissue-specific manner, we took advantage of previously described *Cre* drivers (Figure 5.1A). To remove *Fgf3* in the developing otic placode, a *Pax2-Cre* transgenic allele was utilized (Ohyama and Groves, 2004). In the presence of ROSA26 reporter, the lineage of *Pax2-Cre* expressing cells can be seen throughout the placode (Figure 5.1B). However, in a *Pax2-Cre* background, *Fgf3* would be deleted throughout the otic region, preventing us from identifying distinct roles of the placodal versus late-onset otic vesicle *Fgf3* expression. Therefore, to delete *Fgf3* in the neurogenic region of the otocyst we used the *Foxg1-Cre* targeted line that becomes active at embryonic day (E) 9.5 (Hebert and McConnell, 2000). In ROSA26 reporter mice, *Foxg1-Cre* recombinase activated

ß- galactoside (ß-gal) expression throughout the otic epithelium starting at the vesicle stage (Figure 5.1C). For removal of *Fgf3* in the dorsal hindbrain, we utilized the *Wnt1-Cre* transgenic driver (Chai et al., 2000). Lineage of *Wnt1-Cre*-expressing cells was determined in a ROSA26 background (Soriano, 1999) and we confirmed expression in the dorsal neural tube at E9.5 (Figure 5.1D), a stage immediately prior to the observed *Fgf3* inner ear defects. To conditionally remove *Fgf3* in rhombomeres 5 and 6 of the hindbrain, *Hoxb1 IRES-Cre* (Arenkiel et al., 2003) and *Hoxa3 IRES-Cre* (Bunting et al., 1999) *Cre* mouse lines were utilized. In the presence of ROSA26, *Hoxb1-Cre* recombinase expression activated ß-gal expression diffusely in rhombomeres 5 and 6, adjacent to the otic vesicle at E9.5 (Figure 5.1E). *Hoxa3-Cre* lineage was detected throughout the same region earlier, beginning with the otic cup stage at E8.75 (Figure 5.1F). These results suggest that *Hoxb1* and *Hoxa3* trigger excision of *Fgf3* in the hindbrain in a similar spatial fashion, however, to variable extents; only a subset of cells in the hindbrain expresses *Hoxb1-Cre* recombinase (Figure 5.1E, F). The differential activity of all the described *Cre* drivers allowed us to define the limits of *Fgf3* expression needed for otic morphogenesis.

To generate conditional mutants with the various *Cre* drivers, crosses were set up between $Fgf3^{\Delta 2/+}$, *Cre* males and $Fgf3^{flox/flox}$ females. The efficiency of $Fgf3^{flox}$ allele recombination was demonstrated by crossing it to a *Cre* deleter line (refer to Chapter 4), leading to recombination in all cells, resulting in a complete absence of *Fgf3* protein and the exact phenocopy of the original *Fgf3* null mutant (Mansour et al., 1993).

Figure 5.1 *Cre* drivers used for tissue-specific ablation of *Fgf3*

(A) Schematic representation of *Fgf3* (left) and tissue-specific *Cre* (right) alleles used to generate conditional mutants of *Fgf3*. (B-F) Schematic depiction of half-transverse sections taken through the generic inner ear forming region (right) with *Fgf3* expression domains indicated in red in the placode (B), neurogenic region of the otocyst (C) and hindbrain (D-E). To the left are transverse sections through the otic region in mouse embryos harboring the *Pax2-Cre* (B), *Foxg1-Cre* (C), *Wnt1-Cre* (D), *Hoxb1-Cre* (E), *Hoxa3-Cre* (F) and ROSA26 alleles reacted with X-Gal. Abbreviations: nt, neural tube; ov, otic vesicle.

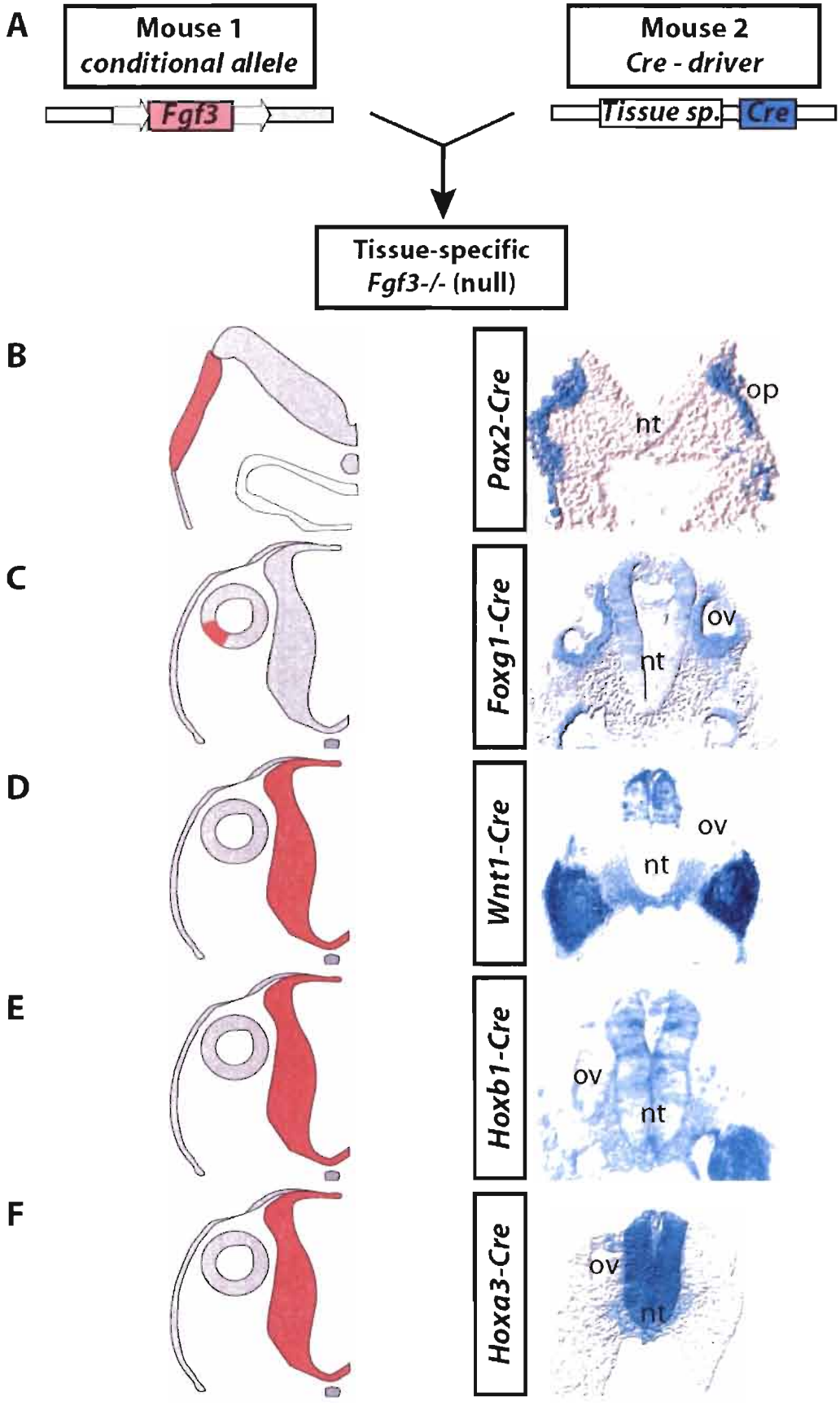
A
Mouse 1
conditional allele
Fgf3
Mouse 2
Cre - driver
Tissue sp.
Cre
Tissue-specific
Fgf3-/- (null)
B
Pax2-Cre
op
nt
C
Foxg1-Cre
ov
nt
D
Wnt1-Cre
ov
nt
E
Hoxb1-Cre
ov
nt
F
Hoxa3-Cre
ov
nt

Phenotypic and marker gene expression analysis in *Fgf3* conditional mutants

Once *Fgf3* conditional animals were generated, their behavior was analyzed at the overt phenotypic level. *Fgf3* germline null animals often exhibit circling behavior of have a tilted head indicative of vestibular dysfunction. In all cases, the conditional mutant animals behaved similarly to wild type. Interestingly both *Hoxb1-Cre/Fgf3* and *Hoxa3-Cre/Fgf3* conditional mutants exhibited characteristic short, curly tails described previously (Figure 4.1B)(Mansour et al., 1993), demonstrating the efficiency of the Cre/loxP system, as in these mutants *Fgf3* is presumably being removed from the primitive streak and/or tail bud mesoderm (data not shown).

Seventy percent of the *Fgf3* null mutant ears described in a previous chapter showed hearing loss. Therefore, we measured auditory brainstem response (ABR) thresholds in each ear individually at approximately 6 weeks of age in *Fgf3* conditional mutant animals generated with the different *Cre* drivers. No significant differences in auditory thresholds were observed between $Fgf3^{\Delta 2/flox}$, *Cre-/-* (n=3) and conditional (n=10, each *Cre*-deleted line) animals, which showed normal thresholds (from 15dB to 25dB) in both ears. These data suggest that inner ear auditory function is normal in the conditional mutants.

To determine whether there might be mild patterning defects in *Fgf3* conditional mutants, we surveyed expression of the two regionally restricted otic vesicle genes, *Gbx2* and *Fgf10*. Dorsally expressed *Gbx2* was strongly affected by E10.5 in the *Fgf3* null mutant otocysts (Figure 4.4C', D'). In addition, the eighth ganglion was reduced and displaced dorsomedially, as marked by *Fgf10* expression, together with a shift of the

Fgf10-expressing anterior domain in the otic epithelium (Figure 4.6E', F'). To determine whether otic molecular patterning is disturbed in *Fgf3* conditional mutants, the expression patterns of *Gbx2* and *Fgf10* were analyzed by whole mount RNA in situ hybridization at E10.5. *Gbx2* expression, which marks a broad dorsomedial region of the vesicle, including the prospective endolymphatic duct as well as more anterior and posterior dorsal otic tissue (Figure 5.2A, A'), was not affected in any *Fgf3* conditional mutants analyzed (n=3, each *Cre*-deleted line) (Figure 5.2C, C', E, E', G, G', I, I' K, K'). *Fgf10* expression was used as a marker of both neural and sensory domains (Pauley et al., 2003; Pirvola et al., 2000). At E10.5, *Fgf10* was detected in the anterior pole of control vesicles, which includes the prospective sensory domain, and in the delaminating neuroblasts of the forming eighth ganglion. During this time, *Fgf10* was also expressed in a second, smaller posterior patch, which is destined to give rise to the posterior crista. No significant differences in the distribution of *Fgf10*-expressing cells were detected between $Fgf3^{\Delta 2/flox}$, *Cre-/-* control (n=3)(Figure 5.2B, B') and $Fgf3^{\Delta 2/flox}$, *Cre+/+* conditional mutant embryos (n=3)(Figure 5.2D, D', F, F', H, H', J, J', L, L'). The size and morphology of otic vesicles of all the conditional mutants analyzed were normal and comparable to wild type and control embryos. In particular, all conditional mutants formed an endolymphatic duct/sac (Figure 5.2). Thus, *Fgf3* function in the otic placode, otic epithelium, and hindbrain later than the cup stage is not required for normal otic morphogenesis.

Discussion

To enhance our understanding of the role of *Fgf3* signaling in early morphogenesis, we set out to determine the tissue-specific effects of *Fgf3* inactivation

Figure 5.2 Expression of *Gbx2* and *Fgf10* inner ear markers is similar in E10.5 *Fgf3* control and tissue-specific mutant embryos

Whole-mount embryos were probed with *Gbx2* (A,C,E,G,I,K) or *Fgf10* (B,D,F,H,J,L) at E10.5 and sectioned transversely as indicated the white lines. *Gbx2* expression in the dorsomedial wall of the otocyst is similar in control (A') and conditional mutant (C',E',G',I',K') embryos. At E10.5, *Fgf10* is expressed in control (B') and *Fgf3* conditional mutant (D',F',H',J',L') embryos in the anterior region of the otocyst, which includes the prospective sensory domain and the delaminating neuroblasts of the forming eighth ganglion. Abbreviations: eds, endolymphatic duct and sac; nt, neural tube; ov, otic vesicle.

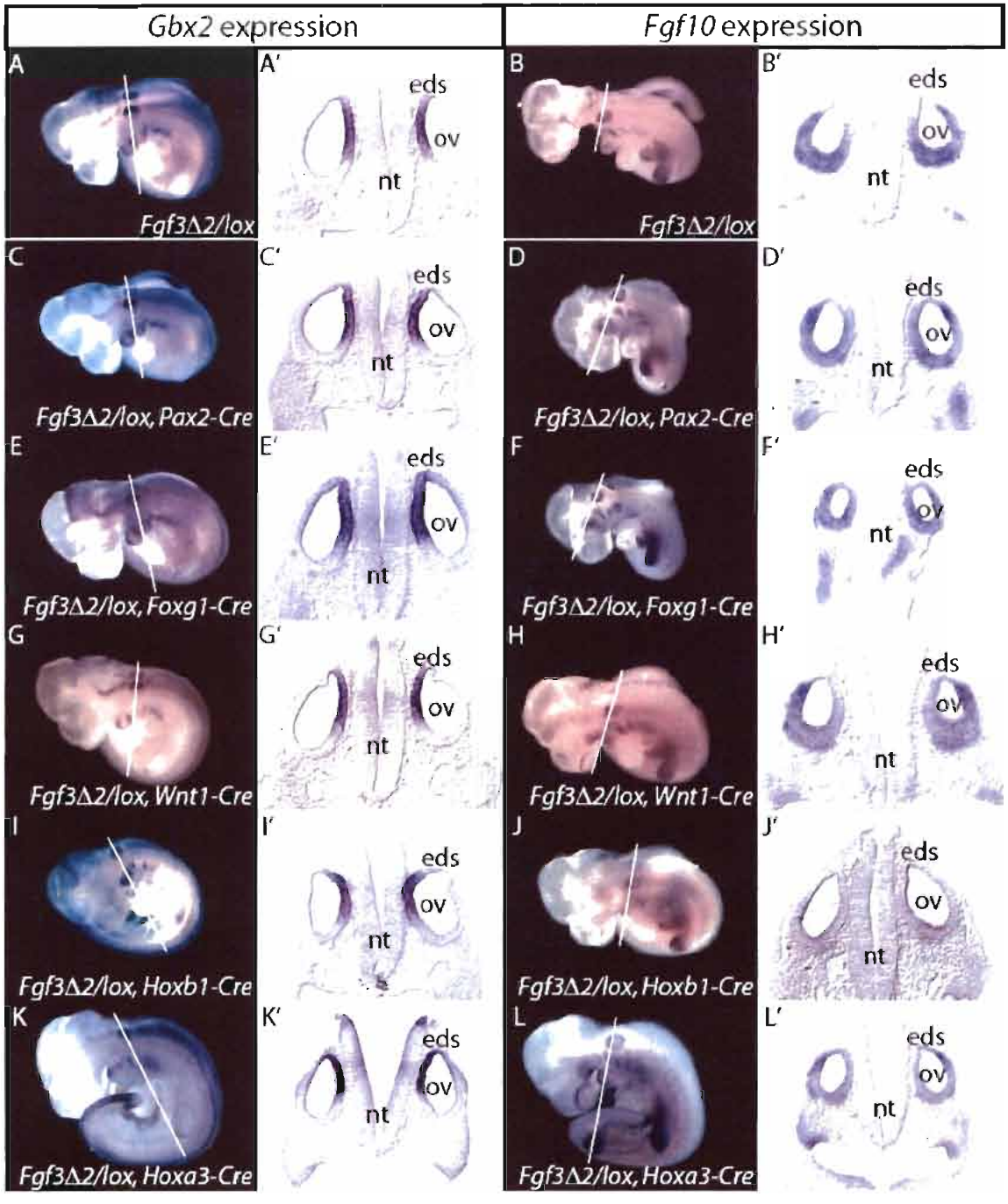
Gbx2 expression
Fgf10 expression
A
A'
B
B'
C
C'
D
D'
E
E'
F
F'
G
G'
H
H'
I
I'
J
J'
K
K'
L
L'
Fgf3Δ2/lox
Fgf3Δ2/lox, Pax2-Cre
Fgf3Δ2/lox, Foxg1-Cre
Fgf3Δ2/lox, Wnt1-Cre
Fgf3Δ2/lox, Hoxb1-Cre
Fgf3Δ2/lox, Hoxa3-Cre
eds
ov
nt

and the timing at which these signaling effects play obligatory roles in the development of the dorsal rudiments of the inner ear. We utilized a conditional mutagenesis approach in which we deleted *Fgf3* in a temporally and spatially controlled fashion. Through this analysis we were not able to generate conditional mutants that phenocopy the *Fgf3* null mutant phenotype. We show that conditional loss of *Fgf3* in the otic placode, the neurogenic region of the otocyst, and the hindbrain adjacent to the otic vesicle does not influence normal inner ear development. In all the conditional mutants analyzed, no significant differences in auditory brainstem response thresholds were observed between control and mutant animals and all of these controls had normal behavior. Furthermore, *Gbx2* and *Fgf10* marker genes used to analyze the effects of the *Fgf3* conditional mutations at the molecular level were not affected.

There are a few potential explanations for the failure to phenocopy the *Fgf3* null mutant phenotype in any of the conditional mutants analyzed in this study. First, coordinated *Fgf3* signaling from multiple tissues might be required for proper vesicle morphogenesis. Removal of *Fgf3* from one source at a time would therefore have no effect. This hypothesis is testable by generating double/triple *Fgf3* conditional mutants in tissues of expression. Second, we can not rule out the possibility that a temporal requirement has not been met in our studies, especially when deleting *Fgf3* in the hindbrain. The initial hypothesis was that FGF3 signaling from the hindbrain is required for dorsal otic morphogenesis at E9.5-E10.5, in the period immediately prior to the observed phenotypic defects. However, the first hindbrain *Fgf3* expression is observed as early as 3 somites (data not shown, but see McKay et al., 1996; Wright and Mansour, 2003), whereas the *Wnt1*, *Hoxb1* and *Hoxa3* hindbrain *Cre* drivers trigger excision of

Fgf3 starting at E9.0. Therefore, it is possible that a short window of early *Fgf3* expression is sufficient to initiate the signaling program required for proper vesicle morphogenesis in *Fgf3* conditional mutants. Ultimately, this possibility would have to be tested by inactivating *Fgf3* in the hindbrain as early as the 0 to 3 somite stages. At the present time, the *Cre* driver that would allow *Fgf3* inactivation specifically in the early hindbrain is not available. However, it has been shown that *Mafb (Kreisler)* is expressed in rhombomeres 5 and 6 of the hindbrain during the time period when *Fgf3* is normally expressed there. *(Mafb)Kreisler-Cre* transgenic animals could potentially be generated and used to delete *Fgf3* in the early hindbrain. If *Fgf3* expressed in the early hindbrain is required for dorsal otic patterning, then deleting it in the hindbrain earlier than the 3 somite stage would phenocopy *Fgf3* null mutant inner ear phenotypes. Phenotypes similar to complete germ line *Fgf3* inactivation can be interpreted to mean that all of the effects of *Fgf3* are a consequence of expression by the hindbrain. Similarly, a partial/less severe phenotype will indicate which aspects of *Fgf3* function are mediated by the early hindbrain expression. Finally, technical imprecision associated with the Cre/LoxP conditional mutagenesis system in the mouse, leading to incomplete deletion of *Fgf3* from the source, could explain the failure to phenocopy the *Fgf3* null mutant phenotype in any conditional mutants used in this study. This is illustrated by the diffused or "patchy" pattern of *Cre*-recombinase expressing cells, seen with the *Hoxb1-Cre* and *Wnt1-Cre* driver alleles. In this case, it can be speculated that a subset of wild type cells present in the tissue of interest produces sufficient levels of *Fgf3* for normal otic development.

Despite the inability to phenocopy any of the inner ear defects associated with *Fgf3* null mutation, some of the questions about the nature of these defects can be answered. Common crus aplasia was one of the most common inner ear phenotypes observed in *Fgf3* null mutants (refer to Chapter 4). Two possible explanations could clarify how this dysmorphology arises. Since the common crus is formed when two distinct central regions of the vertical canal plate fuse and then resorb to form distinct anterior and posterior canals, one possibility is that *Fgf3*, expressed from the developing cristae, normally functions relatively directly to limit the fusion boundaries or the process of cellular resorption. Alternatively, it could be that the abnormal swelling of the epithelium, consequent to failed or incomplete induction of the EDS, is itself the cause of excessive cellular fusion and/or resorption in the vertical canal plate. Conditional ablation of *Fgf3* in the otic epithelium versus hindbrain suggests that common crus aplasia is likely to be caused by the deletion of *Fgf3* in the early hindbrain leading to failed EDS induction and the abnormal swelling, as deleting *Fgf3* in the neurogenic region did not cause inner ear defects.

Our initial hypothesis for the hindbrain *Fgf3* requirement in inner ear patterning is supported by the extensive literature describing the role of the hindbrain for normal inner ear patterning. Removal or rotation of the neural tube in the vicinity of the developing otic tissue disrupts otic vesicle molecular patterning and development (Bok et al., 2005; Hutson et al., 1999). Mutations in hindbrain-expressed genes, such as *Mafb* (*Kreisler*) and *Hoxa1*, which cause defects in the development of r5 and r6, also show aberrant patterning of the otic vesicle that presages inner ear malformations (Choo et al., 2006; Pasqualetti et al., 2001). The expression of *Fgf3* in rhombomeres 5 and 6 is disrupted in

Mafb (Kreisler) and *Hoxa1* mutants, which develop inner ear deformities similar to those described in *Fgf3* mutants (Mansour et al., 1993). Interestingly, the expression of *Fgf3* in the otic region is retained in these mutants, although it is shifted medially. Therefore, it has been suggested that the abnormalities of otic vesicle development seen in *Mafb (Kreisler)* and *Hoxa1* mutants are caused by the disruption of *Fgf3* expression in the hindbrain (McKay et al., 1996; Pasqualetti et al., 2001). The possibility that disturbances of factors other than *Fgf3* cause the inner ear abnormalities in *Mafb (Kreisler)* and *Hoxa1* mutants can not be ruled out. However, the favored interpretation is that *Fgf3* expression in rhombomeres 5 and 6 is necessary for the normal development of the inner ear.

Aside from identifying a more appropriate hindbrain *Cre*-driver, rescuing *Fgf3* function in a null mutant background is one approach that could be pursued to address these issues. A synthetic enhancer element derived from the *Hoxb3* gene together with a minimal promoter element has been described and shown to drive reporter gene expression in rhombomeres 5 and 6 (Manzanares et al., 1997) during the time period when *Fgf3* is normally expressed in the hindbrain. This system can potentially be used to generate transgenic mice that express epitope-tagged FGF3 in the hindbrain, but not at other sites of *Fgf3* expression, to test whether hindbrain expression of *Fgf3* can rescue the null phenotype.

The retinoic acid (RA) rescue study described with *Hoxa1* mutants suggests that *Fgf3* expression in the hindbrain can in fact rescue the inner ear phenotype (Pasqualetti et al., 2001). It was shown that administration of a specific dose of RA can bypass the *Hoxa1* requirement and prevent the inner ear abnormalities observed in *Hoxa*1 mutants (Pasqualetti et al., 2001). The temporal window of RA sensitivity during which the rescue

of inner ear structures is effective in *Hoxa1* mutants was determined to be up to E8.75 and *Fgf3* was described as a direct target of RA rescue. These experiments suggest an early requirement for hindbrain-expressed *Fgf3*, at least before E8.75, which was not met in our conditional inactivation experiments.

Materials and methods

Fgf3 and *Cre*-driver alleles and genotyping

All work with mice complied with protocols approved by the University of Utah Institutional Animal Care and Use Committee. A conditional *Fgf3* allele ($Fgf3^{lox}$) was generated by targeting LoxP sites on either side of exon 2 and then deleting the intervening DNA by exposing the conditional allele to CRE recombinase to produce a $Fgf3^{\Delta 2}$ allele (X. Wang et al., manuscript in preparation). $Fgf3^{\Delta 2/+}$, *Cre-/-* males were crossed to $Fgf3^{flox/flox}$ females to generate conditional mutant embryos. Genotypes were determined by PCR amplification of yolk sac or tail DNA using a 3-primer mix that distinguishes the deletion, conditional and wild type alleles. The $Fgf3^{\Delta 2}$ genotyping mix, contained primers 455C (5'-CTGCCTATGTGCTATATCCATGG-3'), 456C (5'-GTAGATGACTGAGTGTGTAGG-3') and 485B (5'-GGTTCCTCGATCAAACTCTGG-3'). PCR analysis was performed in 20 µl reactions amplified in an MJR thermal cycler for 35 cycles of 30 sec at 94°C, 20 sec at 60°C and 1 min at 72°C. The reaction produced a wild type band of 250 bp, a loxP conditional band of 350 bp and a deletion band of 600 bp. *Cre*-driver alleles were genotyped as described: *Wnt1-Cre* (Chai et al., 2000), *Foxg1* (Hebert and McConnell, 2000), *Pax2* (Ohyama and Groves, 2004), *Hoxb1* (Arenkiel et al., 2003) and *Hoxa3* (Bunting et al., 1999).

X-gal staining

Embryos harboring both the ROSA26 reporter and *Cre* driver alleles were isolated from pregnant females in PBS with 1mM $MgCl_2$. Embryos were then fixed (2% paraformaldehyde, 1.25 mM EGTA, 2 mM $MgCl_2$, 0.1 M PIPES pH6.9), washed in PBS/1mM $MgCl_2$, and immersed into X-gal staining solution (5mM $K_3Fe(CN)_6$/5 mM $K_4Fe(CN)_6$-$3H_2O$/ 1 mM $MgCl_2$/ 0.01% Na Deoxycholate/ 0.02% NP40 in PBS pH7.5). Staining was carried out at 37°C in a humidified atmosphere. Stained embryos were cryoprotected in sucrose and sectioned at 14 µm using a Leica CM1900 cryostat as described (Stark et al., 2000).

RNA in situ hybridization

Otic vesicle and hindbrain patterning was analyzed at E10.5 (30-39 somite pairs) by whole mount RNA in situ hybridization using *Gbx2* and *Fgf10* marker genes. Embryos were isolated on the indicated days following detection of a vaginal plug and age-matched based on the total number of somite pairs. Digoxigenin-labeled probes were prepared, hybridized to the embryos and detected as described (Henrique et al., 1995). Antisense RNA probes were generated from plasmids for *Gbx2* (Wassarman et al., 1997) and *Fgf10* (Pauley et al., 2003). Embryos stained for analysis of gene expression were cryoprotected in sucrose and sectioned at 14 µm using a Leica CM1900 cryostat as described (Stark et al., 2000). Three embryos of each genotype were analyzed for each probe.

Auditory brainstem response threshold measurements

Mice were anesthetized using 0.02 ml/g Avertin. Auditory brainstem response (ABR) thresholds for click stimuli (47 μsec duration, 29.3/sec) presented to each ear individually were determined using high frequency transducers controlled and analyzed by SmartEP software (Intelligent Hearing Systems) according to (Zheng et al., 1999).

Photography

Whole embryos were photographed using a Zeiss SV-11 dissecting microscope fitted with a digital camera (Kodak MDS120 or 240). Sections were photographed using a Zeiss Axioscop fitted with DIC optics and a digital camera (AxioCam).

References

Arenkiel, B. R., Gaufo, G. O. and Capecchi, M. R. (2003). Hoxb1 neural crest preferentially form glia of the PNS. *Dev Dyn* **227**, 379-86.

Bok, J., Bronner-Fraser, M. and Wu, D. K. (2005). Role of the hindbrain in dorsoventral but not anteroposterior axial specification of the inner ear. *Development* **132**, 2115-24.

Bunting, M., Bernstein, K. E., Greer, J. M., Capecchi, M. R. and Thomas, K. R. (1999). Targeting genes for self-excision in the germ line. *Genes Dev* **13**, 1524-8.

Carney, P. R. and Silver, J. (1983). Studies on cell migration and axon guidance in the developing distal auditory system of the mouse. *J Comp Neurol* **215**, 359-69.

Chai, Y., Jiang, X., Ito, Y., Bringas, P., Jr., Han, J., Rowitch, D. H., Soriano, P., McMahon, A. P. and Sucov, H. M. (2000). Fate of the mammalian cranial neural crest during tooth and mandibular morphogenesis. *Development* **127**, 1671-9.

Choo, D., Ward, J., Reece, A., Dou, H., Lin, Z. and Greinwald, J. (2006). Molecular mechanisms underlying inner ear patterning defects in kreisler mutants. *Dev Biol* **289**, 308-17.

Hebert, J. M. and McConnell, S. K. (2000). Targeting of cre to the Foxg1 (BF-1) locus mediates loxP recombination in the telencephalon and other developing head structures. *Dev Biol* **222**, 296-306.

Henrique, D., Adam, J., Myat, A., Chitnis, A., Lewis, J. and Ish-Horowicz, D. (1995). Expression of a Delta homologue in prospective neurons in the chick. *Nature* **375**, 787-90.

Hutson, M. R., Lewis, J. E., Nguyen-Luu, D., Lindberg, K. H. and Barald, K. F. (1999). Expression of Pax2 and patterning of the chick inner ear. *J Neurocytol* **28**, 795-807.

Li, C. W., Van De Water, T. R. and Ruben, R. J. (1978). The fate mapping of the eleventh and twelfth day mouse otocyst: an in vitro study of the sites of origin of the embryonic inner ear sensory structures. *J Morphol* **157**, 249-67.

Mahmood, R., Mason, I. J. and Morriss-Kay, G. M. (1996). Expression of Fgf-3 in relation to hindbrain segmentation, otic pit position and pharyngeal arch morphology in normal and retinoic acid-exposed mouse embryos. *Anat Embryol (Berl)* **194**, 13-22.

Mansour, S. L., Goddard, J. M. and Capecchi, M. R. (1993). Mice homozygous for a targeted disruption of the proto-oncogene int-2 have developmental defects in the tail and inner ear. *Development* **117**, 13-28.

Manzanares, M., Cordes, S., Kwan, C. T., Sham, M. H., Barsh, G. S. and Krumlauf, R. (1997). Segmental regulation of Hoxb-3 by kreisler. *Nature* **387**, 191-5.

McKay, I. J., Lewis, J. and Lumsden, A. (1996). The role of FGF-3 in early inner ear development: an analysis in normal and kreisler mutant mice. *Dev Biol* **174**, 370-8.

Ohyama, T. and Groves, A. K. (2004). Generation of Pax2-Cre mice by modification of a Pax2 bacterial artificial chromosome. *Genesis* **38**, 195-9.

Pasqualetti, M., Neun, R., Davenne, M. and Rijli, F. M. (2001). Retinoic acid rescues inner ear defects in Hoxa1 deficient mice. *Nat Genet* **29**, 34-9.

Pauley, S., Wright, T. J., Pirvola, U., Ornitz, D., Beisel, K. and Fritzsch, B. (2003). Expression and function of FGF10 in mammalian inner ear development. *Dev Dyn* **227**, 203-15.

Pirvola, U., Spencer-Dene, B., Xing-Qun, L., Kettunen, P., Thesleff, I., Fritzsch, B., Dickson, C. and Ylikoski, J. (2000). FGF/FGFR-2(IIIb) signaling is essential for inner ear morphogenesis. *J Neurosci* **20**, 6125-34.

Soriano, P. (1999). Generalized lacZ expression with the ROSA26 Cre reporter strain. *Nat Genet* **21**, 70-1.

Stark, M. R., Biggs, J. J., Schoenwolf, G. C. and Rao, M. S. (2000). Characterization of avian frizzled genes in cranial placode development. *Mech Dev* **93**, 195-200.

Wassarman, K. M., Lewandoski, M., Campbell, K., Joyner, A. L., Rubenstein, J. L., Martinez, S. and Martin, G. R. (1997). Specification of the anterior hindbrain and establishment of a normal mid/hindbrain organizer is dependent on Gbx2 gene function. *Development* **124**, 2923-34.

Wright, T. J. and Mansour, S. L. (2003). Fgf3 and Fgf10 are required for mouse otic placode induction. *Development* **130**, 3379-90.

Zheng, Q. Y., Johnson, K. R. and Erway, L. C. (1999). Assessment of hearing in 80 inbred strains of mice by ABR threshold analyses. *Hear Res* **130**, 94-107.

CHAPTER 6

SUMMARY

The inner ear is a morphologically complex sensory organ that controls the indispensable physiologic functions of audition and balance. Dysfunction of the inner ear is among the most common congenital disorders; affecting at least 1 in 500 births (Morton and Nance, 2006) and up to 39% of sensorineural deafness is associated with inner ear malformations (Mafong et al., 2002; Wu et al., 2005). The mouse inner ear is functionally and structurally very similar to that of humans and thus provides a powerful mammalian model system with which to investigate the genetic mechanisms responsible for the myriad of human inner ear malformations (Fritzsch et al., 2006; Kiernan et al., 2002; Mansour and Schoenwolf, 2005).

The early development of the inner ear occurs in three phases. The first phase is characterized by formation of the early rudiment of the ear, the otic placode. During the second phase, the morphogenetic changes of the placodal region take place, resulting in formation of the otic vesicle that gives rise to the auditory and vestibular compartments of the inner ear. The final stage involves regional patterning of the otocyst, resulting in a unique three-dimensional morphology of the inner ear and is the focus of this study. Particularly of interest is the fact that the complex and the intricate structure of the inner ear arises from a simple patch of ectodermal tissue early in embryonic development.

The final structure of the inner ear is an asymmetric structure with each of its developmental axes having distinct morphologic characteristics. The cellular and molecular aspects of when and how these axes arise are not fully understood. The timing of anterior-posterior (AP) vs. dorsal-ventral (DV) axis formation was addressed in rotation experiments in the chick (Brigande et al., 2000; Fekete and Wu, 2002; Rinkwitz et al., 2001; Rivolta, 1997; Torres and Giraldez, 1998; Wu et al., 1998). It was concluded that the anteroposterior otic axis is established before the dorsoventral axis, and in chick, this development occurs at the otic cup stage. It is also known that the subdivision into the precise inner ear structures is facilitated by the tight regional subdivision into restricted gene expression domains. Most recent models of inner ear development indicate that boundaries of gene expression are in place at the vesicle stage (Brigande et al., 2000; Fekete and Wu, 2002; Rinkwitz et al., 2001), keeping interest in regionally restricted genes. The question of how the complex geometry of the inner ear arises needs active investigation.

This division of the otocyst into gene expression domains required for normal morphogenesis involves signaling interactions within and between otic and non-otic tissues (Fekete, 1999; Kiernan et al., 2002). In particular, signaling coming from the hindbrain is required for inner ear patterning into compartments (Bok et al., 2005; Hutson et al., 1999). The large number of the key transcription factors is also expressed by the epithelium itself, in spatially and temporally complex patterns (Rivolta, 1997; Torres and Giraldez, 1998).

Fibroblast growth factor (FGF) signaling is implicated in different aspects of inner ear development and is a focus of this study. Members of the Fibroblast Growth

Factor family are expressed by tissues relevant for otic development in different species (Ladher et al., 2000; Leger and Brand, 2002; Mahmood et al., 1996; Mansour et al., 1993; Maroon et al., 2002; McKay et al., 1996; Pauley et al., 2003; Phillips et al., 2001; Pirvola et al., 2000; Vendrell et al., 2000; Wilkinson et al., 1988). The phenotypes of mice that individually lack sixteen of the family members have been reported, which began to reveal the ways in which the functions of FGFs are utilized during the normal inner ear development (for review see (Itoh and Ornitz, 2004). Many *Fgf* mutant animals have phenotypes, including otic phenotypes, which are more restricted than might be predicted from the expression patterns of the gene, verifying that combinatorial action of several *Fgfs* from several tissues is required. Because of the functional redundancy associated with *Fgfs*, description of specific inner ear phenotypes associated with each individual mutant would be particularly beneficial.

In an effort to gain a better understanding of the role of *Fgf* genes, this thesis work has focused on the specific roles for *Fgf* genes in patterning inner ear into compartments. More specifically, the goal was to analyze expression patterns of the members of *Fgf* gene family and their receptors and to describe specific roles for *Fgf3* and *Fgf16* in inner ear morphogenesis by using conventional methods of complete and tissue-specific gene inactivation by targeting, cell lineage and expression analyses.

Expression analysis screen of 18 mouse *Fgf* and 3 *Fgf* receptor (*Fgfr*) genes during early otic development identified two novel sites of *Fgf* expression in the otic epithelium region. More specifically, *Fgf4* transcripts were expressed in the pre-placodal and placodal ectoderm, suggesting potential roles in placode induction and/or maintenance. *Fgf16* was expressed in the posterior otic cup and vesicle, suggesting roles

in otic cell fate decisions and/or axis formation. In addition, all three tested members of the *Fgfr* family, *Fgfr2c*, *Fgfr3c*, and *Fgfr4*, were expressed in tissues relevant to inner ear development. Taken together these results provide an opportunity towards better understanding of the general roles of *Fgf* genes in inner ear development.

Previous studies have shown that *Fgf3* null mutants undergo normal otic vesicle formation, but then go on to develop highly variable and incompletely penetrant inner ear dysmorphologies that appear to initiate at the stage of endolymphatic duct outgrowth. These mutants also had a reduction in the size of the otic ganglion (Mansour et al., 1993). This study provides new morphologic data on inner ear dysmorphogenesis in *Fgf3* mutants, which show a range of malformations similar to those seen in *Mafb* (*Kreisler*), *Hoxa1* and *Gbx2* mutants; the most common phenotype being failure of endolymphatic duct and common crus formation, accompanied by epithelial dilatation and reduced cochlear coiling. The range of malformations has close parallels with those seen in hearing impaired patients. The *Fgf3* morphologic data, together with an analysis of changes in the molecular patterning of *Fgf3* mutant otic vesicles and comparisons with other mutations that affect otic morphogenesis, allow placement of *Fgf3* between hindbrain-expressed *Hoxa1* and *Mafb* (*Kreisler*) and otic vesicle-expressed *Gbx2* in the genetic cascade initiated by WNT signaling that leads to dorsal otic patterning and endolymphatic duct and sac formation. In addition, we found that *Fgf3* prevents expansion of *Wnt3a* into more ventral regions of the hindbrain, serving to focus the inductive WNT signals on the dorsal otic vesicle and highlighting a new example of crosstalk between the two signaling systems. Furthermore, we suggest that *Fgf3* also functions, albeit largely redundantly, in the subsequent sensory patch control of non-

sensory development, as a very small number of affected mutants underwent normal endolymphatic duct and sac (EDS) induction, but developed with abnormal or absent posterior semicircular canals. This phenotype is consistent with previous suggestions that FGF signals from the developing sensory patches induce non-sensory (canal) development (Chang et al., 2004). However, to address this issue directly and to assess the relative contributions of *Fgf3* and *Fgf10* to posterior sensory and non-sensory development, analysis of double conditional mutants in which the hindbrain requirement for *Fgf3* in EDS induction is bypassed will be required.

In addition, through a series of conditional mutagenesis experiments, generating chimeric embryos comprised of both wild type and *Fgf3* mutant cells, we demonstrate that conditional loss of *Fgf3* in the otic placode, the neurogenic region of the otocyst and in the hindbrain adjacent to the otic vesicle does not influence normal inner ear development. We further speculate that the early requirement for the hindbrain-expressed *Fgf3* is likely to be in place for proper development of the endolymphatic duct. Another possibility exists, that a combination of tissues participates in endolymphatic duct development. These experiments allowed us to dissociate tissue-specific roles of *Fgf3* and address the timing at which *Fgf3* signals play obligatory roles in the development of the dorsal rudiments of the inner ear, therefore providing further insights into understanding the role of *Fgf3*. Ultimately, analysis of double tissue-conditional mutants, inactivation *Fgf3* in the hindbrain as early as 0 to 3 somite stage, and rescuing *Fgf3* function in a null mutant background would answer all the remaining questions.

The studies with *Fgf16* open up further opportunities towards better understanding of the inner ear development. Our results show that early in development

Fgf16 transcripts are initially detected by whole-mount in situ hybridization in the posterior otic cup and posterior half of the dorsolateral vesicle. Germline deletion of *Fgf16* does not have an effect on inner ear morphogenesis or function. The same allele of *Fgf16* was used to conduct whole-mount *Fgf16* lineage analysis throughout embryogenesis by using the ROSA26 reporter (Soriano, 1999). This genetic approach was used to overcome the limitations associated with traditional lineage tracing experiments in the mouse and expand our knowledge regarding the inner ear compartment/boundary formation. Reporter-positive cells were consistently found at the base of the cochlear stria vascularis, non-sensory region of the anterior and posterior semicircular canals and all the three cristae.

This not only represents the first report of the posterior cup lineage, but also describes a potential role for *Fgf16* in sensory organ development, as reporter positive cells mark semicircular canal sensory organs throughout embryonic development. Furthermore, the *Fgf16* mutant is a genetic tool important in expanding our understanding of patterning and fate specification in different inner ear structures and can be valuable to heart and brown adipose tissue researchers. The lack of the inner ear phenotype might be explained by functional redundancy with another member of the FGF family expressed in the same region. Therefore, the unique role of *Fgf16* in inner ear development ultimately needs to be tested by the generation of double knock-out animals between *Fgf16* and *Fgf10*.

Taken together, the data presented in this study suggests that development of the inner ear is a developmentally coordinated program in which proper formation of one structure is directly dependent upon signaling interactions from different tissues. The

work presented herein describes additional roles for *Fgf* genes, expressed from both the hindbrain and the otic epithelium, in formation of the functional inner ear structures. *Fgf16* lineage analysis described herein has been extremely valuable in supporting compartment boundary model proposed for the inner ear development. These results provide insights at the molecular and genetic levels into how the vertebrate embryo properly coordinates development of such a complex structure as the inner ear through the dynamic regulation of genes in multiple tissues.

References

Bok, J., Bronner-Fraser, M. and Wu, D. K. (2005). Role of the hindbrain in dorsoventral but not anteroposterior axial specification of the inner ear. *Development* **132**, 2115-24.

Brigande, J. V., Kiernan, A. E., Gao, X., Iten, L. E. and Fekete, D. M. (2000). Molecular genetics of pattern formation in the inner ear: do compartment boundaries play a role? *Proc Natl Acad Sci U S A* **97**, 11700-6.

Chang, W., Brigande, J. V., Fekete, D. M. and Wu, D. K. (2004). The development of semicircular canals in the inner ear: role of FGFs in sensory cristae. *Development* **131**, 4201-11.

Fekete, D. M. (1999). Development of the vertebrate ear: insights from knochouts and mutants. *Trends Neusoscience* **22**, 263-269.

Fekete, D. M. and Wu, D. K. (2002). Revisiting cell fate specification in the inner ear. *Curr Opin Neurobiol* **12**, 35-42.

Fritzsch, B., Pauley, S. and Beisel, K. W. (2006). Cells, molecules and morphogenesis: the making of the vertebrate ear. *Brain Res* **1091**, 151-71.

Hutson, M. R., Lewis, J. E., Nguyen-Luu, D., Lindberg, K. H. and Barald, K. F. (1999). Expression of Pax2 and patterning of the chick inner ear. *J Neurocytol* **28**, 795-807.

Itoh, N. and Ornitz, D. M. (2004). Evolution of the Fgf and Fgfr gene families. *Trends Genet* **20**, 563-9.

Kiernan, A. E., Steel, K. P. and Fekete, D. M. (2002). Development of the Mouse Inner Ear. Orlando, FL: Academic Press.

Ladher, R. K., Anakwe, K. U., Gurney, A. L., Schoenwolf, G. C. and Francis-West, P. H. (2000). Identification of synergistic signals initiating inner ear development. *Science* **290**, 1965-7.

Leger, S. and Brand, M. (2002). Fgf8 and Fgf3 are required for zebrafish ear placode induction, maintenance and inner ear patterning. *Mech Dev* **119**, 91-108.

Mafong, D. D., Shin, E. J. and Lalwani, A. K. (2002). Use of laboratory evaluation and radiologic imaging in the diagnostic evaluation of children with sensorineural hearing loss. *Laryngoscope* **112**, 1-7.

Mahmood, R., Mason, I. J. and Morriss-Kay, G. M. (1996). Expression of Fgf-3 in relation to hindbrain segmentation, otic pit position and pharyngeal arch morphology in normal and retinoic acid-exposed mouse embryos. *Anat Embryol (Berl)* **194**, 13-22.

Mansour, S. L., Goddard, J. M. and Capecchi, M. R. (1993). Mice homozygous for a targeted disruption of the proto-oncogene int-2 have developmental defects in the tail and inner ear. *Development* **117**, 13-28.

Mansour, S. L. and Schoenwolf, G. C. (2005). Morphogenesis of the inner ear. In *Development of the Inner Ear*, vol. 26 (ed. M. W. Kelley D. K. Wu A. N. Popper and R. R. Fay), pp. 43-84. New York: Springer-Verlag.

Maroon, H., Walshe, J., Mahmood, R., Kiefer, P., Dickson, C. and Mason, I. (2002). Fgf3 and Fgf8 are required together for formation of the otic placode and vesicle. *Development* **129**, 2099-108.

McKay, I. J., Lewis, J. and Lumsden, A. (1996). The role of FGF-3 in early inner ear development: an analysis in normal and kreisler mutant mice. *Dev Biol* **174**, 370-8.

Morton, C. C. and Nance, W. E. (2006). Newborn hearing screening--a silent revolution. *N Engl J Med* **354**, 2151-64.

Pauley, S., Wright, T. J., Pirvola, U., Ornitz, D., Beisel, K. and Fritzsch, B. (2003). Expression and function of FGF10 in mammalian inner ear development. *Dev Dyn* **227**, 203-15.

Phillips, B. T., Bolding, K. and Riley, B. B. (2001). Zebrafish fgf3 and fgf8 encode redundant functions required for otic placode induction. *Dev Biol* **235**, 351-65.

Pirvola, U., Spencer-Dene, B., Xing-Qun, L., Kettunen, P., Thesleff, I., Fritzsch, B., Dickson, C. and Ylikoski, J. (2000). FGF/FGFR-2(IIIb) signaling is essential for inner ear morphogenesis. *J Neurosci* **20**, 6125-34.

Rinkwitz, S., Bober, E. and Baker, R. (2001). Development of the vertebrate inner ear. *Ann N Y Acad Sci* **942**, 1-14.

Rivolta, M. N. (1997). Transcription factors in the ear: molecular switches for development and differentiation. *Audiol Neurootol* **2**, 36-49.

Soriano, P. (1999). Generalized lacZ expression with the ROSA26 Cre reporter strain. *Nat Genet* **21**, 70-1.

Torres, M. and Giraldez, F. (1998). The development of the vertebrate inner ear. *Mech Dev* **71**, 5-21.

Vendrell, V., Carnicero, E., Giraldez, F., Alonso, M. T. and Schimmang, T. (2000). Induction of inner ear fate by FGF3. *Development* **127**, 2011-9.

Wilkinson, D. G., Peters, G., Dickson, C. and McMahon, A. P. (1988). Expression of the FGF-related proto-oncogene int-2 during gastrulation and neurulation in the mouse. *Embo J* **7**, 691-5.

Wu, C. C., Chen, Y. S., Chen, P. J. and Hsu, C. J. (2005). Common clinical features of children with enlarged vestibular aqueduct and Mondini dysplasia. *Laryngoscope* **115**, 132-7.

Wu, D. K., Nunes, F. D. and Choo, D. (1998). Axial specification for sensory organs versus non-sensory structures of the chicken inner ear. *Development* **125**, 11-20.